MASTERARBEIT

Titel der Masterarbeit

„Comprehensive Process Control for Anaerobic Biotransformation of Petroleum Hydrocarbons *In Situ* using Terminal Electron Acceptor Isotope Ratios“

Verfasser

Martin Kern, BSc

angestrebter akademischer Grad

Master of Science

Wien, im Oktober 2015

Matrikelnummer: 0840584
Studium: Umwelt- und Bioressourcenmanagement
Studienkennzahl: H 066 427
Wissenschaftliche Betreuerin: Priv.-Doz. Dipl.-Ing. Dr.nat.techn. Kerstin Brandstätter-Scherr

Eidesstattliche Erklärung:

Ich erkläre eidesstattlich, dass ich die Arbeit selbständig angefertigt, keine anderen als die angegebenen Hilfsmittel benutzt und alle aus ungedruckten Quellen, gedruckter Literatur oder aus dem Internet im Wortlaut oder im wesentlichen Inhalt übernommenen Formulierungen und Konzepte gemäß den Richtlinien wissenschaftlicher Arbeiten zitiert bzw. mit genauer Quellenangabe kenntlich gemacht habe.

Abstract

Clean-up methods for petroleum hydrocarbon (PH)-contaminated aquifers that rely on the metabolic capability of indigenous microorganisms to convert toxic organic chemicals to innocuous compounds, termed *in situ* bioremediation, are promising and sustainable approaches to reestablish environmental quality. In absence of molecular oxygen, microorganisms require alternative terminal electron acceptors (TEA), e.g. nitrate or sulfate, to perform oxidative PH-degradation. Since anaerobic conditions often prevail in contaminated aquifers and oxygen is slowly replenished, PH-remediation under anaerobic conditions, promoted via addition of alternative, non-oxygen TEA, is gaining importance in recent years. However, qualitative and quantitative *in situ* process control is difficult in the presence of discrete PH-phases, so called non-aqueous phase liquids (NAPL), due to compensation of PH-degradation by resolubilisation from the NAPL.

Thus, the objective of the present study is to determine the practicability of interpreting acceptor sided stable isotopic shifts ($\delta^{15}N$ in nitrate and $\delta^{34}S$ in sulfate) as process parameter for the qualitative and quantitative monitoring of PH-degradation in contaminated aquifers. Long-term anaerobic degradation experiments were carried out in laboratory scale anaerobic microcosms. For this, 250 mL glass reactors equipped with Mininert Valves® were filled with 15 g of PH-contaminated sandy aquifer material, 220 mL mineral medium and supplemented with different concentrations of (i) nitrate, (ii) nitrate+sulfate and (iii) nitrate under sulfate reduction suppression as alternative TEA. Aquifer samples were from a nitrate- and sulfate-reducing zone of a historically PH-contaminated site, respectively. TEA-concentrations were monitored quantitatively via ion chromatography (IC) and their isotopic ratios were analyzed via elemental analyzer connected to an isotope ratio mass spectrometer (EA-IRMS) following precipitation. Total petroleum hydrocarbons (TPH) were analyzed via gas chromatography with flame ionization detector (GC-FID). Aqueous supernatants were analyzed semi-quantitatively for polar degradation products by gas chromatography with mass spectrometry (GC-MS) following derivatisation. A 16S rDNA assay using Illumina-Miseq-Technology of the present eubacterial and archaeal microbiome was performed. Statistical correlation between TPH-degradation and the shift of acceptor sided stable isotope ratios was analyzed via linear regression analysis using the programming language R®.

TPH-degradation was observed under all TEA-conditions and several PH-degrading microorganisms could be identified. Nitrate is used preferentially over sulfate when added concurrently, even if nitrate depletion was found to be most prominent under sulfate reduction suppression. Several metabolites could be identified with nitrate as sole TEA, whereas under amendment of both nitrate+sulfate TPH-degradation was most complete in terms of metabolite recovery. All microcosms showed shifts in $^{15}N/^{14}N$ isotope ratios, while no significant $^{34}S/^{32}S$ isotope fractionation was observed. Good linear correlations between $\delta^{15}N$-shifts in the residual TEA-fraction and the corresponding decline in TPH-concentrations with R^2-values of at least 0.85 were found. Isotope enrichment factors ($\varepsilon_{N\text{-}TPH}$) derived from changes in isotopic ratios were dissimilar under different electron accepting conditions. Thus, $\varepsilon_{N\text{-}TPH}$-values were about -9 ‰ in microcosms with nitrate as

sole TEA, while they only amounted to -3 ‰ in microcosms containing both nitrate and sulfate.

In a first step towards the development of a monitoring technique, these results indicate that the monitoring of acceptor sided stable isotope ratios enables for quantitative insight on the degradation progress. Moreover, linear correlations show different slopes under diverse electron accepting conditions. In addition, a qualitative insight in different anaerobic PH-biotransformation processes can be gained. Further experiments and field observations with different PH-matrices and microbial communities are necessary for the calibration of this technique as an efficient site-independent monitoring approach.

Keywords: petroleum hydrocarbons, in situ bioremediation, anaerobic biodegradation, terminal electron acceptors, stable isotope ratios, monitoring

Zusammenfassung

In situ Bioremediation stellt für die Sanierung von mit Mineralölkohlenwasserstoffen (MKW) kontaminierten Grundwasserleitern und somit für die Wiederherstellung einer guten Umweltqualität eine vielversprechende und nachhaltige Methode dar. Dabei wird die Fähigkeit autochthoner Mikroorganismen diese toxischen Substanzen in unschädliche Komponenten abzubauen genutzt. Steht kein Sauerstoff zur Verfügung benötigen die Mikroorganismen für die Oxidation der MKW im Zuge des Abbaus andere terminale Elektronenakzeptoren (TEA) wie Nitrat oder Sulfat. Da in kontaminierten Grundwasserleitern häufig anaerobe Bedingungen vorherrschen und Sauerstoff nur sehr langsam nachgeliefert wird, gewann die durch die Zugabe von TEA gestützte anaerobe *in situ* Sanierung in den letzten Jahren zunehmend an Bedeutung. Ein großes Problem in der Sanierungspraxis besteht aber darin, dass aufgrund von Konzentrationsabnahmen an MKW im Grundwasser weder qualitativ noch quantitativ auf einen funktionierenden Abbauprozess rückgeschlossen werden kann. Einer der Gründe dafür liegt in der Ausbildung einer eigenen nicht wässrigen Phase, aus welcher sich laufend MKW in die Wasserphase lösen. Dadurch wird die durch Abbau bedingte Schadstoffabnahme teilweise kompensiert und ist somit aus der Analyse der gelösten MKW-Fraktion quantitativ nicht beurteilbar.

Aus diesem Grund soll im Rahmen dieser Arbeit ermittelt werden, ob die akzeptorseitige Verschiebung der Stabilisotopenverhältnisse ($\delta^{15}N$ in Nitrat und $\delta^{34}S$ in Sulfat) als Prozessparameter für das qualitative und quantitative Monitoring des MKW-Abbaus an kontaminierten Standorten herangezogen werden kann. Zur Beantwortung dieser Frage wurden anaerobe Langzeitversuche im Labormaßstab durchgeführt. Dabei wurden 250 mL fassende Glasreaktoren jeweils mit 15 g sandigem Material aus dem nitrat- bzw. sulfatreduzierenden Bereich eines historisch mit MKW kontaminierten Grundwasserleiters befüllt. Anschließend wurden den Reaktoren 220 mL Mineralmedium sowie verschiedene Konzentrationen an (i) Nitrat, (ii) Nitrat+Sulfat sowie (iii) Nitrat (bei Hemmung der Sulfatreduktion) als TEA beigefügt. Im Rahmen des Versuches wurden die in den einzelnen Reaktoren vorherrschenden Konzentrationen an TEA laufend mittels Ionenchromatographie (IC) ermittelt. Die Erhebung der akzeptorseitigen Stabilisotopenverhältnisse erfolgte durch Fällung und anschließender Analyse mittels Elementaranalysator gekoppelt an ein Isotopenmassenspektrometer (EA-IRMS). Der Gesamtgehalt an MKW wurde mittels Gaschromatographie und Flammenionisationsdetektor (GC-FID) erhoben. Die wässrigen Überstände wurden derivatisiert und anschließend mittels Gaschromatographie und Massenspektrometrie (GC-MS) semi-quantitativ auf polare Abbauprodukte untersucht. Zur Identifizierung der in den einzelnen Mikrokosmen vorhandenen Eubakterien und Archaeen wurde eine 16S rDNA Sequenzierung mittels Illumina-Miseq-Technolgie durchgeführt. Für die statistische Analyse der Korrelation zwischen MKW-Konzentration und Verschiebung der akzeptorseitigen Stabilisotopenverhältnisse wurde mittels der Programmiersprache R® eine lineare Regressionsanalyse durchgeführt.

In allen Mikrokosmen konnte eine Abnahme der MKW-Konzentrationen beobachtet werden. Außerdem konnten etliche Mikroorganismen mit der Fähigkeit MKW abzubauen identifiziert werden. Lagen sowohl Sulfat als auch Nitrat vor, so nutzten die Mikroorganismen bevorzugt Nitrat, wobei die Nitratzehrraten bei Hemmung der Sulfatreduktion am höchsten waren. Während in jenen Mikrokosmen, in welche nur Nitrat als TEA beigefügt wurde, verschiedenste Zwischenprodukte des Abbaus identifiziert werden konnten, verlief der Abbau in den Reaktoren mit beiden TEA am vollständigsten. Während sich bei allen Mikrokosmen eine Verschiebung der $^{15}N/^{14}N$ Stabilisotopenverhältnisse zeigte, konnte keine signifikante $^{34}S/^{32}S$ Fraktionierung beobachtet werden. Schließlich konnten bei allen Mikrokosmen lineare Korrelationen zwischen der Verschiebung der Stabilisotopenverhältnisse in der noch vorhandenen TEA-Fraktion und der MKW-Abnahme festgestellt werden, wobei die R^2-Werte immer über 0,85 lagen. Dabei zeigten sich unter Zugabe verschiedener TEA unterschiedliche Isotopen-Anreicherungsfaktoren ($\varepsilon_{N\text{-}TPH}$). So lagen die $\varepsilon_{N\text{-}TPH}$-Werte bei den mit Nitrat versetzten Mikrokosmen bei -9 ‰, während sie in den sowohl mit Nitrat wie auch mit Sulfat versetzten Reaktoren nur -3 ‰ betrugen.

Aus diesen Ergebnissen kann geschlussfolgert werden, dass durch das Monitoring der akzeptorseitigen Stabilisotopenverhältnisse ein guter Einblick in den quantitativen Sanierungsfortschritt ermöglicht wird, auch wenn die Regressionsgeraden je nach vorhandenen TEA unterschiedliche Steigungen aufweisen. Zusätzlich kann ein guter Einblick in verschiedene anaerobe MKW-Biotransformationsprozesse gewonnen werden. Nichtsdestotrotz sind für einen standortunabhängigen und effizienten Einsatz dieser Monitoringmethode noch weitere Experimente beziehungsweise Feldversuche mit verschiedenen MKW-Zusammensetzungen und unterschiedlichen mikrobiellen Gemeinschaften notwendig.

Schlüsselwörter: Mineralölkohlenwasserstoffe, in situ Bioremediation, anaerober biologischer Abbau, terminale Elektronenakzeptoren, Stabilisotopenverhältnisse, Monitoring

Danksagung

An dieser Stelle möchte ich mich bei allen bedanken, die mich während der Erstellung meiner Masterarbeit motiviert und unterstützt haben.

Mein ganz besonderer Dank gilt dabei meiner wissenschaftlichen Betreuerin **Kerstin**, welche mir die Möglichkeit gegeben hat diese Masterarbeit am Institut für Umweltbiotechnologie zu verfassen, mir immer mit ihrer gewohnt freundlichen und fachlichen Art zur Seite stand, mich auch in schwereren Zeiten unterstützte bzw. motivierte und mir überdies die Präsentation des Inhalts dieser Arbeit auf der „European Bioremediation Conference“ in Kreta ermöglichte.

Außerdem bedanke ich mich bei **Andrea** und **Joachim** für das Durchführen der Isotopiemessungen sowie bei **Tanja** und **Diana** für das Ausführen der mikrobiologischen Analysen.

Weiters möchte ich mich bei **Marion** für ihre immerwährende Hilfsbereitschaft im Labor bedanken.

Mein ganz besonderer Dank gilt auch **Karin**, die mir zu Beginn im Labor alles gezeigt hat und mir auch zwischendurch immer wieder mit Rat und Tat zur Seite stand.

Des Weiteren danke ich auch **Astrid** und **Stefan**, welche mich in Gesprächen öfters auf neue Ideen gebracht haben.

Markus und **Robert** danke ich für ihre technische Unterstützung.

Thomas und **Andreas** danke ich für die Organisation des Projekts ISOMON, im Rahmen dessen diese Arbeit verfasst wurde.

Natürlich bedanke ich mich auch **bei allen anderen Mitarbeiterinnen und Mitarbeitern am Institut**, die ebenfalls zum Gelingen dieser Arbeit beigetragen haben.

Daneben bedanke ich mich bei meinen Eltern **Günther und Barbara**, bei meinem Onkel **Reinhold** und bei den Eltern meiner Freundin **Horst und Christine** für ihre großartige Unterstützung.

Zu guter Letzt gilt mein ganz besonderer Dank meiner Freundin **Karin**, welche in letzter Zeit auf viel gemeinsame Stunden verzichten musste, immer ein offenes Ohr für mich hatte und mich auch so gut wie möglich unterstützte.

Table of contents

1 Problem statement

Today, more than two-thirds of worldwide energy consumption is based on fossil energy sources (IEA, 2014). Thus, crude oil and its refinery products like motor fuel, fossil burning and lubricants are very important in the global economy (Caldwell et al., 1998; Widdel and Rabus, 2001). All of these fossil fuels contain petroleum hydrocarbons (PH) as the main constituent and as a consequence these compounds are amongst the most produced and transported chemicals around the world (Bian et al., 2015; Boley et al., 2012; Callaghan et al., 2006; Wang and Fingas, 2003). Since crude oil and its refinery products are consistently released into the environment due to accidents or improper handling, PH have become the most frequently occurring contaminants worldwide (Förstner, 2012; Hollinger and Zehnder, 1996; Scherr et al., 2012). For this reason, remediation of PH-contaminated sites represents an important global task (Kiss et al., 1998). Since crude oil and its refinery products are complex mixtures of hundreds of individual hydrocarbons, the remediation of these sites constitutes a big challenge (Atlas, 1981; Bian et al., 2015). Moreover, many clean-up technologies like chemical and physical treatment approaches are very elaborate and expensive (Blume et al., 2010; Hamby, 1996).

One very useful method for remediation of these sites is therefore the so-called *in situ* bioremediation, where the ability of autochthone microorganisms to transform these pollutants into innocuous compounds is used (Blume et al., 2010; Caldwell et al., 1998; Hasinger et al., 2011). Already at the beginning of the 20th century a number of microorganisms able to degrade PH have been identified (Boopathy, 2004; Widdel and Rabus, 2001). It was assumed for a long time, that this degradation process can only take place in presence of oxygen and as a consequence performed clean-up methods have been exclusively based on aerobic conditions (Boopathy, 2004; Heider et al., 1999; Heider, 2007; SLUG, 2000). Today it is known that numerous microorganisms can also degrade PH in absence of oxygen and, since at contaminated soils and aquifers often prevail anaerobic conditions, this possibility of remediation gains in importance (Boopathy, 2003; Spormann and Widdel, 2000; Widdel and Rabus, 2001). For biodegradation to proceed in a scale useful for site treatment, sufficient quantities of terminal electron acceptors (TEA), nutrients and trace elements have to be provided to microorganisms (Haeseler et al., 2010; Hasinger et al., 2011; Michels et al., 2001). Furthermore, site environmental conditions, including pH, absence of other inhibitors such as heavy metals, temperature and water content must be adequate (Atlas, 1981; SLUG, 2000).

In *in situ* bioremediation, qualitative and quantitative monitoring of anaerobic degradation process is very important to determine the success of the measures, however made difficult by the poor accessibility of aquifers (Stelzer, 2008). Since the analysis of aquifer cores is expensive and drilling often difficult, the focus lies on aqueous samples obtained from monitoring wells. However, the problem arises that also abiotic processes like volatilization and partitioning processes result in a decline of determined PH-concentrations and therefore observation of decreasing aqueous PH-concentrations is insufficient (Förstner, 2012; Meckenstock et al., 2004; Stelzer et al., 2006; Wisotzky, 2011). For this reason there have been accretive efforts to use stable isotope shifts for monitoring anaerobic degradation processes (Förstner, 2012; Meckenstock et al., 2004;

Stelzer, 2008). Many studies focused on the prediction of the degradation progress from shifts in pollutant sided $^{13}C/^{12}C$ stable isotope ratios (e.g. Jaeckel et al., 2014; Meckenstock et al., 1999; Morasch et al., 2001; Richnow et al., 2003; Stelzer et al., 2006). This is efficient for simple, low-molecular-weight hydrocarbons such as BTEX and to monitor the reductive dehalogenation of chlorinated hydrocarbons, but since structure and chain length of PH are very diverse, this method is problematic (Aelion et al., 2009; Hunkeler et al., 2008; Meckenstock et al., 2004; Morasch et al., 2004). For this reason it may be more useful to predict biodegradation of PH from changes in acceptor sided stable isotope ratios ($^{15}N/^{14}N$ in nitrate or $^{34}S/^{32}S$ in sulfate). To make this possible, correlations between PH-degradation and shifts in acceptor sided stable isotope ratios must be found, which constitutes the objective of this study. For this reason, within this study shifts in stable isotope ratios of possible amendments in *in situ* bioremediation, nitrate and sulfate, and the combination thereof, were monitored during anaerobic biodegradation of a crude oil comprising high- and low-molecular-weight hydrocarbons of different structure in an acclimated environment.

2 Fundamentals

2.1 Petroleum hydrocarbons

PH are the main constituents of crude oil and its refinery products, like motor fuel, fossil burning or lubricants (Reichenauer et al., 2011; SLUG, 2000; Werner, 2009). They represent a very versatile group of reduced organic compounds, which only contain carbon and hydrogen and are widespread in the environment (Ehrenreich et al., 2000; Heider et al., 1999; Spormann and Widdel, 2000; Werner, 2009; Widdel and Rabus, 2001).

Basically, hydrocarbons can be subdivided into aliphatic and aromatic compounds *(see Tab. 1).* According to their bonding features aliphatic hydrocarbons can further be divided into alkanes (containing only single bonds), alkenes (containing double bonds) and alkynes (containing triple bonds). Alkanes are also known as saturated and alkenes as well as alkynes are counted among the unsaturated hydrocarbons. Depending on their structure, saturated and unsaturated hydrocarbons can be subdivided again into straight-chain (n- or normal-), branched (iso-) and cyclic (cyclo-) compounds. In contrast aromatic hydrocarbons consist of one or more benzene rings as structural components and have a delocalized electron system. Among aromatics, common contaminants are monocyclic substances (contain one benzene ring), like benzene, toluene, ethylbenzene and xylene (BTEX), and polycyclic compounds (contain two or more fused benzene rings), such as polycyclic aromatic hydrocarbons (PAH) (Atlas, 1981; Mortimer et al., 2014; Wawra et al., 2003).

Because of the lack of functional groups hydrocarbons are apolar and as a consequence, hydrophobic and lipophilic, and their water solubility decreases with increasing chain length (Fuchs et al., 2014; Haeseler et al., 2010; Hasinger et al., 2011; Wentzel et al., 2007; Widdel and Rabus, 2001). Depending on their chain length they can occur in various states of aggregation. Thus, at normal conditions alkanes with a chain length up to four carbon atoms are gaseous, while longer-chain alkanes occur as liquids or solids (Hasinger et al., 2011; Michels et al., 2001; Wawra et al., 2003). Furthermore, the chemical reactivity of hydrocarbons strongly depends on their structure and chain length. Long-chain alkanes and aromatics exhibit low chemical reactivity, while unsaturated hydrocarbons show higher responsiveness (Atlas, 1981; Callaghan et al., 2006; Callaghan et al., 2009; Ehrenreich et al., 2000; Spormann and Widdel, 2000; Werner, 2009; Widdel and Rabus, 2001).

Naturally, PH are formed in a complex geochemical process over several million years, where decaying organic material is primarily converted through microorganisms and then temperature and pressure are decreasing (Ehrenreich et al., 2000; Widdel and Rabus, 2001). However, considerable amounts of hydrocarbons can also be formed contemporarily in strictly biological processes as degradation products or as compounds with protective functions (Widdel and Rabus, 2001), e.g. methane, which is the most prevalent hydrocarbon among biological degradation products and is produced by methanogenic bacteria or through respirative reduction of CO_2 by archaea (Heider et al., 1999; Widdel and Rabus, 2001). Besides, hydrocarbons occur in the lipophilic cuticles of

many plants and insects, where they are probably formed from fatty acids and serve inter alia as protection against water loss (Heider et al., 1999; Spormann and Widdel, 2000).

Tab. 1: Examples for different aliphatic and aromatic hydrocarbons inclusive their chemical structural formulae (author's representation based on NIST, 2015)

Aliphatics

	Saturated	**Unsaturated**	
	Alkanes	**Alkenes**	**Alkynes**
Straight-chain (n- or normal-)	 Butane	 1-Pentene	 1-Propyne
Branched (iso-)	 2-Methylpentane	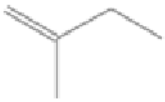 2-Methyl-1-butene	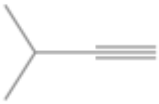 2-Methyl-3-butyne
Cyclic (cyclo-)	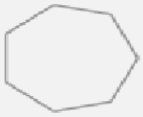 Cycloheptane	 Cyclopentene	 Cyclooctyne

Aromatics

Monocyclic	 Benzene	 p-Xylene	 Ethylbenzene
Polycyclic	 Benzo(a)pyrene		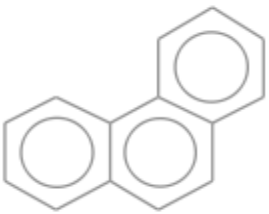 Phenanthrene

Since the industrial revolution humans gather increasing amounts of PH-containing crude oil for production of motor fuel (benzene, diesel, kerosene), fossil burning, lubricant or chemicals (HLUG, 2005). Crude oil and its refinery products are consisting of an extremely complex and heterogeneous mixture of thousands of substances, whereas their composition can vary depending on their origin and production (Atlas, 1981; Bian et al., 2015; Hasinger et al., 2012; Wang and Fingas, 2003). Basically it can be distinguished between paraffinic (contain mainly n- and iso-alkanes), naphthenic (contain mainly cyclo-alkanes) and mixed (contain n-, iso- and cyclo-alkanes in relatively equal proportions) crude oils (Michels et al., 2001). Nevertheless, PH are the main constituents of all crude oils (Bian et al., 2015; Callaghan et al., 2006; Wang and Fingas, 2003). Thereby, the proportion of PH lies between 50 % for heavy and 97 % for light crude oil (Schauer and Sietmann, 2010; Werner, 2009). Among PH, n-, iso- and cyclic-alkanes as well as aromatic hydrocarbons are dominating (~80 % by mass), while unsaturated hydrocarbons, like alkenes and alkynes, and nitrogen-, oxygen and sulfur-rich chemical compounds, like asphaltenes and resins, are minor components (Ehrenreich et al., 2000; HLUG, 2005; Hollinger and Zehnder, 1996; Reichenauer et al., 2011; Scherr et al., 2012; Spormann and Widdel, 2000; Widdel and Rabus, 2001). Furthermore, crude oil and its refinery products contain several metals like iron, nickel and vanadium (Peters et al, 2005; Wang and Fingas, 2003; Werner, 2009).

Today, crude oil and its refinery products are of fundamental importance for our industrialized civilization and thus, PH are the most produced and transported chemicals worldwide (Boley et al., 2012; Caldwell et al., 1998; Widdel and Rabus, 2001). During handling with these substances consistently accidents are taking place, where PH are released into soil, water and air (Hasinger et al., 2012; Scherr et al., 2012). In comparison, natural marine and terrestrial releases from shallow reservoirs, such as in the Caspian Sea, the Gulfs of Mexico and Arabia, or Pitch Lake on Trinidad, are quantitatively of minor importance. Frequently, spills at production sites, storage tanks or filling stations, leakages of pipelines and underground storage tanks as well as accidents during transport arise. Besides, PH-containing products frequently are released into the environment through improper or careless handling and illegal disposal (Boley et al., 2012; Förstner, 2012). Consequently, many soils, aquifers and oceans are contaminated with PH and as a consequence these compounds have become the most frequently occurring pollutions worldwide (Boopathy, 2003; Boopathy, 2004; Hollinger and Zehnder, 1996). For example according to International Oil Tanker Spill Statistics alone in the years between 2000 and 2014 more than 200000 tons of crude oil were spilled into the oceans by oil tankers (ITOPF, 2015), whereat the estimated number of unreported cases is much higher. Furthermore, alone in Austria there are about 75 known PH-contaminated sites, wherefore these substances are second most abundant pollutants in registered sites (Granzin and Valtl, 2015).

When PH-containing crude oil and its refined products spill into subsoil, these pollutants migrate with gravity. While a fraction of the pollutants is retained in the pores of the vadose zone, another fraction may reach the aquifer. The amount of PH remaining in the unsaturated zone depends on sorption- and diffusion-processes and mainly on capillary forces. From the portion of PH reaching the aquifer, only a small proportion is dissolved

due low aqueous solubility. The other part of PH is forming discrete phases, prevailing in dependence on the specific gravity at the capillary fringe (Light Non Aqueous Phase Liquid; LNAPL) or at top of poor permeability layers or the aquitard (Dense Non Aqueous Phase Liquid; DNAPL). Depending on groundwater flow the aqueous dissolved portion is forming a contaminant plume affecting groundwater quality in large distances (Boley et al., 2012; Fuchs et al., 2014; Hasinger et al., 2011; SLUG, 2000; Wentzel et al., 2007). If PH-contamination expends in groundwater reservoirs the water supply of communities or private households can be endangered (Boopathy, 2004).

Once PH are released into nature, they pose a threat to humans and their surrounding environment. Many aromatic hydrocarbons, like PAH or BTEX are classified as toxic substances, because they can affect human health, cause cancer or have mutagenic effects (Boley et al., 2012; Gieg and Suflita, 2002; Hollinger and Zehnder, 1996; Reichenauer et al., 2011; Widdel and Rabus, 2001). In contrast, mid- to high-molecular-weight alkanes are less toxic (Ehrenreich et al., 2000), but at higher concentrations they also can affect biological membranes (Sikkema et al., 1995) or have narcotic effects (Widdel and Rabus, 2001). PH can be toxic as well by physical as by chemical mean. The physical toxicity is based on the fact that lipophilic PH intrude into cells, where they accumulate on the cytoplasm surrounding membranes of phosholipides and disturb their function or even lead to membrane disruption. In contrast, the chemical toxicity arises from the formation of bonds with molecules that thereby are denatured and thus biologically inactivated. From this, carcinogenic and mutagenic effects may result. However, this toxic effect is assumed to be caused mainly by degradation products, because PH have low reactivity (Marquardt et al., 2013). For this reason, contaminated sites were becoming more common in the public debate in recent years, many regulations were created and there are strong efforts to remediate these sites (Callaghan et al., 2006).

2.2 Microbial degradation of PH

In recent decades, several clean-up technologies for remediation of PH-contaminated sites were developed. Basically, these technologies can be divided into *ex situ* and *in situ* methods. While for *ex situ* remediation the contaminated material is removed from the site, *in situ* remediation takes place directly in the subsurface (Blume et al., 2010; Das, 2014; Hasinger et al., 2011; SLUG, 2000). Therefore, a great advantage of *in situ* methods consists in the fact that no major excavations are needed which is cost-saving and allows remediation even below settlements or other infrastructure facilities (Hasinger et al., 2011; Lu et al., 2014; Stroo et al., 2010).

Besides a number of chemical and physical treatment approaches, recently *in situ* bioremediation of PH-contaminated sites using microorganisms became more and more promising (Gödeke et al., 2003; Nagel et al., 2011; Stelzer, 2008). In this method, the ability of microorganisms to break down these pollutants is used (Blume et al., 2010; Caldwell et al., 1998; Hasinger et al., 2011). Thereby, microorganisms incorporate PH and then oxidize them under reduction of TEA, like oxygen, nitrate, sulfate, ferric iron(III), manganese(IV) and CO_2, in a number of metabolic steps for gaining energy (Dissimilation)

and generating biomass (Assimilation). This complex process can take place under aerobic as well as anaerobic conditions and in the best case leads to complete mineralization of PH to CO_2, H_2O and/or CH_4 (Blume et al., 2010; Boopathy, 2003; Hasinger et al., 2011; SLUG, 2000; Spormann and Widdel, 2000; Wisotzky, 2011). In order to achieve remediation success all factors required for microbial growth and proliferation have to be, or made to be, around a certain optimum. The most prevalent factors inhibiting degradation are lack of terminal electron acceptors and lack of macronutrients. Furthermore, process control represents a very important part. Since these approaches rely on naturally occurring processes, they are often referred to as *enhanced natural attenuation* (ENA), while at other, naturally highly active sites merely *monitored natural attenuation* (MNA) may be chosen as an option (Lu et al., 2014; Michels et al., 2001; Nagel et al., 2011; Stelzer, 2008).

2.2.1 PH-degrading microorganisms

Since the beginning of earth's history large accumulations of PH are ubiquitous in biosphere. Long before their industrial use these compounds were formed by natural geochemical and biological processes. This fact explains why many microorganisms were able to adapt on this type of pollutants and thus, over time metabolic pathways for energy and carbon recovery by degradation of PH evolved (Blume et al., 2010; Spormann and Widdel, 2000; Wentzel et al., 2007; Widdel and Rabus, 2001). Today, PH-degrading microorganisms are widely distributed in soils, aquifers and marine environments (Atlas, 1981). Besides naturally formed PH, these microorganisms are also able to biodegrade a wide range of industrial produced, refined or converted PH and therefore can be used for bioremediation of contaminated sites (Heider et al., 1999).

According to the different structure of ribosomal ribonucleic acid (rRNA) microorganisms can be divided into Bacteria (Eubacteria), Archaea and Eukaryota, including Fungi (Blume et al., 2010; Cypionka, 2010; Fuchs et al., 2014). While Bacteria and Archaea are unicellular organisms without a cell nucleus, Eukaryota consist of both cell nucleus and membrane. Moreover, Eukaryota usually are much larger than Bacteria and Archaea (Blume et al., 2010). According to their occurrence microorganisms can be divided into autochthonous species, which are naturally present at a given site, and allochthone species, that were introduced by humans in their habitat (Michels et al., 2001). With respect to their preferred living conditions, they can be further divided into aerobic, obligatory anaerobic and facultative anaerobic microorganisms. While obligatory anaerobic microorganisms are inhibited or even devitalized under influx of molecular oxygen, facultative anaerobic organisms are able to live under aerobic as well as anaerobic conditions (Blume et al., 2010; Michels et al., 2001). With regard to their nutrition, microorganisms can be classified into heterotrophic species, which gain carbon from organic material and so in regard to PH-degradation are most important, and autotrophic ones, that use the carbon from CO_2 (Michels et al., 2001; SLUG, 2000).

Already in 1946, the action of microorganisms on PH was reviewed by Zobell (1946), collecting early evidence that some microorganisms have the ability to reduce PH and that these organisms are very widespread in the environment. Today, numerous aerobic and

anaerobic microorganisms using PH as a carbon and energy source and thereby degrading these compounds have been isolated and characterized, of which the majority counts to Bacteria (Boopathy, 2003; Wentzel et al., 2007; Widdel et al., 2010). Tab. 2 shows a range of Bacteria, which are demonstrably capable of degrading aliphatic and aromatic PH under different electron acceptor conditions. Nevertheless, there exist still many other microorganisms able to biodegrade PH, which could not be identified to date due to their poor culturability (Widdel and Rabus, 2001).

Among Bacteria especially those of the phylum Proteobacteria are well known for biodegradation of PH (Werner, 2009; Widdel and Rabus, 2001). Thus, many nitrate-reducing bacteria belong to the class of β- and γ-Proteobacteria and several sulfate-reducing ones to the class of δ-Proteobacteria (Blume et al., 2010; Wentzel et al., 2007). Moreover, PH-degrading Bacteria like Arthrobacter and Bacillus belonging to other phyla have been identified (Leahy and Colwell, 1990). In addition to the Bacteria also PH-degrading Archaea and Fungi were found (Boetius et al., 2000; Hinrichs et al., 1999; Leahy and Colwell, 1990; Van Beilen et al., 2003). However, these organisms represent only a small portion compared to Bacteria (Leahy and Colwell, 1990; Widdel and Rabus, 2001). Thus, in a comparative study of PH-degradation by Bacteria and Fungi performed by Song et al. (1986) only 13 % of n-hexadecane degradation was performed by Fungi, while the other much larger part was degraded by Bacteria.

Tab. 2: Overview of bacterial taxa capable of biodegradation of PH under different electron accepting conditions (author's representation)

Phylum	Species, strain	Carbon source	Type of metabolism	Reference(s)
β-Proteobacteria	*Alcaligenes odorans*	$<C_{33}$	AE	*Lal and Khanna, 1996*
	Strain EbN1	Ethylbenzene, Toluene	NR	*Rabus and Widdel, 1995*
	Strain HxN1	C_6-C_8	NR	*Ehrenreich et al., 2000*
	Strain OcN1	C_8-C_{12}	NR	*Ehrenreich et al., 2000*
	Thauera aromatica	Toluene	NR	*Evans et al., 1991*
δ-Proteobacteria	*Desulfatibacillum aliphaticivorans*	C_{13}-C_{18}	SR	*Cravo-Laureau et al., 2004*
	Desulfobacula toluolica	Toluene	SR	*Rabus et al., 1993*
	Geobacter metallireducens	Toluene	FR	*Lovley et al., 1989*
	Strain AK01	C_{13}-C_{18}	SR	*So and Young, 1999*
	Strain BuS5	C_3-C_4	SR	*Kniemeyer et al., 2007*
	Strain EbS7	Ethylbenzene	SR	*Widdel and Rabus, 2001*
	Strain Hxd3	C_{12}-C_{20}	SR	*Aeckersberg et al., 1991*
	Strain TD3	C_6-C_{15}	SR	*Rueter et al., 1994*

γ-Proteobacteria	*Alcanivorax borkumensis*	C_8-C_{32}	AE	*Schneiker et al., 2006*
	Halomonas sp.	Toluene	NR	*Widdel and Rabus, 2001*
	Pseudomonas aeruginosa	C_{12}-C_{34}	AE	*Yuste et al., 2000*
	Pseudomonas balearica	C_{15}-C_{18}	NR	*Grossi et al., 2008*
	Pseudomonas sp.	Naphthalene	NR	*Rockne et al., 2000*
	Strain HdN1	C_{14}-C_{20}	NR	*Ehrenreich et al., 2000*
	Vibrio sp.	Naphthalene	NR	*Rockne et al., 2000*
Actinobacteria	*Arthrobacter nicotianae*	C_{10}-C_{40}	AE	*Radwan et al., 1996*
	Rhodococcus erythropolis	C_6-C_{36}	AE	*Van Beilen et al., 2002*
Firmicutes	*Bacillus thermoleovorans*	C_9-C_{30}	AE	*Kato et al., 2001*
	Geobacillus thermodenitrificans	C_{15}-C_{36}	AE	*Wang et al., 2006*

AE…aerobic ; NR…nitrate-reduction ; SR…sulfate-reduction ; FR…Fe(III)-reduction

2.2.2 Requirements for biodegradation and inhibitory effects

For ensuring good biodegradation rates generating optimal surrounding conditions as well as reducing inhibiting effects is very important, wherefore knowledge of requirements of and inhibitory effects on microorganisms is crucial (Scherr et al., 2012; SLUG, 2000).

First, for reaching high biological PH-degradation rates, site- and pollutant-adapted microorganisms with the ability to crack PH are necessary (Förstner, 2012; Gödeke et al., 2003; Leahy and Colwell, 1990; Michels et al., 2001; Spormann and Widdel, 2000). For biodegradation microorganisms need degradable pollutants, which serve them as energy and carbon source and don't have toxic effects on their metabolism (Gödeke et al., 2003; SLUG, 2000; Wisotzky, 2011). Whether or not a pollutant has these properties, largely depends on the structural properties of the compound (Hasinger et al., 2012; Michels et al., 2001). So for example synthetic organic substances, called Xenobiotics, can be degraded only very slightly or over long periods (Wisotzky, 2011). Among PH n-alkanes can be biodegraded easiest, followed by iso-alkanes, alkenes and alkynes as well as low-molecular-weight aromatics. In contrast cyclo-alkanes and high-molecular-weight aromatics show very low degradability (Leahy and Colwell, 1990; Schinner and Sonnleitner, 1997; Wang and Fingas, 2003; Wisotzky, 2011). Nevertheless, these order is not universal, as for example Cooney et al. (1985) found higher degradation rates for naphthalene then for n-hexadecane in the sediment of a freshwater lake.

Additionally, pollutants have to be bioavailable (Spormann and Widdel, 2000; Wisotzky, 2011). As microorganisms live in the water phase, the availability of the pollutants for biodegradation highly depends on their water solubility (Förstner, 2012; Haeseler et al., 2010). Since PH are widely insoluble in water (Haeseler et al., 2010; Hasinger et al., 2011; Wentzel et al., 2007; Widdel and Rabus, 2001), microorganisms have to create special mechanisms in order to incorporate them into their cells (Michels et al., 2001). For this purpose PH-degrading microorganisms secrete special biosurfactants of diverse chemical nature, which emulsify hydrocarbons and thus make them accessible (Haeseler et al., 2010; Michels et al., 2001; Rosenberg and Ron, 1999; Singer and Finnerty, 1984). Furthermore, many microorganisms have lipophilic membranes that allow them to attach directly on hydrocarbons and so to create an oil-water interface (Haeseler et al., 2010; Michels et al., 2001). Besides, the bioavailability of pollutants is lowered if compounds are sequestrated in soil pores or lipophilic phases (Hasinger et al., 2011; SLUG, 2000).

Moreover, it is very important that the pollutants occur in a suitable concentration for biodegradation. So, if the concentration of PH is too low, microorganisms are not able to obtain sufficient energy for maintaining their metabolism (Michels et al., 2001). Moreover, in this case production of enzymes necessary for degradation is not induced (Michels et al., 2001; SLUG, 2000). In contrast, very high concentrations of PH contribute to the formation of thick oil slicks in water that are difficult to attack for microorganisms (Leahy and Colwell, 1990). In addition, high concentrations have toxic effects on organisms (Michels et al., 2001; SLUG, 2000).

High concentrations of toxic accompanying substances like heavy metals or salts, can reduce or even inhibit microbial activity (Atlas, 1981; Hasinger et al., 2011; Leahy and Colwell, 1990; SLUG, 2000). In addition, inhibitory effects of a number of organic compounds, like chlorinated hydrocarbons, were determined. At high concentrations these substances can change nature of cell membranes and thus disrupt their transport function (Blume et al., 2010).

Available TEA play a key role in biodegradation of PH because during degradation generated reducing equivalents must be transferred to an electron acceptor for energy conservation. If the available amount of TEA is not enough, the degradation process comes to a complete standstill. So in practice TEA are the most predominant limiting factor of PH-degradation (Haeseler et al., 2010; Heider et al., 1999; SLUG, 2000). Besides, microorganisms need nutrients for holding up their metabolism. The amount of required nutrients is usually given in relation to the quantity of carbon, which has to be degraded. So for aerobic degradation a stoichiometric relation for carbon:nitrogen:phosphorous:potassium (C:N:P:K) of around 100:10:1:1 and for anaerobic degradation of around 150:5:1:1 is required (Atlas, 1981; Gödeke et al., 2003; Hasinger et al., 2011; Michels et al., 2001; Wisotzky, 2011). Furthermore, trace elements like Mg, Ca, Fe, Na, Cl, Zn, Mn and so on are essential for growth and activity of microorganisms. As these elements generally occur in sufficient quantity in the subsurface, in most cases no addition is necessary (Hasinger et al., 2011; Michels et al., 2001).

Additionally, the rate of biological PH-degradation highly depends on at contaminated site existing environment conditions (Atlas, 1981). So biodegradation rates are influenced by

prevailing temperatures. Many PH-degrading microorganisms with diverse temperature optima have already been isolated. While most of them show maximal degradation rates at temperatures around 30 to 40 °C, lower and especially higher temperatures lead to slower rates (Atlas, 1981; Blume et al., 2010; Hasinger et al., 2011; Leahy and Colwell, 1990; Michels et al., 2001). Anyway, at for soils and aquifers common temperatures of 10 to 14 °C adequate degradation rates can be expected (Hasinger et al., 2011). Furthermore, most PH-degrading microorganisms prefer pH-values between 6 and 8, whereat some organisms can also adapt on extreme conditions (Hasinger et al., 2011; Leahy and Colwell, 1990; Michels et al., 2001; SLUG, 2000). Nevertheless, too low or high pH-values decelerate PH-degradation rates, wherefore in these cases pH-values should be balanced by adding for example chalk (Hasinger et al., 2011; Leahy and Colwell, 1990). Besides, prevailing redox conditions influence biodegradation processes (Förstner, 2012; Gödeke et al., 2003; Michels et al., 2001). So nitrate-reducing microorganisms need a higher redox potential than sulfate-reducing ones (Michels et al., 2001; Wiedemeier et al., 1999). In general, microorganisms need widely stable environmental conditions and as a consequence high fluctuations can interrupt the degradation process (SLUG, 2000).

If biodegradation takes place in the unsaturated zone, the type, fabric and permeability of soil should be considered (Michels et al., 2001). So at hydraulic conductivity beyond 10^{-5} $m*s^{-1}$ microbial degradation of PH is not possible (Hasinger et al., 2011). Additionally, in this case microorganisms need enough available water for transport of educts and products as well as for metabolism (Förstner, 2012; Leahy and Colwell, 1990). Generally, high water contents beyond saturation foster microbial activity (Leahy and Colwell, 1990; Michels et al., 2001).

When at a contaminated site requirements for biodegradation are not fulfilled or occurring inhibitory effects are too big, other methods for remediation like thermic or chemical techniques have to be envisaged (Blume et al., 2010).

2.2.3 Aerobic biodegradation of PH

The ability of many microorganisms to mineralize PH aerobically by using oxygen as TEA has been known for a long time (Haeseler et al., 2010; Spormann and Widdel, 2000; Werner, 2009). Already at the beginning of the 20th century many Bacteria and Fungi capable of metabolizing aliphatic and aromatic hydrocarbons under aerobic conditions have been isolated from contaminated sites (Boopathy, 2003; Boopathy, 2004; Widdel and Rabus, 2001). In the subsequent decades it was assumed that the largely chemical inert PH can only be biodegraded in the presence of oxygen as a reactive and strong oxidant (Heider, 2008; Spormann and Widdel, 2000; Widdel and Rabus, 2001), wherefore performed studies and clean-up methods have been exclusively based on aerobic mechanisms (Boopathy, 2004; SLUG, 2000). Today it is known that PH can also be degraded under anaerobic conditions (Das, 2014; Fuchs et al., 2014; Hasinger et al., 2012).

Nevertheless, PH are preferentially metabolized and higher degradation rates are observed in the presence of oxygen because in this case the Gibbs free energy (ΔG^0_r)

obtained from microorganisms per unit metabolized carbon is largest (Blume et al., 2010; Michels et al., 2001; SLUG, 2000; Thauer et al., 1977; Widdel and Rabus, 2001). Generally, Gibbs free energy (ΔG^0_r) declares maximal energy change for a chemical reaction at a constant temperature and pressure and is defined as follows (Wiedemeier et al., 1999):

$$\Delta G_r^0 = \sum \Delta G_{products}^0 - \Delta G_{reactants}^0$$

If ΔG^0_r-values are negative this indicates an exothermic reaction, while positive ΔG^0_r-values exhibit endothermic reactions (Wiedemeier et al., 1999). Therefore, microorganisms prefer those TEA, where ΔG^0_r-values are most negative and so energy yield is maximum (Dendrou et al., 2000; Thauer et al., 1977).

Basically, the degradability of hydrocarbons under aerobic conditions is depending on their molecular weight and structures, which results from lower water solubility of long-chain hydrocarbons and from the fact that more complex structures hinder enzymatic attack (Hasinger et al., 2011; Setti et al., 1993; SLUG, 2000). So in the presence of oxygen preferential biodegradation of (i) short-chain hydrocarbons over long-chain ones, (ii) n-alkanes over iso- and cyclo-alkanes, (iii) saturated hydrocarbons over unsaturated as well as (iv) aliphatics over aromatics prevails (Haeseler et al., 2010; Michels et al., 2001; Scherr et al., 2007; SLUG, 2000; Wang and Fingas, 2003).

Generally, the stoichiometric mineralization equation for aerobic degradation of hydrocarbons can be written as follows (Haeseler et al., 2010; Wisotzky, 2011):

$$C_xH_y + \left(x + \frac{1}{4}y\right)O_2 \rightarrow xCO_2 + \left(\frac{1}{2}y\right)H_2O$$

So for example for mineralization of n-C_{25} (pentacosane) the chemical equation is:

$$C_{25}H_{52} + 38O_2 \rightarrow 25CO_2 + 26H_2O$$

From this equation results a requirement of 3.44 g O_2 as TEA for biodegradation of 1 g $C_{25}H_{52}$.

The mechanism of aerobic biodegradation follows the same pattern for all groups of PH and is well described in many studies (Callaghan et al., 2006; Prince et al., 2003; SLUG, 2000; Watson et al., 2002). First, relatively inert hydrocarbons are activated by oxidation which leads to formation of more polar and therefore water-soluble substances like alcohols, aldehydes, ketones and fatty acids. Subsequently, fatty acids are further mineralized by β-Oxidation to CO_2 and H_2O (SLUG, 2000).

The activation of n-alkanes can take place in three different ways, which are illustrated in Fig. 1. Usually it starts with by monooxygenases-enzyme catabolized oxidation at the terminal carbon atom (C1). This reaction results in the formation of primary alcohols, which are further oxidized to aldehydes and fatty acids *(see way 1 in Fig. 1)*. In rare cases terminal oxidation can also be catalyzed by dioxygenases-enzyme, which leads to formation of alkane-peroxids and then by elimination of water to fatty acids *(see way 2 in Fig. 1)*. Sometimes, oxidation takes place at the subterminal carbon atom (C2), which results in the formation of secondary alcohols that are further oxidized to ketones and acetylesters. Accordingly, acetylesters are cleaved into acetic acid and primary alcohols that are onward oxidized to fatty acids *(see way 3 in Fig. 1)* (Fuchs et al., 2014; Michels et al., 2001; Rehm and Reiff, 1981; Wentzel et al., 2007; Werner, 2009). For further mineralization to CO_2 and H_2O fatty acids are activated by coenzymeA-ligase and then oxidized in repeated reaction-cycles by elimination of acetyl-units. Since in this process β-C-atoms of fatty acids are oxidized, this mechanism is called β-Oxidation (Fuchs et al., 2014; Michels et al., 2001; SLUG, 2000; Wentzel et al., 2007; Werner, 2009). Iso- and cyclo-alkanes are metabolized in almost the same manner. The only difference is that degradation of iso-alkanes begins with separation from branching and depletion of cyclo-alkanes with opening of ring structures (SLUG, 2000).

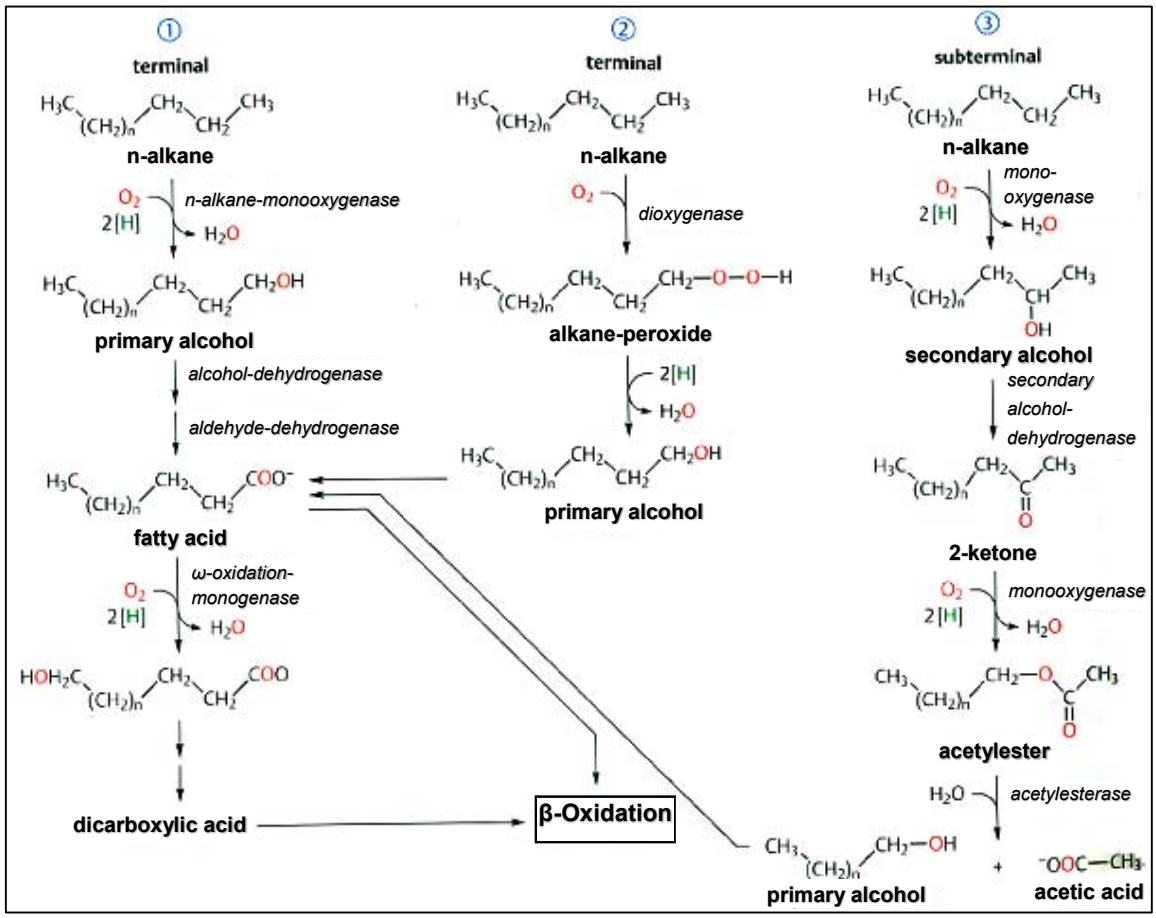

Fig. 1: Presentation of the three different metabolic pathways for aerobic biodegradation of n-alkanes (modified from Fuchs et al., 2014)

At aromatics activation is performed by implementation of hydroxyl-groups (OH-groups) at 1,2-position or 1,4-position catalyzed by either monooxygenases or dioxygenases. Afterwards aromatic C-C-bonds can be cleaved by using oxygen, which results in formation of non-cyclic compounds. This cleavage can either take place between the OH-groups carrying carbon atoms (ortho cleavage) or between an OH-group carrying carbon atom and an adjacent carbon atom (meta cleavage). Afterwards cleavage products are mineralized following same metabolic pathways as at degradation of n-alkanes (Fuchs et al., 2014; Heider et al., 1999; Michels et al., 2001; SLUG, 2000). Fig. 2 schematically shows aromatic degradation process using the example of benzene.

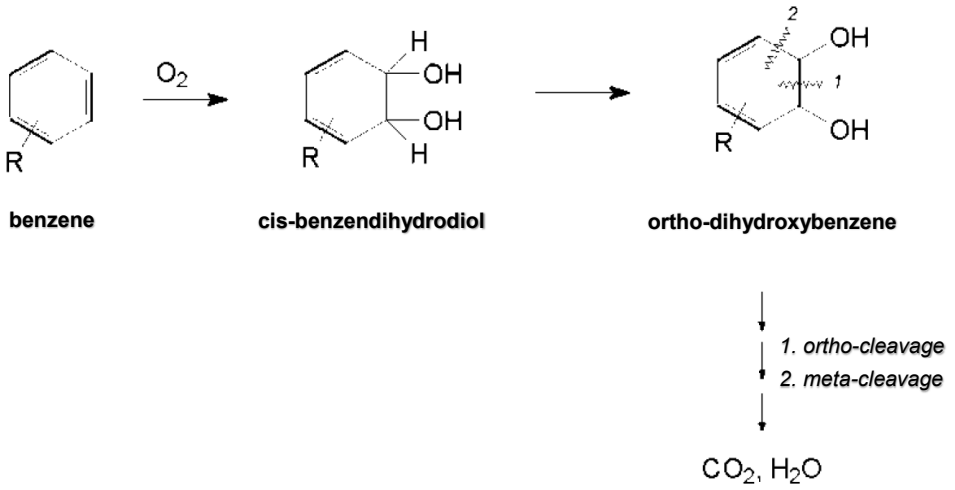

Fig. 2: Schematic representation of aerobic biodegradation of aromatics on the example of benzene (modified from SLUG, 2000)

2.2.4 Anaerobic biodegradation of PH

In comparison to aerobic biodegradation of PH, metabolic pathways for mineralizing these compounds at anaerobic conditions have been unknown until the early 1980s (Atlas, 1981; Grossi et al., 2008; Werner, 2009). In subsequent years many PH-degrading microorganisms using alternative TEA like nitrate, sulfate and ferric iron instead of oxygen have been identified and isolated (Grossi et al., 2008; Spormann and Widdel, 2000; Wentzel et al., 2007; Werner, 2009; Widdel and Rabus, 2001). Hence, numerous studies about anaerobic biodegradation pathways were performed, which led to a better understanding of the underlying processes (e.g. Grossi et al., 2008; Heider et al., 1999; Heider, 2007; So et al., 2003; Spormann and Widdel, 2000; Widdel and Rabus, 2001). Today, there is emerging interest on anaerobic biodegradation of PH as a promising alternative to aerobic treatment processes (Boopathy, 2003; Boopathy, 2004; Hasinger et al., 2012; Xiong et al., 2015). As oxygen is consumed through occurring biological respiration processes, at contaminated soils or aquifers often prevail anaerobic conditions (Boopathy, 2003; Gödeke et al., 2003; Widdel and Rabus, 2001). So for aerobic remediation current supply of oxygen is necessary, which can be very costly (Boopathy, 2003; Boopathy, 2004). Besides, aerobic biodegradation comes along with high biomass production, which can result in blockage of soil pores called Bioclogging. Subsequently,

this can lead to a complete stop of the degradation process caused by insufficient oxygen supply (Hasinger et al., 2011; Hollinger and Zehnder, 1996). Furthermore, aerobic remediation of aquifers is very ineffective because the water solubility of oxygen at normal conditions is only around 8.6 mg/L (Hasinger et al., 2011; Widdel and Rabus, 2001). In contrast alternative TEA like nitrate or sulfate are more soluble as well as consumed more slowly during oxidation of pollutants and therefore can be transported over long distances (Widdel and Rabus, 2001). Despite these advantages over aerobic methods, for anaerobic biodegradation longer remediation periods have to be taken into account, since in the absence of oxygen degradation processes are slower due to less Gibbs free energy (ΔG^0_r) obtained from microorganisms (Blume et al., 2010; Cypionka, 2010; Heider et al., 1999; SLUG, 2000; Thauer et al., 1977; Wentzel et al., 2007). So for example Hasinger et al. (2012) obtained degradation rates of 470 mg TPH per kg soil dry weight and day at aerobic conditions, while under nitrate-reducing and sulfate-reducing conditions rates were only at 28 mg TPH/kg*d and 18 mg TPH/kg*d, respectively. Furthermore, preferential degradation of less complex and lower-weight hydrocarbons as known for aerobic conditions do not necessarily occur in absence of oxygen. So Hasinger et al. (2012) found inverse degradation pattern under sulfate-reducing conditions, where long-chain and branched hydrocarbons were preferentially degraded over short-chain and unbranched ones.

2.2.4.1 Stoichiometry and energy gain under different electron accepting conditions

Anaerobic biodegradation of PH was demonstrated under reduction of alternative TEA like nitrate (Boopathy, 2003; Boopathy, 2004; Callaghan et al., 2009; Ehrenreich et al., 2000; So and Young, 2001), sulfate (Boopathy, 2003; Boopathy, 2004; Caldwell et al., 1998; So and Young, 2001; So et al., 2003), ferric iron (So and Young, 2001), manganese (Langenhoff et al., 1997a; Langenhoff et al., 1997b; Myers and Nealson, 1988) and CO_2 under methanogenic conditions (Boopathy, 2003; Jones et al., 2008; So and Young, 2001). Therefore, by addition of these alternative TEA biological degradation processes at anaerobic sites can be initiated and enhanced. Generally, alternative TEA are introduced into the subsurface in salt form like KNO_3 for nitrate or Na_2SO_4 for sulfate. The type of the supplied alternative TEA should be selected in relation to at contaminated site present pollutants as well as to prevailing underground conditions (Hasinger et al., 2011). So nitrate is especially suited for short-chain hydrocarbons, while under sulfate-reducing conditions long-chain and complex PH are preferentially degraded (Hasinger et al., 2011; Hasinger et al., 2012). Furthermore, alternative TEA must not be supplemented in high concentrations because this can lead to adverse effects on groundwater quality. In order to enable adaptation of microorganisms at the beginning of remediation lesser amounts of alternative TEA should be added, before the quantity can be increased successively (Hasinger et al., 2011).

According to decreasing Gibbs free energy (ΔG^0_r) obtained from microorganisms per unit metabolized carbon unit *(see Tab. 3)* nitrate is used preferential followed by manganese(IV), ferric iron(III), sulfate and CO_2 for methanogenesis (Gödeke et al., 2003; Haeseler et al., 2010; Werner, 2009; Wisotzky, 2011). So if an alternative TEA completely

has been consumed, microorganisms use the energetically next best one (Ulrich and Edwards, 2003). This sequence is accompanied by a decrease in the prevailing redox-conditions *(see Tab. 3)* (Wiedemeier et al., 1999).

Tab. 3: Common redox-potentials and yielded Gibbs free energy (ΔG^0_r) per mol mineralized PH on the example of benzene (C_6H_6) at different anaerobic electron accepting conditions (author's representation based on Dendrou et al., 2000 and Wiedemeier et al., 1999)

Electron accepting conditions	**Redox-potential** *[mV]*	**ΔG^0_r** *[kJ*mol^{-1} C_6H_6]*
Nitrate-reduction	+740	-3245
Mn(IV)-reduction	+520	-3202
Fe(III)-reduction	-50	-2343
Sulfate-reduction	-220	-514.3
Methanogenesis / CO_2-reduction	-240	-135.6

Most identified microorganisms capable for anaerobic degradation of PH use nitrate, sulfate or CO_2 as alternative TEA (Widdel and Rabus, 2001). Thereby, alternative TEA are assimilated by means of specific transport systems and then are reduced in several steps (Cypionka, 2010; Fuchs et al., 2014). So for example nitrate (NO_3^-) is reduced over nitrite (NO_2^-), nitric oxide (NO) and nitrous oxide (N_2O) to elemental nitrogen (N_2) or from nitrite directly to ammonium (NH_4^+) (Fuchs et al., 2014; Weiner, 2012). In the following relevant stoichiometric mineralization equations in general form and for degradation of n-C_{25} (pentacosane) are shown (Gödeke et al., 2003; Haeseler et al., 2010; So and Young, 2001):

<u>Nitrate-reduction:</u>

$$C_xH_y + \left(\frac{4}{5}x + \frac{1}{5}y\right)NO_3^- + \left(\frac{4}{5}x + \frac{1}{5}y\right)H^+ \rightarrow xCO_2 + \left(\frac{2}{5}x + \frac{1}{10}y\right)N_2 + \left(\frac{2}{5}x + \frac{3}{5}y\right)H_2O$$

$$C_{25}H_{52} + 30.4NO_3^- + 30.4H^+ \rightarrow 25CO_2 + 15.2N_2 + 41.2H_2O$$

From this equation results a stoichiometric requirement of 5.34 g NO_3^- as TEA for biodegradation of 1 g $C_{25}H_{52}$.

Sulfate-reduction:

$$C_xH_y + \left(\frac{1}{2}x + \frac{1}{8}y\right)SO_4^{2-} + \left(x + \frac{1}{4}y\right)H^+ \rightarrow xCO_2 + \left(\frac{2}{4}x + \frac{1}{8}y\right)H_2S + \left(\frac{1}{2}y\right)H_2O$$

$$C_{25}H_{52} + 19SO_4^{2-} + 38H^+ \rightarrow 25CO_2 + 19H_2S + 26H_2O$$

From this equation results a stoichiometric requirement of 5.17 g SO_4^{2-} as TEA for biodegradation of 1 g $C_{25}H_{52}$.

Methanogenesis / CO_2-reduction:

$$C_xH_y + \left(x - \frac{1}{4}y\right)H_2O \rightarrow \left(\frac{1}{2}x - \frac{1}{8}y\right)CO_2 + \left(\frac{1}{2}x + \frac{1}{8}y\right)CH_4$$

$$C_{25}H_{52} + 12H_2O \rightarrow 6CO_2 + 19CH_4$$

During degradation of PH under methanogenic conditions on the one hand CO_2 serves as alternative TEA and thus is reduced to CH_4 but on the other hand additional CO_2 is formed by oxidation of hydrocarbons (Weiner, 2012).

Microbial anaerobic degradation under reduction of ferric iron and manganese was mainly demonstrated for aromatic hydrocarbons (Widdel and Rabus, 2001). Thereby, solid bound ferric iron(III) or manganese(IV) is reduced to well water soluble ferric iron(II) and manganese(II), respectively (Blume et al., 2010; Cypionka, 2010; Wisotzky, 2011). In the following stoichiometric mineralization equations in general form and for degradation of C_6H_6 (benzene) are shown (Le Corfec, 2011; So and Young, 2001):

Fe(III)-reduction:

$$C_xH_y + (4x + y)Fe^{3+} + 2xH_2O \rightarrow xCO_2 + (4x + y)Fe^{2+} + (4x + y)H^+$$

$$C_6H_6 + 30Fe^{3+} + 12H_2O \rightarrow 6CO_2 + 30Fe^{2+} + 30H^+$$

From this equation results a stoichiometric requirement of 21.45 g Fe^{3+} as TEA for biodegradation of 1 g C_6H_6.

Mn(IV)-reduction:

$$C_xH_y + (2x + 0.5y)Mn^{4+} + 2xH_2O \rightarrow xCO_2 + (2x + 0.5y)Mn^{2+} + (4x + y)H^+$$

$$C_6H_6 + 15Mn^{4+} + 12H_2O \rightarrow 6CO_2 + 15Mn^{2+} + 30H^+$$

From this equation results a stoichiometric requirement of 10.55 g Mn^{4+} as TEA for biodegradation of 1 g C_6H_6.

2.2.4.2 Degradation pathways and formed metabolites

While biodegradation mechanism of PH under aerobic conditions always follows the same pattern and is well known, hydrocarbon activation in absence of oxygen follows fundamentally different and diverse pathways (Andrade et al., 2012; Grossi et al., 2008; Spormann and Widdel, 2000; Widdel and Rabus, 2001). Today, some of these degradation pathways are well studied, whereas others are still incompletely described (Callaghan et al., 2006; SLUG, 2000; Wentzel et al., 2007). So for example biological mechanisms for breaking down hydrocarbons with more than 20 carbon atoms under anaerobic conditions are not yet fully understood (Grossi et al., 2008). Typical metabolites formed during anaerobic degradation pathways are succinates (salts or esters of succinic acid), alcohols, aldehydes, ketones and fatty acids (Bian et al., 2015; Gieg and Suflita, 2002; Grossi et al., 2008; SLUG, 2000). In comparison to their parent compounds these intermediates show higher reactivity, polarity and therefore better water solubility (Blume et al., 2010; Cravo-Laureau et al., 2005).

n-alkanes:

Today, for biological degradation of n-alkanes under anaerobic conditions two pathways are well described: (i) alkane addition to fumarate and (ii) carboxylation of the alkane (Callaghan et al., 2006; Grossi et al., 2008). While the first mechanism has been observed both under nitrate- (e.g. strain HxN1) and sulfate-reducing (e.g. strain AK-01) conditions (Callaghan et al., 2006; Davidova et al., 2005; Kniemeyer et al., 2007; Kropp et al., 2000; Rabus et al., 2001; Wilkes et al., 2002), the second one has only be shown for sulfate reducers like strain Hxd3 (Callaghan et al., 2006; So et al., 2003).

Mechanism (i) *(see Fig. 3)* starts with addition of the n-alkane to fumarate catalyzed by the enzyme alkylsuccinate synthase (Callaghan et al., 2008; Callaghan et al., 2010). Fumarate is the salt of fumaric acid, contains one double bond and occurs in many microorganisms capable for anaerobic degradation of PH (Fuchs et al., 2014). Thereby, the n-alkane is added to the double bond of fumarate at the subterminal carbon atom (C2) or in rare cases at the terminal carbon atom (C1), which results in methyl branched alkyl-succinates as first metabolites. In the next step 4-methyl-branched fatty acids are formed by carbon skeleton rearrangement followed by elimination of one CO_2-molecule (carboxylation). In succession

4-methyl-branched fatty acids are degraded by β-oxidation over 2-methyl-branched and linear fatty acids to CO_2 as final product (Callaghan et al., 2006; Cravo-Laureau et al., 2005; Davidova et al., 2005; Kniemeyer et al., 2007; Kropp et al., 2000; Rabus et al., 2001; Wilkes et al., 2002). During this process microorganisms are able to regenerate fumarate (Wilkes et al., 2003). A special feature of this degradation mechanism is that the alkyl-succinates and fatty acids formed as metabolites have the same chain length than the original n-alkane. So C-even alkyl-succinates and fatty acids are formed when grown on C-even alkanes and vice versa (Aeckersberg et al., 1998; Cravo-Laureau et al., 2005; So and Young, 1999).

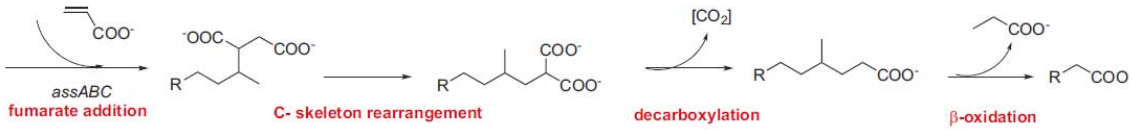

Fig. 3: Schematic representation of anaerobic n-alkane biodegradation by fumarate-addition (Bian et al., 2015)

In contrast mechanism (ii) *(see Fig. 4)* starts with addition of an exogenous carbon atom at the C3-position of the n-alkane by carboxylation. The reason for carboxylation at the subterminal C3-atom lies in the fact, that at this position C-H-bonds are weaker than those on the terminal carbon atom and thus can be more easily broken. As a result of carboxylation 2-ethyl-fatty acids should be formed but these metabolites have not been detected to date. Consequently, the two terminal carbon atoms are removed which leads to formation of fatty acids, that are one carbon atom shorter than the original n-alkane. So in contrast to fumarate-addition C-even fatty acids are formed from C-odd n-alkanes and vice versa. In further steps fatty acids are either subsequently mineralized to CO_2 by β-oxidation or transformed to other fatty acids by mechanisms like chain-elongation or C10-methylation (Callaghan et al., 2006; So et al., 2003).

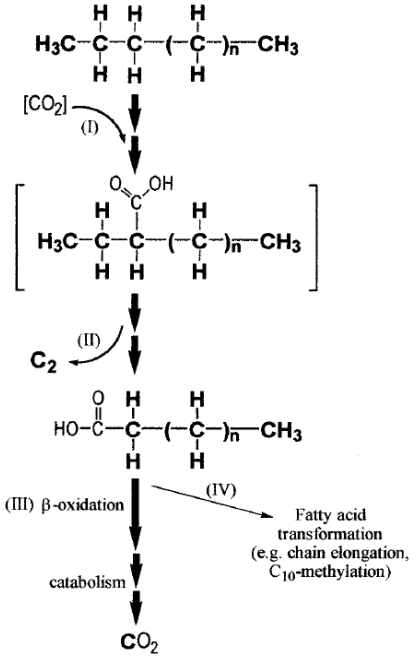

Fig. 4: Proposed pathway for anaerobic biodegradation of n-alkanes by carboxylation (So et al., 2003)

In addition to these two well described pathways, a third anaerobic mechanism for activation of n-alkanes has recently been found. Thereby, hydrocarbons are hydroxylated which leads to formation of alcohols as first intermediate products (Brückner, 2004; Fuchs et al., 2014). This process was found to be catalyzed by special molybdenum-containing enzymes, called molybdenum-hydroxylases, which have the ability for deriving therefore necessary oxygen atoms from cleavage of water rather than from O_2 *(see Chapter 2.3.2)*. However, metabolic pathways for further mineralization of alcohols are very diverse and not fully explored (Dobbek, 2000; Hille, 1996; Hille, 2004).

Moreover, recently Grossi et al. (2008) isolated the denitrifying bacterium *Pseudomonas balearica*, which is able to degrade C_{15}-C_{18} n-alkanes. Degradation experiments with this strain have shown the formation of C-even fatty acids grown on C-even n-alkanes and vice versa as it is usual for degradation mechanism of fumarate-addition. But typical metabolites of this mechanism like alkyl-succinates and 4- or 2-methyl-branched fatty acids could not be detected which lead to the conclusion that there must be a fourth metabolic pathway for anaerobic biodegradation of n-alkanes. However, to date no fourth pathway could be identified.

n-alkenes:

Anaerobic microbial degradation of n-alkenes has been reported under nitrate-reducing (Gilewicz et al., 1991), sulfate-reducing (Cravo-Laureau et al., 2004) as well as methanogenic (Schink, 1985) conditions but underlying degradation mechanisms are still incompletely understood (SLUG, 2000). So anaerobic degradation pathways of polyenes and monounsaturated alkenes with an internal double bond have not been studied (Grossi et al., 2008). Only for monounsaturated alkenes with the double bond between C1 and C2 (1-alkenes) two degradation pathways were described by Grossi et al. (2007) and Grossi et al. (2011). In these studies it was shown that 1-alkenes can be activated either by oxidation of the double bond at C1 or by addition of organic carbon at C2, C3 and at the subterminal carbon atom of the saturated end. The first way leads to formation of primary alcohols and linear fatty acids, whereas the second one results in formation of methyl- and ethyl-branched fatty acids. Subsequently, fatty acids are mineralized to CO_2 by β-oxidation or transformed into other fatty acids by chain-elongation or C10-methylation.

Aromatics:

Activation of aromatic hydrocarbons is due to the high stability of their ring structures always related to high energy input. Nevertheless, many microorganisms have developed metabolic pathways for degradation of these compounds under anaerobic conditions (Werner, 2009). Today four pathways for anaerobic biodegradation of aromatics are known: (i) hydroxylation, (ii) fumarate-addition, (iii) carboxylation and (iv) methylation (Heider, 2007). All mechanisms lead to formation of benzoylacetyl-CoA as central degradation metabolite of aromatics which is further dearomatized to a cyclic dien by catalysis via benzoyl-CoA-reductase. Afterwards, ring structures are cracked and chain-like compounds can be mineralized to CO_2 by β-oxidation (Boll et al., 2002; Fuchs et al., 2014; Harwood et al., 1999).

Mechanism (i) *(see Fig. 5)* has been observed during anaerobic degradation of ethylbenzene under nitrate-reducing conditions (e.g. strain EbN1) (Ball et al., 1996; Heider, 2007; Rabus and Widdel, 1995). Thereby, first ethylbenzene is activated by adding a hydroxyl-group (hydroxylation) to the C1-methylene carbon atom of the sidechain (Heider et al., 1999; Kniemeyer and Heider, 2001a). This reaction is catalyzed by ethylbenzene dehydrogenase, which belongs to the molybdenum-containing enzymes and was the first known enzyme capable for oxidizing hydrocarbons in absence of oxygen (Hagel, 2006;

Kniemeyer and Heider, 2001b; Johnson et al., 2001). For this purpose the oxygen atom of the hydroxyl-group is derived from water (Hagel, 2006; Heider et al., 1999). In the course of hydroxylation ethylbenzene is transformed into 1-phenylethanol which microorganisms can incorporate into cytoplasm (Heider et al., 1999; Kniemeyer and Heider, 2001a). Moreover, 1-phenylethanol is oxidized to acetophone which in turn is carboxylated to benzoylacetate. After further activation and thiolytically cleavage the central intermediate benzoylacetyl-CoA is formed (Heider et al., 1999; Rabus et al., 2005).

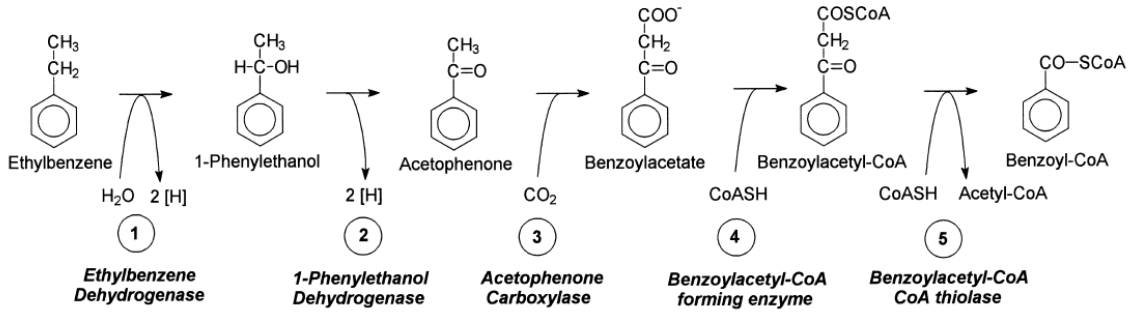

Fig. 5: Anaerobic biodegradation pathway of ethylbenzene commenced by hydroxylation (Heider et al., 1999)

Mechanism (ii) *(see Fig. 6)* has been detected for biodegradation of toluene or xylene under nitrate- (e.g. *Thauera aromatica*), sulfate- (e.g. *Desulfobacula toluolica*) and ferric iron-reducing (e.g. *Geobacter metallireducens*) as well as at methanogenic conditions (Beller and Edwards, 2000; Biegert et al., 1996; Kane et al., 2002; Kube et al., 2004; Rabus et al., 1993). Besides, Kniemeyer et al. (2003) observed this pathway in the degradation of ethylbenzene by sulfate-reducing strain EbS7. In this mechanism the aromatic hydrocarbon is added to the double bond of fumarate enzymatically catalyzed by benzylsuccinate synthase (Beller and Spormann, 1997; Biegert et al., 1996). This process leads to formation of benzyl-succinates in case of toluene (Biegert et al., 1996), methylbenzene-succinates in case of xylene (Morasch and Meckenstock, 2005) and (1-phenylethyl)-succinates in case of ethylbenzene (Kniemeyer et al., 2003). Further degradation of these intermediates is done via a special β-oxidation-pathway that is indicated by CoA-transferase enzyme. Finally, this process leads to formation of benzoylacetyl-CoA as central metabolite (Leuthner and Heider, 2000; Leutwein and Heider, 2002).

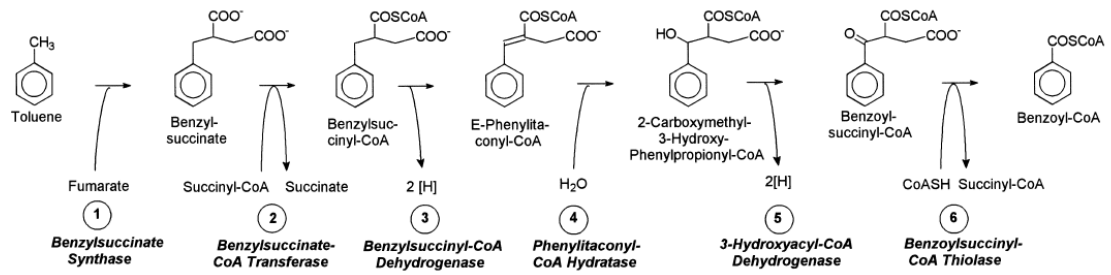

Fig. 6: Anaerobic biodegradation pathway commenced by addition to fumarate on example of toluene (Heider et al., 1999)

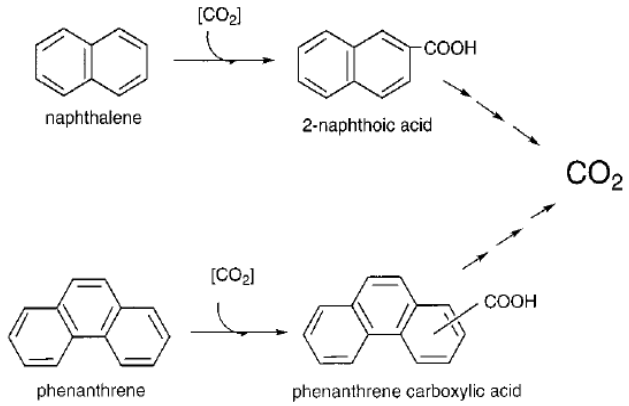

Fig. 7: Proposed anaerobic pathways for biodegradation of naphthalene and phenanthrene under sulfate-reducing conditions (Zhang and Young, 1997)

Mechanism (iii) *(see Fig. 7)* was shown for degradation of naphthalene and phenanthrene under sulfate-reducing conditions by Zhang and Young (1997). In this study degradation metabolites like 2-naphthoic acid or phenanthrene carboxylic acid were determined, which indicates activation of hydrocarbons by incorporation of CO_2 into the ring structures (carboxylation). Subsequent degradation steps for converting these intermediates to benzoylacetyl CoA have not been fully investigated.

Recently, Safinowski and Meckenstock (2006) detected mechanism (iv) as a completely new way for activation of naphthalene under sulfate-reducing conditions. Thereby, naphthalene is initially methylated to 2-methylnaphthalene, which is metabolized further via fumarate-addition and β-oxidation to benzoylacetyl-CoA as central metabolite.

2.3 The function of molybdenum in biological microcosms

The transition metal molybdenum with the atomic number 42 is located in the sixth group of the periodic table (Wawra et al., 2003). Naturally it occurs as a component of minerals in the earth crust, where it accounts for only a small proportion in comparison to other metals like ferric iron. So the ratio of ferric iron to molybdenum in the earth crust constitutes 3000:1 (Hagel, 2006). Depending on prevailing redox-conditions molybdenum arises in bivalent to hexavalent form (Ternes, 2013). While highly reduced molybdenum is insoluble in water, oxidized molybdates (consist of Mo(VI) and oxoanions; MoO_4^{2-}) show great solubility and therefore are readily bioavailable (Hagel, 2006). For microorganisms molybdenum constitutes an essential trace element which at too high concentrations has toxic effects (Blume et al., 2010). Furthermore, molybdenum is present in the active center of a large number of enzymes (Ternes, 2013). Under anaerobic conditions several bacterial species are capable to reduce Mo(VI) to Mo(IV) which leads to formation of insoluble compounds like MoS_2 (Biswas et al., 2009; Blume et al., 2010; Tucker et al., 1997).

2.3.1 The inhibition of sulfate-reduction by molybdate

Many studies have shown that molybdate inhibits the microbial process of sulfate-reduction under anaerobic conditions (e.g. Mizuno et al., 1998; Mosey, 1983; Ranade et al., 1999). For this effect two reasons were found:

(i) Molybdate has a similar stereochemical structure to sulfate and as a consequence it competes in biochemical reactions (Ranade et al., 1999; Smith and Klug, 1980). Thus, molybdate often blocks microbial uptake system, which leads to lower incorporation of sulfate via cell membranes (Biswas et al., 2009; Ranade et al., 1999; Reuveny, 1976).

(ii) Molybdate can inhibit the first enzyme in the pathway of sulfate-reduction, called ATP-sulfurylase (Ranade et al., 1999; Reuveny, 1976; Smith and Klug, 1980). This enzyme catalyzes the activation of inorganic sulfate by adenosine triphosphate (ATP) which leads to formation of adenosine-5'-phosphosulfate (APS) and pyrophosphate (PPi) (Biswas et al., 2009; Fuchs et al., 2014; Parey et al., 2013; Reuveny, 1976):

$$SO_4^{2-} + ATP + 2H^+ \xrightarrow[ATP-sulfurylase]{} APS + PPi$$

Usually, APS is reduced on further steps to sulfite and sulfide (Eggeling and Bott, 2005; Fuchs et al., 2014). But in the presence of molybdate no APS can be generated due to suppression of the enzyme. In this case only a molecule equivalent to APS is formed, whereby further sulfate-reduction cannot take place (Biswas et al., 2009).

Since higher concentrations of molybdate have toxic effects on organisms and environment, only small amounts of this compound should be added for suppression of sulfate-reduction (Biswas et al., 2009; Blume et al., 2010; Ranade et al., 1999). Fortunately, the inhibiting effect on sulfate-reducing microorganisms appears even at low concentrations of molybdate. So Biswas et al. (2009) and Hasnain and Anderson (2005) already observed immediate and complete suppression of sulfate-reduction with addition of 3 mM. However, it could also be shown that sulfate-reducing microorganisms possess high adaptiveness to molybdate, which requires its continuous amendment (Hasnain and Anderson, 2005). Moreover, only bacteriostatic effects of molybdate were observed, wherefore microorganisms are able to recover thoroughly after removing molybdate (Hasnain and Anderson, 2005; Ranade et al., 1999). In contrast, Biswas et al. (2009) determined no recovery of microorganisms.

2.3.2 Molybdenum containing enzymes

Molybdenum forms the active center of many enzymes, in which it occurs as Mo (IV), Mo(V) or Mo(VI) (Blume et al., 2010; Hagel, 2006). Basically, molybdenum containing enzymes can be divided into two groups: (i) polynuclear nitrogenases and (ii) mononuclear oxo-molybdenum enzymes (Dobbek, 2000; Hille, 1996). Nitrogenases catalyze the metabolization of molecular nitrogen to ammoniac and thus play an important role in

biological nitrogen fixation (Blume et al., 2010; Wisotzky, 2011). Among oxo-molybdenum enzymes already more than 30 types are known, whose catalytic reactions play an important role in many metabolic cycles (Hille, 1996; Hille, 2002). Oxo-molybdenum enzymes can further be subdivided based on their spectroscopic properties into two subgroups: (i) molybdenum-oxotransferases and (ii) molybdenum-hydroxylases (Hille, 1996). Molybdenum-oxotransferases typically catalyze redox-reactions, where a substrate is either oxidized or reduced by adding or removing an oxygen atom, respectively (Hille, 1996; Hille, 2002). To this group belongs for example nitrate reductase, which catalyzes reduction of nitrate to nitrite (Cypionka, 2010; Fuchs et al., 2014; Wisotzky, 2011). Furthermore, dimethylsulfoxid-reductases (DMSO) like ethylbenzene dehydrogenase as key enzyme of anaerobic ethylbenzene activation by adding OH-groups to carbon atoms (hydroxylation) are among this group (Hagel, 2006; Hille, 1996). Ethylbenzene dehydrogenase was the first detected enzyme capable for hydrocarbon-oxidation under anaerobic conditions deriving necessary oxygen atoms by cleavage of water (Hagel, 2006; Heider et al., 1999; Johnson et al., 2001; Kniemeyer and Heider, 2001b). Chemically, this process can be described by the following equation (Hille, 1996):

$$RH + H_2O \rightarrow ROH + 2H^+ + 2e^-$$

Where:

R … attached hydrocarbon

Today this capability is also known for all enzymes belonging to the group of molybdenum-hydroxylases (Dobbek, 2000; Hille, 2004). But in contrast to ethylbenzene dehydrogenase this enzymes are able to hydroxylate a large number of aliphatic and aromatic hydrocarbons, whereat metabolic pathways are extremely diverse (Hille, 1996; Hille, 2004).

2.4 Methods for monitoring of PH-biodegradation processes

If a PH-contaminated site or aquifer is remediated *in situ* via MNA, qualitative and quantitative assessment of biodegradation is very important to ensure a working process (Stelzer, 2008). Therefore, surveillance of PH-degradation is insufficient, since not only biological degradation processes lead to a decrease in measured pollutant concentrations. Aside, also abiotic processes, like sorption, desorption, volatilization, dilution, dispersion and chemical transformation can result in a decline of imposed PH-concentrations. But through these processes pollutants are only relocated in other environmental compartments and there is no real reduction in their quantities (Förstner, 2012; Kopinke et al., 2005; Meckenstock et al., 2004; Stelzer et al., 2006; Stelzer, 2008; Wisotzky, 2011). Furthermore, monitoring is difficult in presence of LNAPL- and DNAPL-phases due

compensation of PH-degradation by resolubilisation from the NAPL (Wiedemeier et al., 1999). Hence, many methods for monitoring biological PH-degradation processes were developed, whereat the bigger part of these methods only allows indirect evidence for biodegradation and is coupled with many uncertainties (Stelzer, 2008).

2.4.1 Indirect methods

Indirect methods for detection of *in situ* biodegradation are frequently used (Stelzer, 2008). In this connection, one option is the combined measurement of PH-degradation, TEA-depletion (O_2, NO_3^-, SO_4^{2-}) and occurrence of products of microbial activity (CO_2, N_2, S^{2-}). However, practical application of this method is very limited because TEA are implemented also for growth of microorganisms and microbial respiration products are produced by other processes, too (Förstner, 2012; Gödeke et al., 2003; Meckenstock et al., 2004; Stelzer, 2008; Wisotzky, 2011). Another way of monitoring relies on decreasing biodegradability from n-alkanes over iso-alkanes to cyclo-alkanes and aromatics. Here, it is assumed that a relative increase of the more readily degradable n-alkanes compared to the more persistent iso- and cyclo-alkanes as well as aromatics is an indication of biodegradation. In practice ratios of n-C_{17} to pristane as well as n-C_{18} to phytane are frequently consulted. Again, this method is critical because the chemical composition of PH also can change in absence of biodegradation for instance by solution- and sorption-processes (Hasinger et al., 2012; Kopinke et al., 2005; Meckenstock et al., 2004; Wang and Fingas, 2003). Furthermore, biodegradation of PH can be verified by detection of specific polar metabolites. However, in many cases only a few or even not any metabolites can be detected, even if biodegradation is working (Förstner, 2012; Gieg and Suflita, 2002; Meckenstock et al., 2004; Stelzer, 2008; Widdel and Rabus, 2001). Another indication for biological PH-degradation relies on the detection of the presence of depleting active microorganisms at the contaminated site by fingerprinting methods like Polymerase Chain Reaction (PCR). But again, this approach provides no evidence for a functioning biodegradation process because there can be no assurance that the organisms are active (Meckenstock et al., 2004; Stelzer, 2008). Moreover, increasing values for Dissolved Organic Carbon (DOC) and Dissolved Inorganic Carbon (DIC) at the contaminated site constitute an indication of PH-degradation (Hasinger et al., 2011).

2.4.2 Stable isotope fractionation analysis for direct detection of PH-degradation

In recent years one of the most promising and commonly applicated approaches for qualitative and quantitative monitoring of PH-biodegradation in the subsurface is the so called stable isotope fractionation analysis (SIFA), which in contrast to other methods allows direct detection of biodegradation (Förstner, 2012; Hunkeler et al., 2008; Meckenstock et al., 2004; Stelzer, 2008). Atoms of the same element with diverse numbers of neutrons and therefore different masses are named isotopes (Aelion et al., 2009; Stelzer, 2008; Stögbauer, 2004). While many isotopes decay and thereby emit radioactive

radiation, plenty of naturally occurring elements consist of several stable isotopes, which can be used for SIFA (Aelion et al., 2009; Stelzer, 2008). The method relies on the fact, that microorganisms use lighter isotopes in preference to heavier ones, whereby isotope ratios are shifted. This occurs because lighter isotopes have a higher zero-point energy than heavier ones and so microorganisms need less activation energy for cracking chemical bonds formed by lighter isotopes (Cichocka et al., 2008; Fischer et al., 2004; Meckenstock et al., 2004; Nagel et al., 2011).

As well PH as different TEA consist of mixtures of lighter and heavier stable isotopes (Meckenstock et al., 2004). So PH contain ^{12}C and ^{13}C isotopes, whereas oxygen is composed of ^{16}O, ^{17}O and ^{18}O, nitrate of ^{14}N and ^{15}N and sulfate of ^{32}S, ^{33}S, ^{34}S and ^{36}S isotopes (Aelion et al., 2009; Kendall and Caldwell, 1998; Stögbauer, 2004; Wisotzky, 2011). For analytical online measurement of stable isotope ratios at given compounds frequently an elemental analyzer connected to an isotope ratio mass spectrometer (EA-IRMS) is used (Aelion et al., 2009; Hunkeler et al., 2008). Commonly, results are demonstrated as δ-values, which represent the ratio of heavier to lighter isotopes in comparison to an international standard expressed in ‰ (Aelion et al., 2009; Meckenstock et al., 2004; Stelzer, 2008; Stögbauer, 2004; Wisotzky, 2011). Thereby, for all international standards δ-values were set at 0 ‰ and as a consequence samples with higher isotopic ratios have positive δ-values while those with lower isotopic ratios exhibit negative δ-values (Aelion et al., 2009).

The calculation of δ-values is defined as following (Fischer et al., 2004; Johnston et al., 2008; Meckenstock et al., 2004; Stelzer et al., 2006; Stelzer, 2008):

Carbon:

$$\delta^{13}C = \left(\frac{\left(\frac{^{13}Cs}{^{12}Cs}\right)}{\left(\frac{^{13}Cst}{^{12}Cst}\right)} - 1 \right) * 1000$$

Oxygen:

$$\delta^{18}O = \left(\frac{\left(\frac{^{18}Os}{^{16}Os}\right)}{\left(\frac{^{18}Ost}{^{16}Ost}\right)} - 1 \right) * 1000$$

Nitrogen:

$$\delta^{15}N = \left(\frac{\left(\frac{^{15}Ns}{^{14}Ns}\right)}{\left(\frac{^{15}Nst}{^{14}Nst}\right)} - 1 \right) * 1000$$

Sulfur:

$$\delta^{34}S = \left(\frac{\left(\frac{^{34}Ss}{^{32}Ss}\right)}{\left(\frac{^{34}Sst}{^{32}Sst}\right)} - 1 \right) * 1000$$

Where:

$\left(\frac{^{13}Cs}{^{12}Cs}\right)$ … isotope ratio in sample

$\left(\frac{^{13}Cst}{^{12}Cst}\right)$ … isotope ratio in international standard

Tab. 4 shows for respective calculation used international standards and appropriate relative frequency of stable isotopes. All standards were determined by International Atomic Energy Agency (IAEA) in Vienna and the National Institute of Standards and Technology (NIST) in the United States (Aelion et al., 2009; Meckenstock et al., 2004).

Tab. 4: Relative Frequency [%] of stable isotopes in for calculation of δ-values used international standards (author's representation based on Aelion et al., 2009 and Hoefs, 2015)

Isotope	Relative Frequency [%]	Int. Standard	Description
$^{12}C/^{13}C$	99.89 / 1.11	Vienna Pee Dee Belemnite *(VPDB)*	Stable isotope ratio of a crushed white marble designated as NBS-19, which is very similar to that of originally used belemnite fossil collected in the cretaceous Pe Dee Formation in South Carolina, USA
$^{16}O/^{18}O$	99.76 / 0.02	Vienna Standard Mean Ocean Water *(VSMOV)*	Stable isotope ratio of a mixture of distilled ocean water collected at many places around the world
$^{14}N/^{15}N$	99.64 / 0.36	Atmospheric Air	Stable isotope ratio of atmospheric air
$^{32}S/^{34}S$	94.02 / 4.21	Vienna Canyon Diablo Troilite *(VCTD)*	Stable isotope ratio of troilite from the Canyon Diablo meteorite, which was found in Arizona, USA; since this standard is not available anymore, today a special silver sulfide designated as IAEA-S-1 is used instead

While abiotic concentration-reducing processes, like volatilization, sorption or dilution, don't lead to significant isotope fractioning (Harrington et al., 1999; Hunkeler et al., 2004; Slater et al., 2000), biodegradation goes along with noticeable isotope shifts *(see Fig. 8)* (Aelion et al., 2009; Hofstetter et al., 2008; Hunkeler et al., 2008; Kopinke et al., 2005; Wisotzky, 2011). If microorganisms degrade compounds like PH, a significant enrichment of heavier isotopes in residual substrates and of lighter isotopes in degradation products appears. So as well at side of PH as of TEA kinetic isotope effects consisting of a shift from lighter to heavier isotopes arise, whereby δ-values are increasing (Cichocka et al., 2008; Fischer et al., 2004; Meckenstock et al., 2004; Nagel et al., 2011; Stelzer et al., 2006; Widdel and Rabus, 2001). Nevertheless, the isotope fractioning can also be affected by temperature or redox conditions, the involved microorganisms or enzymes and other processes like substrate uptake and transport into cells (Cichocka et al., 2008; Knöller et al., 2011; Morasch et al., 2001; Nijenhuis et al., 2005; Nikolausz et al., 2006). Anyway, the impact of these processes is not very high, wherefore an estimation of biodegradation from changing isotope ratios is possible (Aelion et al., 2009; Fischer et al., 2004; Hunkeler et al., 2008; Stelzer, 2008).

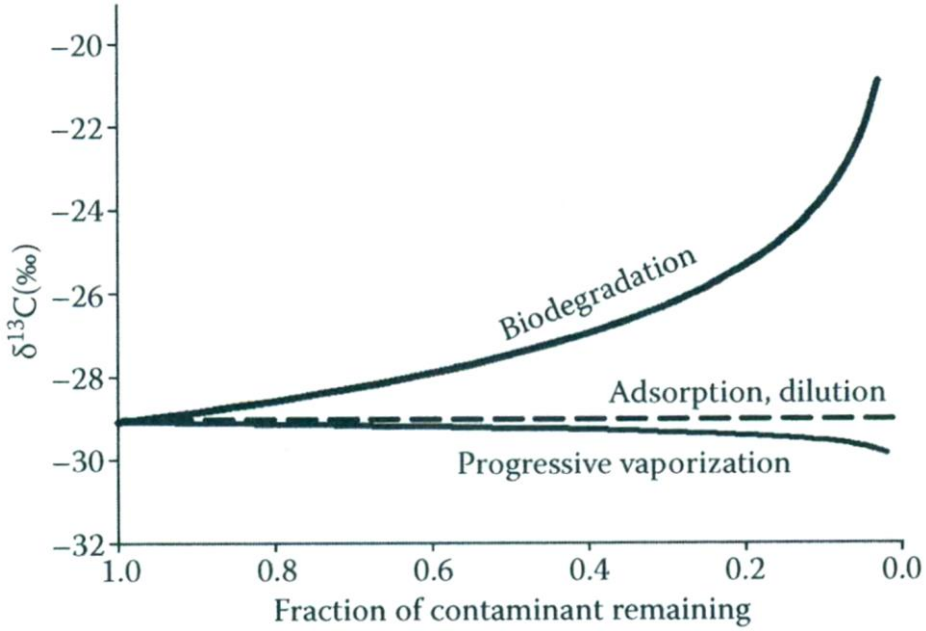

Fig. 8: Illustration of the potential for using SIFA to differentiate between abiotic concentration-reducing processes and biodegradation (Aelion et al., 2009)

For quantification of the extent of PH-biodegradation at a contaminated site by SIFA, first the prevailing on-site conditions must be ascertained. Then laboratory studies under these specific conditions must be carried out, under which concentrations and δ-values of the not yet degraded PH or TEA are analyzed (Aelion et al., 2009; Hunkeler et al., 2008; Meckenstock et al., 2004). Afterwards as well the kinetic isotope fractionation factor (α) as the isotope enrichment factor (ε), which both are a constant for given conditions and characterize the magnitude of isotope fractionation (Aelion et al., 2009), can be calculated using the so called Rayleigh Equation (Rayleigh, 1896). This equation describes the mathematical relation between changes in substrate concentrations and simultaneously occurring shifts in isotope ratios (Stelzer, 2008). In literature there can be found several forms of Rayleigh Equation, whereas following forms are commonly used (Clark and Fritz, 1997; Hoefs, 2015; Meckenstock et al., 2004; Stelzer, 2008):

$$\frac{R_t}{R_0} = \left(\frac{C_t}{C_0}\right)^{(\alpha-1)} \qquad ln\left(\frac{R_t}{R_0}\right) = (\alpha - 1) * ln\left(\frac{C_t}{C_0}\right)$$

With:

$$\frac{R_t}{R_0} = \frac{(\delta_t + 1000)}{(\delta_0 + 1000)}$$

Where:

R_t … stable isotope ratio of remaining substrate at time t calculated from determined δ-value

R_0 … initial isotope ratio of substrate calculated from determined δ-value

C_t … remaining concentration of substrate at time t

C_0 … initial concentration of substrate

α … kinetic isotope fractionation factor

According to the Rayleigh Equation α-value can be obtained by plotting $\ln(C_t/C_0)$ over $\ln(R_t/R_0)$ and laying a linear regression line through all data points. The slope (b) of regression line corresponds to α-1 and so the kinetic isotope fractionation factor (α) can be determined (Meckenstock et al., 2004). Furthermore, ε-value expressed in ‰ can be calculated by multiplying b with 1000 (Clark and Fritz, 1997; Meckenstock et al., 2004).

After specific α-value was determined, expected percentage biological degradation (B) at contaminated site can be calculated. Therefore Rayleigh Equation must be transformed in such a way, that the term (C_t/C_0) can be replaced (Fischer et al., 2004; Meckenstock et al., 2004; Stelzer, 2008):

$$B[\%] = \left(1 - \frac{C_t}{C_0}\right) * 100 = \left(1 - \left(\frac{R_t}{R_0}\right)^{\left(\frac{1}{(1/\alpha)-1}\right)}\right) * 100$$

Nevertheless, in practice prediction of PH-biodegradation from pollutant sided $^{13}C/^{12}C$ stable isotope ratios is problematic because chain lengths of PH are very diverse. While PH are degraded by microorganisms, not all carbon atoms are involved into the reaction. Therefore, an isotope effect only occurs in those carbon atoms that are involved into the reaction, while other carbon atoms stay isotopically stable. In context of SIFA it is always integrated over the entire range of carbon atoms, whereby the calculated isotope effect is less than the real intrinsic isotope effect. The higher the chain length of PH-molecules, the more pronounced is this effect (Aelion et al., 2009; Hunkeler et al., 2008; Meckenstock et al., 2004; Morasch et al., 2004; Stelzer, 2008). In a study of Morasch et al. (2004) it was shown, that molecules with more than 12 carbon atoms are not appropriate for SIFA, since in this case measured isotope shifts are not significantly different from analytical errors. Furthermore, at many contaminated sites PH come from multiple sources and therefore have different original isotope compositions. In this case the prediction of biodegradation based on SIFA should be made very carefully because this can indicate isotope fractioning and thus biodegradation, which does not take place in reality (Hunkeler et al., 2008; Meckenstock et al., 2004). For this reasons it may be more useful to predict biological degradation of PH from acceptor sided stable isotope shifts. For this purpose at aerobic degradation processes $^{18}O/^{16}O$ isotope ratios and at anaerobic degradation processes

$^{15}N/^{14}N$ isotope ratios under nitrate-reducing or $^{34}S/^{32}S$ isotope ratios under sulfate-reducing conditions can be used.

Besides application for quantitative assessment of PH-biodegradation, SIFA can also be used for detection of predominant degradation pathways (Aelion et al., 2009; Hunkeler et al., 2008). However, for this purpose exclusive investigation of acceptor sided stable isotope ratios is insufficient. So for identification of specific metabolic pathways shifts in pollutant sided stable isotope ratios have to be imposed, too. Since different degradation pathways can show the same or equal isotope fractionation for one element, in many cases investigation of isotope ratios must be performed for several elements contemporaneously (Hofstetter et al., 2008; Hunkeler et al., 2008). Thereby, for assessment of aerobic and anaerobic pathways of PH-biodegradation usually shifts in pollutant sided carbon and hydrogen isotope ratios are investigated, as it was even conducted in several studies (e.g. Hunkeler et al., 2001; Jaeckel et al., 2014; Morasch et al., 2002; Steinbach et al., 2004).

3 Materials and Methods

3.1 Chemicals

All used chemicals were purchased from Sigma Aldrich (Sigma Aldrich, Vienna, Austria), Merck (Merck GmbH, Vienna, Austria) as well as Macherey-Nagel (Macherey-Nagel GmbH & Co. KG, Düren, Germany) and were of analytical quality.

3.2 Aquifer material and crude oil

The aquifer material used in the experiments was originally collected from a nitrate- and sulfate-reducing zone of a historically PH-contaminated site in Lower Austria. It has a sandy texture and was used in previous anaerobic degradation experiments under nitrate- and sulfate-reducing conditions (Hasinger et al., 2012), wherefore microbial consortia of anaerobic PH-degraders were already present. For this experiment the aquifer material was sieved to < 2mm and carefully homogenized in an anaerobic glove-box (MECAPLEX, Grenchen, Switzerland) flushed with argon 5.0 (Messer GmbH, Gumpoldskirchen, Austria). To avoid limitation by poor intrinsic and structural degradability and so to ensure good degradation rates (Scherr et al., 2007) it was additionally spiked with a paraffin-rich crude oil. Here, the appropriate amount of crude oil was selected to reach a concentration of around 18000 mg TPH per kilogram soil dry weight. The crude oil was added with a Pasteur pipette and afterwards mixed with a spoon to achieve homogenous distribution under anaerobic conditions.

3.3 Mineral medium

For mineral medium macronutrients, trace elements and vitamins were dissolved in MilliQ®-Water (Merck Millipore, Darmstadt, Germany) with an electrical resistance of 18.5 MΩ*cm. To yield an approximate stoichiometric C(contaminant):N:P:K-relationship of 150:5:1:1 (Hasinger et al., 2011) nutrients were added as NH_4Cl, KH_2PO_4 and Na_2HPO_4 as described in Scherr et al. (2011), where the amount of C was calculated from the TOC of the aquifer material and the carbon from the contaminant. Additionally, 10 mL/L of a trace element solution consisting of (mg/L): H_3BO_3 (3), $CaCl_2*2H_2O$ (703.2), $CoCl_2$ (3.9), $CuSO_4*5H_2O$ (17.3), $FeSO_4*7H_2O$ (206), KI (101), $MnSO_4*1H_2O$ (14), $Na_2MoO_4*2H_2O$ (5.3), Na_2SeO_4 (0.6), $NiCl_2*6H_2O$ (4.6), $ZnSO_4*7H_2O$ (20.5), H_2SO_4 (concentration 1 mL/L) and 1 mL/L of a vitamin-solution containing (mg/L): 4-aminobenzoic acid (5), biotin (2), folic acid (2), lipoic acid (5), nicotinic acid (5), panthothenic acid (5), pyridoxine hydrochloride (10), riboflavin (5), thiamin hydrochloride (5) and vitamin B12 (0.1) were added (modified from Scherr et al., 2009 and Scherr et al., 2011). Furthermore, 2.2 mg/L Resazurin as redox- and pH-indicator was supplemented. To remove oxygen the mineral medium was boiled in a VARIOKLAV® Series autoclave (H+P Labortechnik AG, Oberschleissheim, Germany) at an operating temperature of 125 °C and an operating

pressure of 1.4 bar, followed by gassing with argon 5.0 in an anaerobic glove-box (MECAPLEX, Grenchen, Switzerland). Additionally, the amount of liquid lost by autoclaving was replenished.

3.4 Anaerobic microcosms

Long-term anaerobic degradation experiments with PH-contaminated aquifer material under different electron accepting conditions (nitrate; nitrate+sulfate; nitrate under sulfate reduction suppression) were carried out in 250 mL glass reactors. Therefore each reactor was filled with 15 g of contaminated aquifer material and 220 mL mineral medium. Afterwards different TEA were added. To 42 of the microcosms only nitrate (32.2 mmol/L) was added, whereas to another 42 reactors both nitrate (32.2 mmol/L) and sulfate (20.8 mmol/L) were added. Thereby, the added TEA-amounts were chosen so, that they are sufficient for biodegradation of the total PH-fraction. Nitrate was supplemented as KNO_3 and sulfate as Na_2SO_4. To detect the influence of sulfate reduction on nitrate depletion under nitrate-reducing conditions further 42 reactors were filled with nitrate (32.2 mmol/L) as TEA as well as Na_2MoO_4 (3 mmol/L) as sulfate reduction suppressor (Biswas et al., 2009; Ranade et al., 1999; Reuveny, 1976; Smith and Klug, 1980). All bioreactors were charged in an anaerobic glove-box (MECAPLEX, Grenchen, Switzerland) flushed with argon 5.0 and then sealed airtight with Mininert Valves® (Sigma Aldrich, Vienna, Austria). Afterwards microcosms were incubated horizontally without shaking in shaded boxes at 20±2 °C *(see Fig. 9)*.

Fig. 9: Anaerobic microcosms incubated horizontally in shaded boxes

3.5 Quantification of TEA-concentrations

In all microcosms nitrate- and sulfate-concentrations were monitored on a weekly basis to calculate the percentage depletion of TEA. Therefore 30 µL of the aqueous supernatant were removed with a gas-tight syringe (Hamilton, Reno, USA) and analyzed according to ÖNORM EN ISO 10304-1:2009 for nitrate- and sulfate-concentrations on a Dionex ICS 900 ion chromatography system (ThermoFisher Scientific, Waltham, USA) with guard column AG14A, separation column AS14A, micro membrane suppressor AMMS, conductivity detector DS5 and an eluent of 8 mM Na_2CO_3 and 1 mM $NaHCO_3$ at a flow rate of 1 mL/min. Also concentrations of chloride, nitrite and phosphate were analyzed by default, where chloride concentrations were used as a quality parameter for the measurement due its high stability. After sampling the microcosms were slewed lightly and then stored again horizontally in the dark.

Additionally, from some reactors 6 mL of the aqueous supernatant were removed, stabilized with four drops HNO_3 and analyzed via ULTIMA ICP-AES system (Horiba Jobin Yvon, Kyoto, Japan) for its content of dissolved iron- and manganese-concentrations as described in Scherr et al. (2011). Furthermore, molybdenum concentrations were determined at Na_2MoO_4-containing reactors.

3.6 Analysis of TPH-concentrations

Periodically, a triplicate of reactors was sacrificed and the solids were analyzed qualitatively and quantitatively for their total petroleum hydrocarbon (TPH)-content according to DIN EN ISO 16703:2011. Therefore 20 mL acetone p.a. and 20 mL of retention time window (RTW) standard (30 µL/L n-C_{10} and 30 µL/L n-C_{40} in n-C_7) were added, followed by 1 min shaking and 60 min ultrasound extraction. After centrifugation for 10 min at 2300 rpm (5810 Series centrifuge, Eppendorf, Hamburg, Germany) the extracts were dried over Na_2SO_4, cleaned up by filtering through MgO_3Si (Florisil®) and diluted with RTW. Extracts were analyzed by a HP 5890 Series II gas chromatograph with a flame ionization detector (Hewlett Packard, Palo Alto, USA), which had been calibrated with a diesel fuel standard. For separation a DB-5HT capillary column (30 m x 0.25 mm x 0.1 µm) (Agilent Technologies, Santa Clara, USA) at a constant helium carrier gas flow rate of 1.6 mL/min was used. Samples of 1 µl were injected splitless by a HP 7673 Series autosampler (Hewlett Packard, Palo Alto, USA) via 11 mm Bleed Temperature Optimized septa (Agilent Technologies, Santa Clara, USA). To pass into the gaseous phase samples were heated in a 4 mm Single Taper Ultra Inert liner with glass wool (Agilent Technologies, Santa Clara, USA). At the beginning oven temperature was set at 60 °C for 1 min, then increased by 20 °C/min to 390 °C and finally held 5 min at 390 °C to ensure complete passage of all substances. Injector and detector temperatures were 320 °C and 400 °C, respectively. To calculate TPH-concentrations chromatograms were integrated between n-C_{10} and n-C_{40} using the Agilent GC ChemStation Software (Version B.04.03 - SP2) and results were multiplied by sample weight and dilution factor followed by division through dry matter and extract volume. For conversion to mmol molecular weight of n-C_{25} was used, since this alkane is located in the middle of the investigated RTW. The determined TPH-concentrations were used to calculate percentage degradation compared to initial values.

3.7 Detection of intermediate products of PH-degradation

Polar intermediate products of PH-degradation were analyzed semi-quantitatively. Therefore around 20 mL of the aqueous supernatant were extracted three times with 15 mL ethyl acetate, respectively. After centrifugation for 5 min at 2500 rpm (5810 Series centrifuge, Eppendorf, Hamburg, Germany) extracts were dried with Na_2SO_4 over night, concentrated down to 1 mL by TurboVap® II Concentration Workstation (Zymark, Corporation, Hopkinton, USA) under a stream of nitrogen at a bath temperature of 38 °C and transferred into GC-Vials. Then extracts were completely blown dry with nitrogen. In

a next step extracts were derivatized with 20 µL N,O-Bis(trimethylsilyl)trifluoroacetamide (BSTFA) at 70 °C to form less polar trimethylsilyl (TMS) esters. Finally, 1 mL of CH_2Cl_2 was added to each extract. Derivatized extracts were analyzed on a Agilent 7890A Series gas chromatograph with a coupled Agilent 5975C Series mass selective detector (Agilent Technologies, Santa Clara, USA). Separation was performed on a DB-17MS capillary column (30 m x 0.25 mm x 0.25 µm) (Agilent Technologies, Santa Clara, USA). Helium was used as carrier gas with a constant flow rate of 1.2 mL/min. Samples of 1 µl were injected splitless by a CTC Combi Pal Series autosampler (CTC Analytics AG, Zwingen, Switzerland) via 11 mm Bleed Temperature Optimized septa (Agilent Technologies, Santa Clara, USA). To pass into the gaseous phase, samples were heated in a 4 mm Single Taper Ultra Inert liner with glass wool (Agilent Technologies, Santa Clara, USA). Oven temperatures were set as follows: held at 60 °C for 0.5 min, increased by 10 °C/min to 100 °C, held at 100 °C for 1 min, increased by 6 °C/min to 220 °C, held at 220 °C for 2 min, increased by 20 °C/min to 340 °C, held at 340 °C for 9 min. Injector temperature and pressure were 300 °C and 10.42 psi. The mass selective detector was operated with a source temperature of 230 °C and a quad temperature of 190 °C at an electron energy of 1824 eV over a mass range of 33-330 amu in the scan mode. Data analysis were performed with MSD ChemStation Software (Version E.02.01.1177) using NIST08 and Wiley10/NIST11 databases.

3.8 Pre-treatment for stable isotope analysis

3.8.1 Nitrate precipitation

To avoid re-oxidation of nitrite to nitrate, precipitation was performed in an anaerobic glove-box (MECAPLEX, Grenchen, Switzerland) flushed with argon 5.0. First, the aqueous supernatants were carefully removed from the reactors with a Pasteur pipette without taking oil phase and aquifer material off. Then the supernatants were filtered through Al_2O_3 for eliminating humic matter, followed by pH adjustment to 12 by adding 10N KOH. Further, aqueous supernatants were dried first by heating and then for at least four hours at 70 °C in an incubator. After drying precipitation residues were crushed, filled in a small tube and flushed with argon 5.0.

3.8.2 Sulfate precipitation

After removal and filtration of the aqueous supernatants as described above, pH was set to values of 2-2.5 using 6N HCl. Then the aqueous supernatants were heated to 75 °C and supplemented with 10 mL of a 0.2-molar $BaCl_2$-solution to precipitate sulfate as $BaSO_4$, followed by incubation at 70 °C for three hours. Furthermore, aqueous supernatants were sucked off over blue ribbon filters with 0.45 µm pore size (Schleicher & Schuell BioScience GmbH, Dassel, Germany) to collect precipitated $BaSO_4$ and the loaded

filters were dried at 95 °C in an incubator. After drying $BaSO_4$-precipitates were filled in a small tube and flushed with argon 5.0.

3.9 Analysis of stable isotope ratios

Stable isotope ratios ($\delta^{15}N$ for nitrate; $\delta^{34}S$ for sulfate) were measured with a Vario EL III Series elemental analyser (Elementar GmbH, Hanau, Germany) and a Delta Plus XP Series isotope ratio mass spectrometer (ThermoFisher Scientific, Bremen, Germany). Therefore precipitation residues were oxidized in an oxidation furnace filled with $W(IV)O_3$ at a temperature of 1150 °C. The NO_3 formed in this process was reduced to N_2 in a furnace filled with elementary copper at a temperature of 850 °C, while the formed SO_2 was hold in a trap. Subsequently, N_2 and SO_2 were passed to the isotope ratio mass spectrometer for isotope ratio measurement. Nitrate samples were calibrated against the international standard IAEA-NO-3 (KNO_3) and $\delta^{15}N$-values were based on N_2 in air. Barium sulfate samples were calibrated against the standard NBS 127 ($BaSO_4$) and $\delta^{34}S$-values were based on Vienna Canyon Diablo Troilite (VCDT). For nitrogen isotope analysis the taken sample amount was aliquot to 1.3-1.5 mg KNO_3 and the device-specific measuring inaccuracy was <0.4 ‰, while for sulfur isotope analysis 0.6-0.7 mg $BaSO_4$ were weighted in and the device-specific measuring inaccuracy was <0.6 ‰.

3.10 Identification of present eubacterial and archaeal microbiome

For determination of present eubacterial and archaeal microbiome in anaerobic microcosms first genomic DNA was extracted from the samples using PowerSoil® DNA Isolation Kit (MO BIO Laboratories Inc., Carlsbad, USA). Since extracted genomic DNA-amounts were too small for further analyzation, DNA was amplified with Polymerase Chain Reaction (PCR) method using universal primer pairs and native Taq-Polymerase (ThermoFisher Scientific, Waltham, USA). Further amplification of eubacterial and archaeal 16S rDNA was performed using universal primers and KAPAHiFi™ DNA-Polymerase (Peqlab Biotechnologie GmbH, Erlangen, Germany). For identification of different microbial communities 500 µL of amplified genomic DNA was sent to the company Microsynth AG (Balgach, Switzerland), respectively. There eubacterial and archaeal 16S rDNA sequencing was done with Illumina-Miseq-Technology using the primer set 16S V4 (515f/806r).

3.11 Statistical analysis

Do determine the statistical correlation between TEA-depletion and TPH-degradation as independent variables and the shift of stable isotope ratios ($\delta^{15}N$ for nitrate; $\delta^{34}S$ for sulfate) as dependent variables, linear regression analysis using the programming language R® were performed. Diagnostic plots, including a QQ-Plot, were used in order to check whether the conditions for a linear regression are given. Furthermore, the existence

of autocorrelation between variables and errors was checked by Durbin-Watson-Test. For testing the statistical significance of the correlations calculated p- and t-values were used. The quality of the statistical models was ascertained via the coefficients of determination (R^2-values). For graphic presentation scatterplots were created with R®. Kinetic isotope fractionation factors (α) and isotope enrichment factors (ε) were calculated from the slope (b) of the linear regression lines.

4 Results

For better readability microcosms amended with different alternative TEA are designated with shortcuts in the following chapters: (i) microcosms amended with nitrate (NIT), (ii) microcosms with both nitrate and sulfate (COM), (iii) microcosms with nitrate under sulfate reduction suppression (SUP).

4.1 Depletion of alternative TEA in anaerobic microcosms

With increasing experiment duration all microcosms showed a decline of nitrate- and sulfate-concentrations. Tab. 5 and Fig. 10 provide an overview of the detected analytical results. In individual microcosms determined values are very similar under the same electron accepting conditions. For each test series mean values and their corresponding standard deviations are given.

Tab. 5: Averaged alternative TEA-concentrations and resulting decreases detected under different electron accepting conditions (n = 42)

Nitrate in NIT

Exp. Dur.	Mean Value		Standard Deviation		Decrease		
[d]	*[mg*L^{-1}]*	*[mmol*L^{-1}]*	*[mg*L^{-1}]*	*[mmol*L^{-1}]*	*[mg*L^{-1}]*	*[mmol*L^{-1}]*	*[%]*
0	1917	30.91	7	0.11	0	0.00	0.00
84	1826	29.45	30	0.48	90	1.46	4.72
168	1625	26.20	36	0.58	292	4.71	15.23
252	1542	24.87	39	0.62	375	6.04	19.55

Nitrate in COM

Exp. Dur.	Mean Value		Standard Deviation		Decrease		
[d]	*[mg*L^{-1}]*	*[mmol*L^{-1}]*	*[mg*L^{-1}]*	*[mmol*L^{-1}]*	*[mg*L^{-1}]*	*[mmol*L^{-1}]*	*[%]*
0	2097	33.83	3	0.06	0	0.00	0.00
84	1945	31.36	28	0.44	153	2.47	7.29
168	1784	28.76	12	0.19	314	5.06	14.97
252	1688	27.22	46	0.74	409	6.60	19.52

Sulfate in COM

Exp. Dur.	Mean Value		Standard Deviation		Decrease		
[d]	*[mg*L^{-1}]*	*[mmol*L^{-1}]*	*[mg*L^{-1}]*	*[mmol*L^{-1}]*	*[mg*L^{-1}]*	*[mmol*L^{-1}]*	*[%]*
0	2209	23.00	1	0.02	0	0.00	0.00
84	2089	21.74	26	0.27	121	1.26	5.46
168	2016	20.98	22	0.23	193	2.01	8.75
252	1907	19.85	28	0.29	302	3.14	13.67

Nitrate in SUP

Exp. Dur.	Mean Value		Standard Deviation		Decrease		
[d]	*[mg*L^{-1}]*	*[mmol*L^{-1}]*	*[mg*L^{-1}]*	*[mmol*L^{-1}]*	*[mg*L^{-1}]*	*[mmol*L^{-1}]*	*[%]*
0	1971	31.79	4	0.06	0	0.00	0.00
84	1719	27.73	30	0.48	252	4.06	12.77
168	1563	25.21	26	0.41	408	6.58	20.70
252	1473	23.75	23	0.37	498	8.04	25.29

Exp. Dur. = Experiment duration

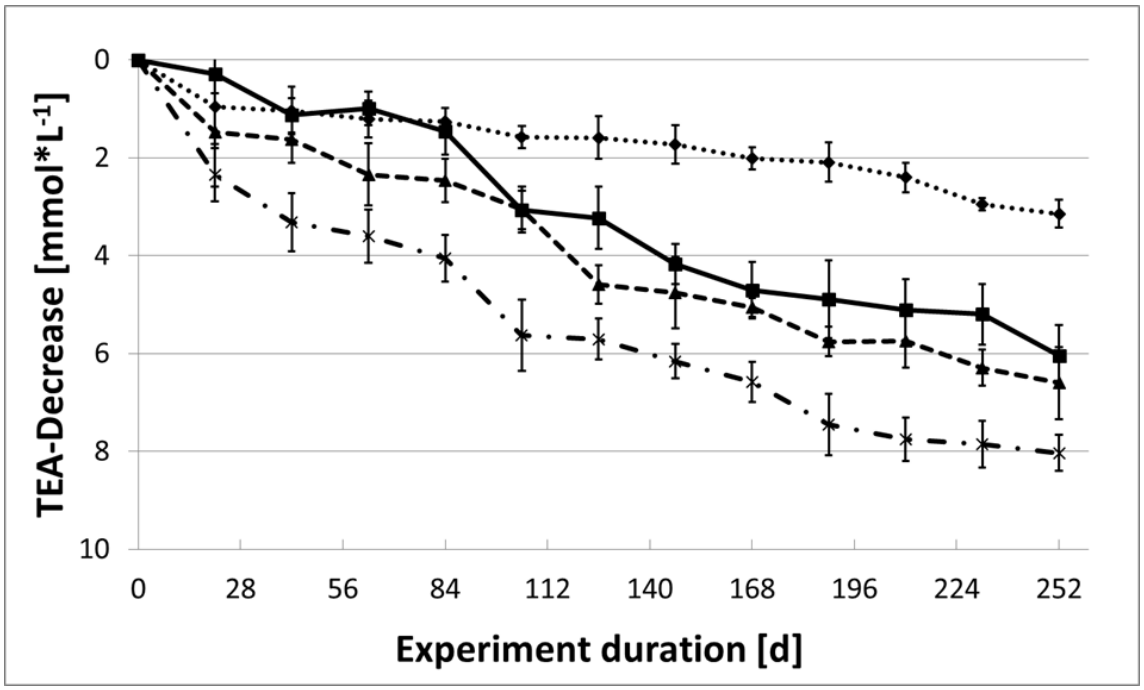

Fig. 10: Averaged depletion of alternative TEA in NIT (solid line), in COM (nitrate=dashed line // sulfate=dotted line) as well as in SUP (dashed-dotted line) (n = 42; Bars = 1 SD)

All mean values show standard deviations below 0.8 mmol*L^{-1}. The decrease of nitrate was similar in NIT and COM, while nitrate reduction was higher in SUP. If both alternative TEA are added together (COM) nitrate was used preferentially over sulfate.

Looking at nitrite as generated intermediate product of nitrate reduction *(see Fig. 11)*, NIT as well as COM showed slightly increasing concentrations. In contrast, in SUP nitrite concentrations increased strongly during the first 28 days, then decreased to approximately the same level, before they again began to rise slightly.

In microcosms containing also sulfate (COM) detected concentrations of sulfide as intermediate product of sulfate reduction were only around 0.05 mmol*L^{-1} and remained stable over the entire experiment period.

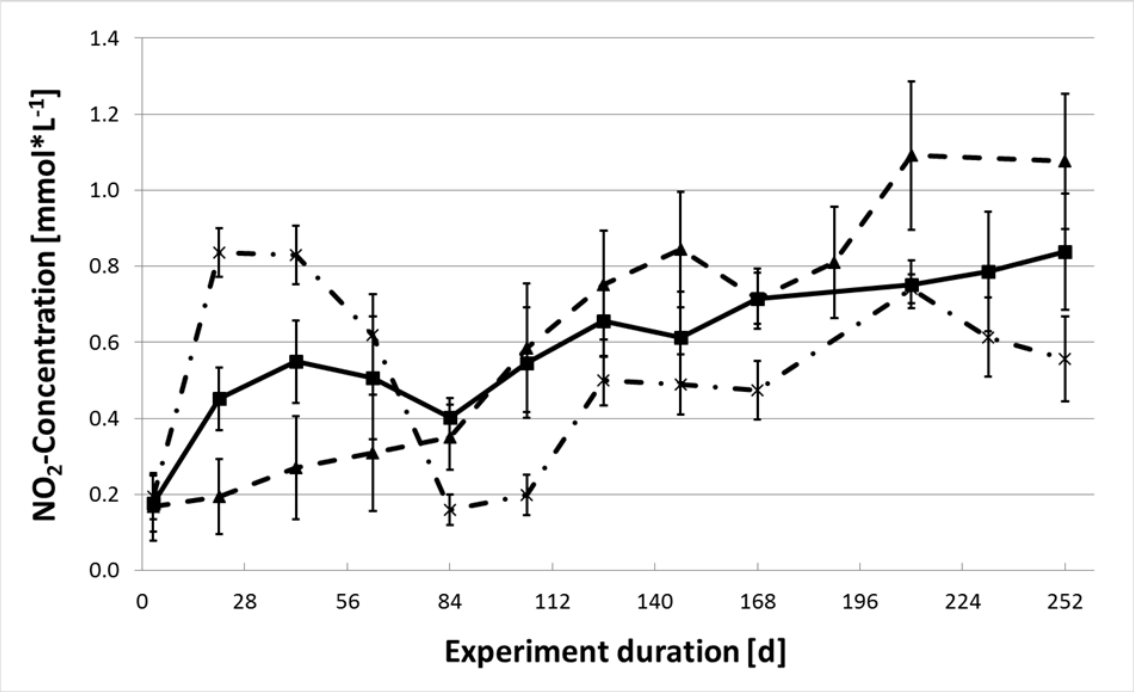

Fig. 11: Averaged nitrite concentrations in NIT (solid line), in COM (dashed line) as well as in SUP (dashed-dotted line) (n = 42; Bars = 1 SD)

Since microorganisms can also use ferric iron(III) and manganese(IV) as alternative TEA beside nitrate and sulfate, in addition concentrations of reduced ferric iron(II) and manganese(II) in the aqueous phase were determined (data not shown). Thereby, all microcosms showed increasing concentrations of ferric iron(II) over time, whereat increases only amounted to around 0.03 mmol*L^{-1}. Furthermore, in all microcosms manganese(II) concentrations were below analytical detection limit. Since no iron- and manganese-precipitation in form of for example FeS_2 (pyrite) or $Fe[CO_3]$ (siderite) could be observed, it can be assumed that effects of ferric iron(III) and manganese(IV) reduction are negligible. Moreover, it can be expected that almost no methanogenic degradation took place because no pressure increase was noted in different reactors.

4.2 Quantitative TPH-degradation in anaerobic microcosms

Decreasing TPH-concentrations in microcosms were adjoined by qualitative shifts. TPH eluting between n-C_{10} and n-C_{40} were monitored, selected GC-FID chromatograms are shown in Fig. 12.

TPH-concentrations collected during the experiments are presented in Tab. 6 and Fig. 13. All values are given per kg soil dry weight. Each extraction was performed in triplicate and results were averaged. Standard deviations did not exceed 1.9 mmol*kg^{-1}. For conversion to mmol molecular weight of n-C_{25} was used because it is located in the middle of the investigated retention time window between n-C_{10} and n-C_{40}.

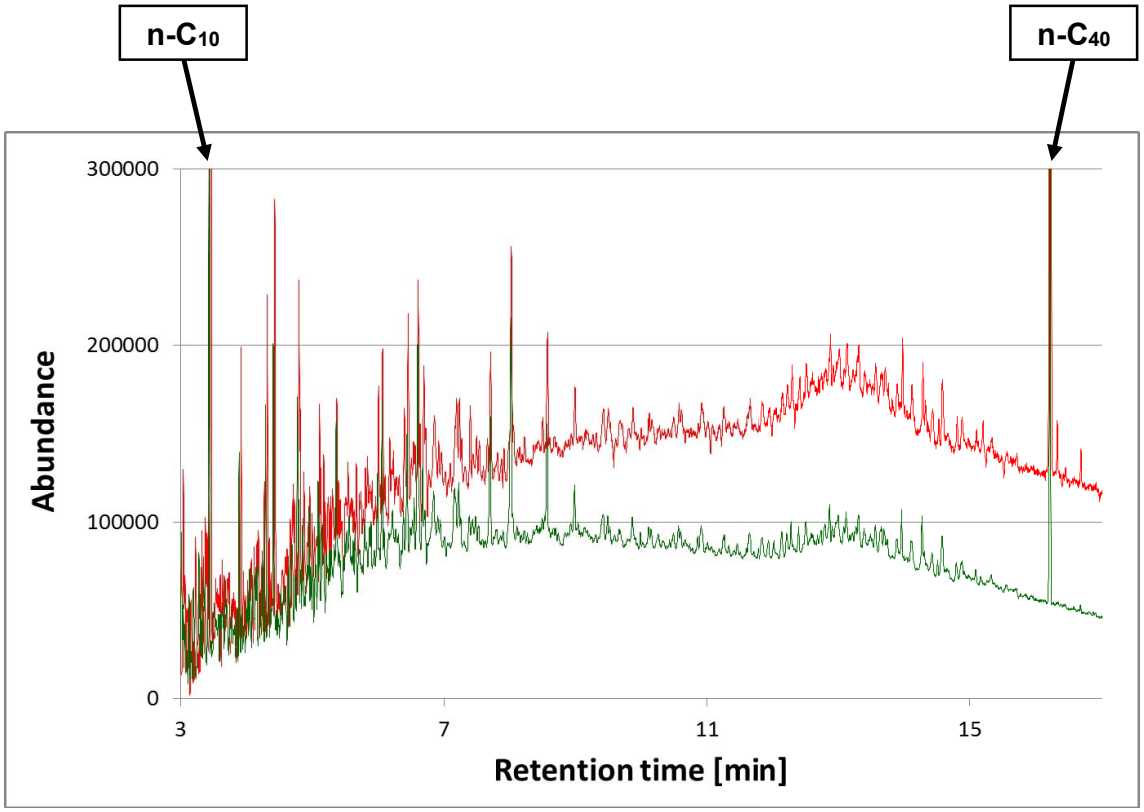

Fig. 12: Contrasting juxtaposition of GC-FID chromatograms obtained at the beginning of the experiment (red, upper line) and at day 22 (green, lower line) using the example of NIT

Tab. 6: Averaged TPH-concentrations and resulting decreases detected in different microcosms (n = 3; mmol related to n-C_{25})

NIT

Exp. Dur.	Mean Value		Standard Deviation		Decrease		
[d]	*[mg*kg^{-1}]*	*[mmol*kg^{-1}]*	*[mg*kg^{-1}]*	*[mmol*kg^{-1}]*	*[mg*kg^{-1}]*	*[mmol*kg^{-1}]*	*[%]*
0	18260	51.77	137	0.39	0	0.00	0.00
22	15497	43.94	283	0.80	2763	7.83	15.13
113	13628	38.64	255	0.72	4631	13.13	25.36
133	12959	36.74	577	1.64	5301	15.03	29.03
233	12493	35.42	645	1.83	5766	16.35	31.58

COM

Exp. Dur.	Mean Value		Standard Deviation		Decrease		
[d]	*[mg*kg^{-1}]*	*[mmol*kg^{-1}]*	*[mg*kg^{-1}]*	*[mmol*kg^{-1}]*	*[mg*kg^{-1}]*	*[mmol*kg^{-1}]*	*[%]*
0	18716	53.07	388	1.10	0	0.00	0.00
22	16679	47.29	330	0.94	2037	5.78	10.88
139	12255	34.75	165	0.47	6461	18.32	34.52
242	12039	34.14	600	1.70	6677	18.93	35.67

SUP

Exp. Dur.	Mean Value		Standard Deviation		Decrease		
[d]	*[mg*kg^{-1}]*	*[mmol*kg^{-1}]*	*[mg*kg^{-1}]*	*[mmol*kg^{-1}]*	*[mg*kg^{-1}]*	*[mmol*kg^{-1}]*	*[%]*
0	15260	43.27	137	0.39	0	0.00	0.00
8	11814	33.50	368	1.04	3446	9.77	22.58
57	9865	27.97	523	1.48	5395	15.30	35.35
113	9740	27.62	126	0.36	5520	15.65	36.17
233	8663	24.56	137	0.39	6596	18.70	43.23

Exp. Dur. = Experiment duration

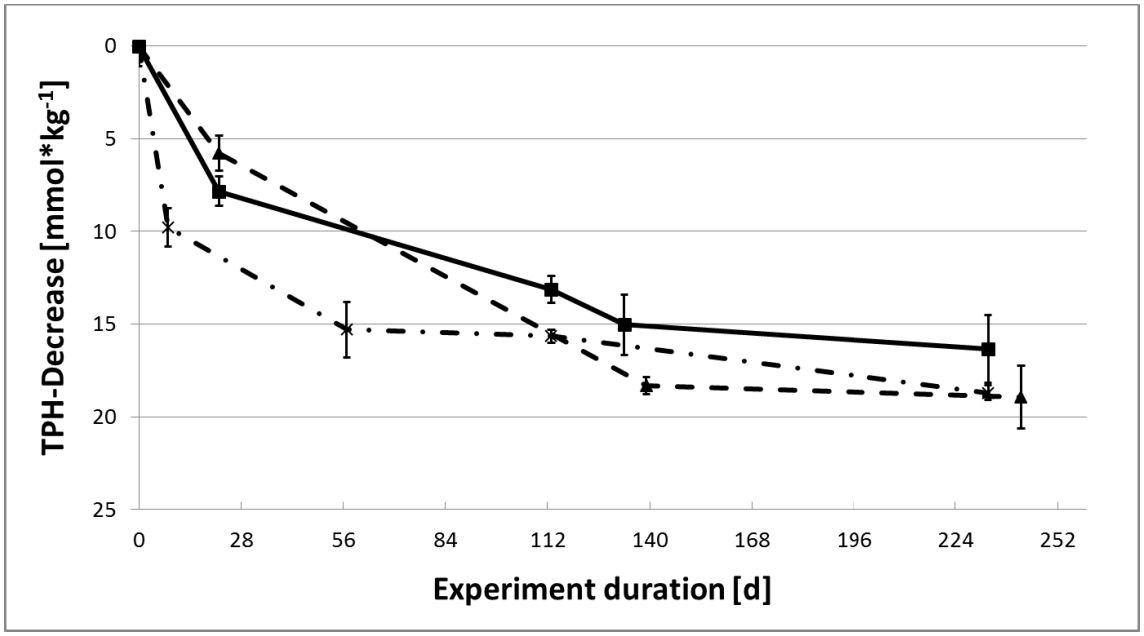

Fig. 13: Averaged TPH-concentrations in NIT (solid line), in COM (dashed line) as well as in SUP (dashed-dotted line) (n = 3; Bars = 1 SD; mmol related to n-C_{25})

After an experiment duration of around 250 days, all microcosms showed similar quantitative TPH-decrease. Thus, the detected TPH-decline was around 5700 to 6700 mg*kg^{-1} and 16 to 19 mmol*kg^{-1} (related to n-C_{25}), respectively. This implicates an average TPH-degradation rate about 25 mg*kg^{-1}d^{-1} or 0.07 mmol*kg^{-1}d^{-1} (related to n-C_{25}). Generally, in all microcosms around one third of the originally present TPH were degraded. The possible extent of degradation is discussed below.

A comparison of TPH-degradation and concurrent depletion of TEA is provided in Tab. 7. For complete degradation of 1 mmol n-C_{25} stoichiometric 30.4 mmol nitrate or 19 mmol sulfate are necessary. In these experiments considerably lower requirements were observed. So after an experiment duration of around 250 days in NIT and SUP only 5-6 mmol nitrate were reduced per mmol n-C_{25} consumed. Furthermore, at COM detected requirements were even lower.

Tab. 7: Comparison of TPH-decrease and alternative TEA-depletion inclusive therefrom calculated requirements of TEA per mmol TPH consumed in different microcosms (mmol related to n-C_{25})

NIT

Exp. Dur.	TPH-Decrease	NO_3-Depletion	TEA-Requirement
[d]	*[mmol]*	*[mmol]*	*[mmol NO_3^- per mmol TPH]*
22	0.12	0.31	2.61
113	0.20	0.77	3.92
133	0.23	1.12	4.95
233	0.25	1.31	5.32

COM

Exp. Dur.	TPH-Decrease	NO_3-Depletion	TEA-Requirement NO_3	SO_4-Depletion	TEA-Requirement SO_4
[d]	*[mmol]*	*[mmol]*	*[mmol NO_3^- per mmol TPH]*	*[mmol]*	*[mmol SO_4^{2-} per mmol TPH]*
22	0.09	0.14	1.62	0.12	1.44
139	0.27	1.33	4.83	0.58	2.11
242	0.28	1.43	5.02	0.57	1.99

SUP

Exp. Dur.	TPH-Decrease	NO_3-Depletion	TEA-Requirement
[d]	*[mmol]*	*[mmol]*	*[mmol NO_3^- per mmol TPH]*
8	0.15	0.41	2.78
57	0.23	1.02	4.43
113	0.23	1.22	5.21
233	0.28	1.72	6.12

Exp. Dur. = Experiment duration

4.3 Detected metabolites of PH-degradation

For all microcosms GC-MS chromatograms of derivatized supernatants showed many peaks which indicates existence of several polar metabolites of PH-degradation *(see Fig. 14)*. Thereby, semi-quantitatively most metabolites were detected in NIT and SUP. In contrast, only small amounts were found in COM, which indicates more complete PH-degradation under amendment of both alternative TEA. Qualitatively it was not possible to assign each peak to a certain compound because many peaks were overlapping each other or were too small for a reliable identification. Nevertheless, several polar metabolites of PH-degradation like succinates, alcohols and fatty acids have been identified. Tab. 8 provides an overview of in different microcosms detected silylated metabolites.

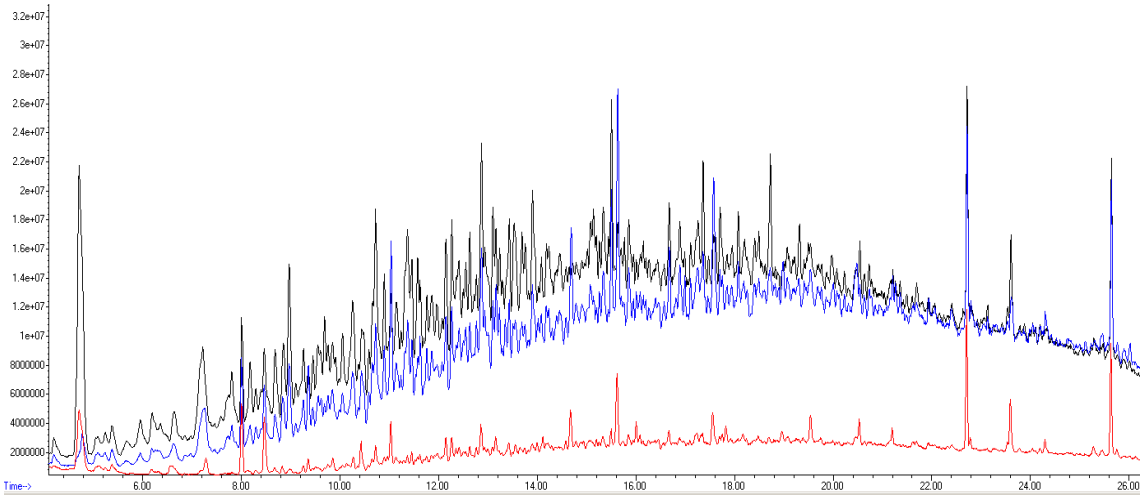

Fig. 14: GC-MS chromatograms of derivatized supernatants for SUP (black, upper line), NIT (blue, middle line) as well as COM (red, lower line)

Tab. 8: Detected silylated metabolites of PH-degradation and appropriate mass spectra for NIT (i), COM (ii) as well as SUP (iii)

Runtime	Silylated metabolite	Mass spectrum	Original metabolite	Found in
[min]				
4.71	Silane, trimethyl(octyloxy)-	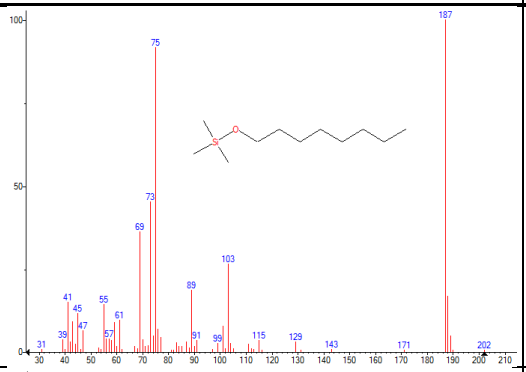	1-Octanol	(i-iii)
5.09	Hexanoic acid, trimethylsilyl ester	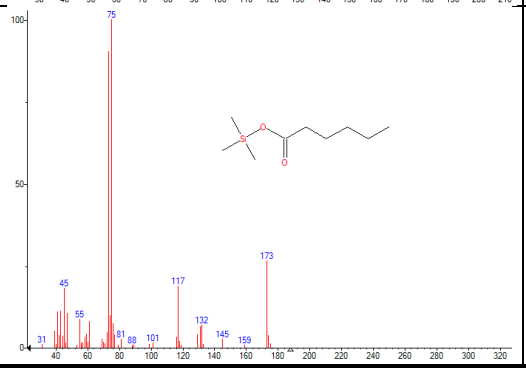	Hexanoic acid	(i; iii)

6.19	Octanoic acid, trimethylsilyl ester	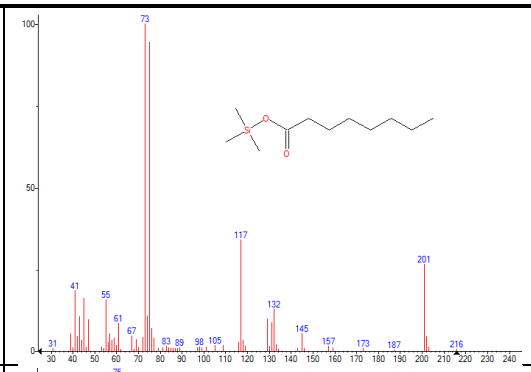	Octanoic acid	(i; iii)
6.57	2-[2-(Trimethylsilyloxy)ethoxy]ethanol	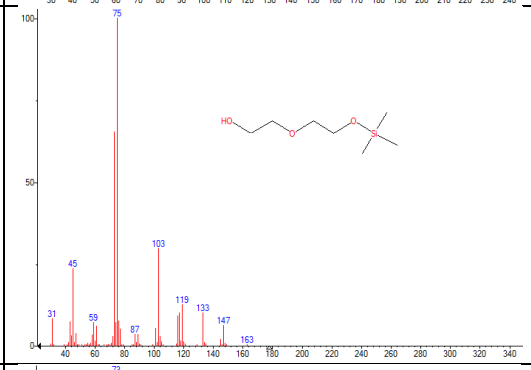	2-(2-Hydroxyethoxy)ethan-1-ol	(ii)
7.28	Glycerol, tris(trimethylsilyl) ether	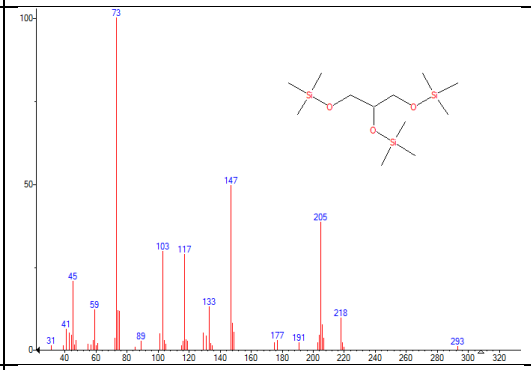	1,2,3-Propanetriol	(ii)
7.80	Silane, trimethyl[(1-methylnonyl)oxy]-	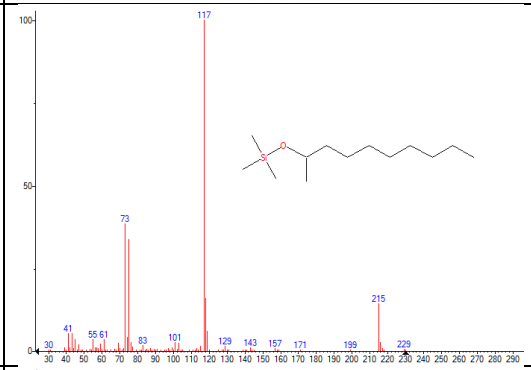	2-Decanol	(i; iii)
8.00	3,6,9-Trioxa-2,10-disilaundecane, 2,2,10,10-tetramethyl-	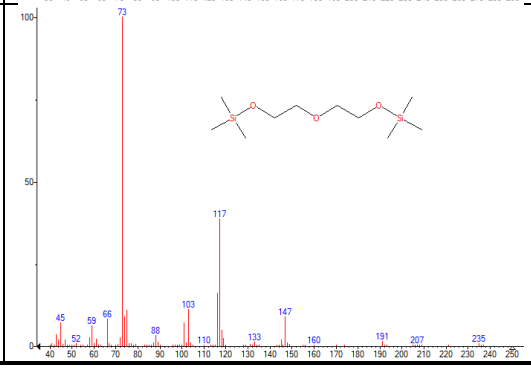	2-(2-Hydroxyethoxy)ethan-1-ol	(i-iii)

8.29	Cyclohexane acetic acid, trimethylsilyl ester	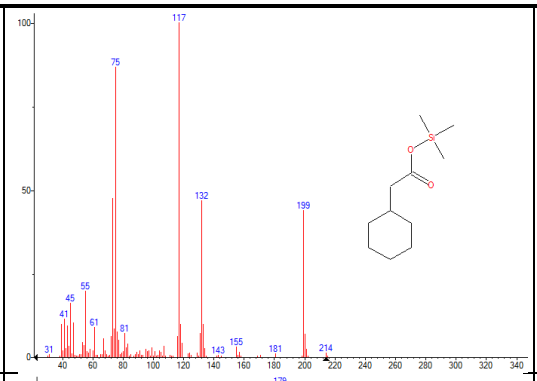	Phenylacetic acid	(i-iii)
9.85	Benzoic acid trimethylsilyl ester	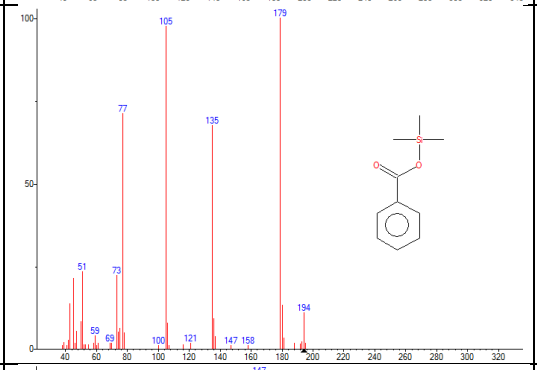	Benzoic acid	(ii)
10.26	Butanedioic acid, bis(trimethylsilyl) ester	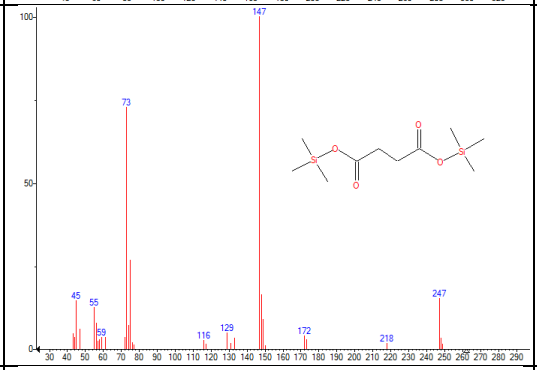	Butanedioic acid	(ii)
10.42	Nonanoic acid, trimethylsilyl ester	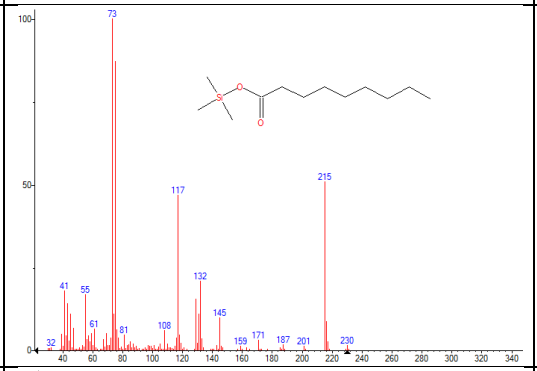	Nonanoic acid	(ii)
12.26	Undecenoic acid, trimethylsilyl ester	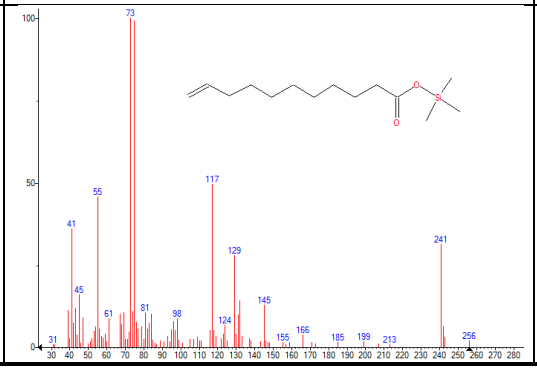	Undecenoic acid	(i; iii)

15.49	10-Undecynoic acid, trimethylsilyl ester	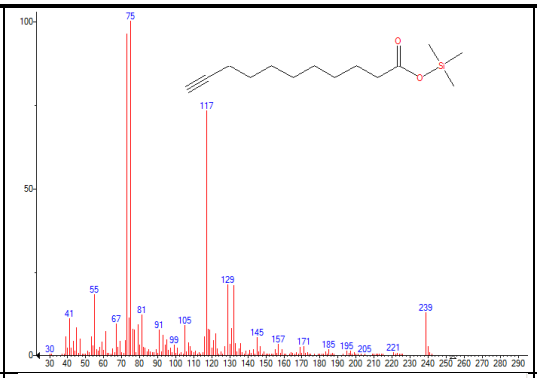	10-Undecynoic acid	(i-iii)
16.08	Dodecanoic acid, trimethylsilyl ester	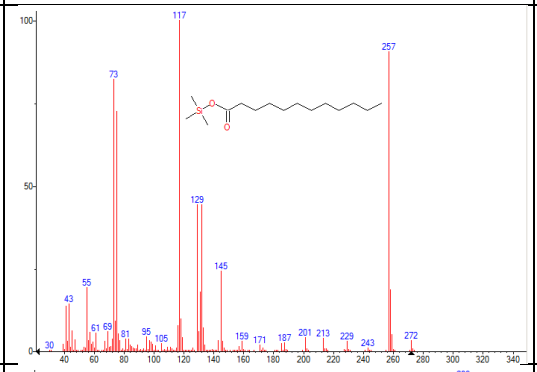	Dodecanoic acid	(ii)
20.52	Silane, (hexadecyloxy)trimethyl-	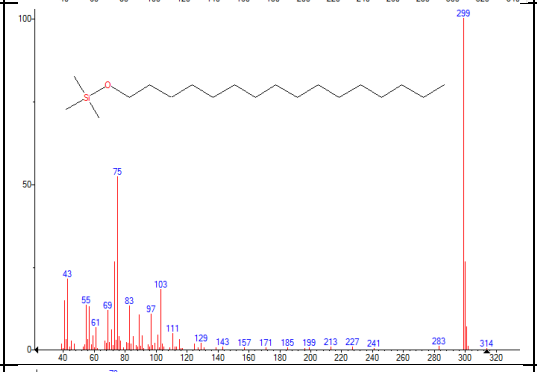	1-Hexadecanol	(ii)
22.71	Hexa decanoic acid, trimethylsilyl ester	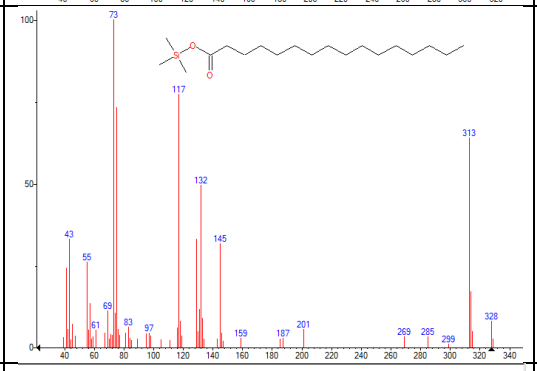	Hexadecanoic acid	(i-iii)
23.59	Silane, trimethyl(octadecyloxy)-	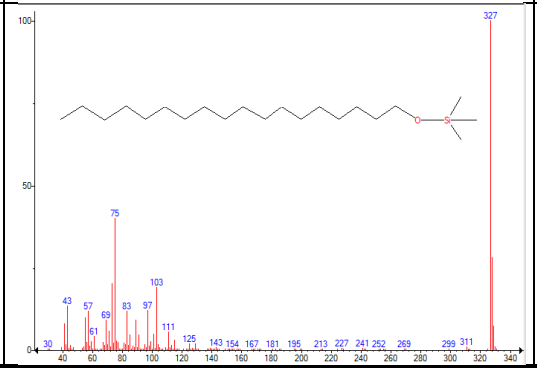	1-Octadecanol	(i-iii)

25.64	Tetra decanoic acid, trimethylsilyl ester	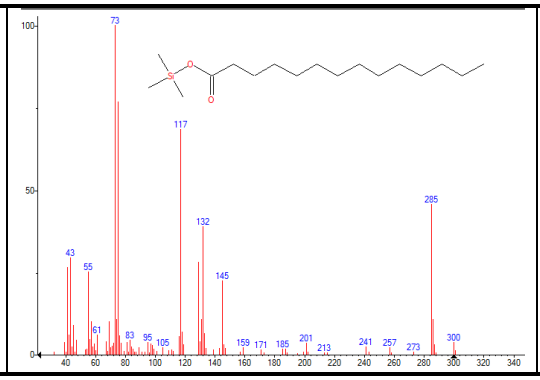	Tetradecanoic acid	(i-iii)

4.4 Detected PH-degrading microorganisms

In all microcosms several PH-degrading microorganisms were identified *(see Fig. 15 and Fig. 16)*, of which the biggest part belonged to the taxonomic group of Bacteria (around 98-99 %). However, only around 1-2 % of identified microorganisms were Archaea. Among detected Bacteria just over 60% were Proteobacteria belonging to the classes of β- and γ-Proteobacteria and Firmicutes belonging to the class of Bacilli. Thereby, in NIT and SUP γ-Proteobacteria dominated while in COM β-Proteobacteria and Bacilli were most prominent. In addition, further bacterial phyla known for their ability to degrade PH like α-Proteobacteria and Chloroflexi were found. In COM also sulfate-reducing Bacteria belonging to the class of δ-Proteobacteria were detected. Among Archaea almost exclusively Euryarchaeota belonging to the class of Methanobacteria were identified. Generally, COM showed higher microbial diversity (Chao-Index: 5942 // Shannon-Index: 8) than NIT and SUP (Chao-Index: 3858 // Shannon-Index: 6).

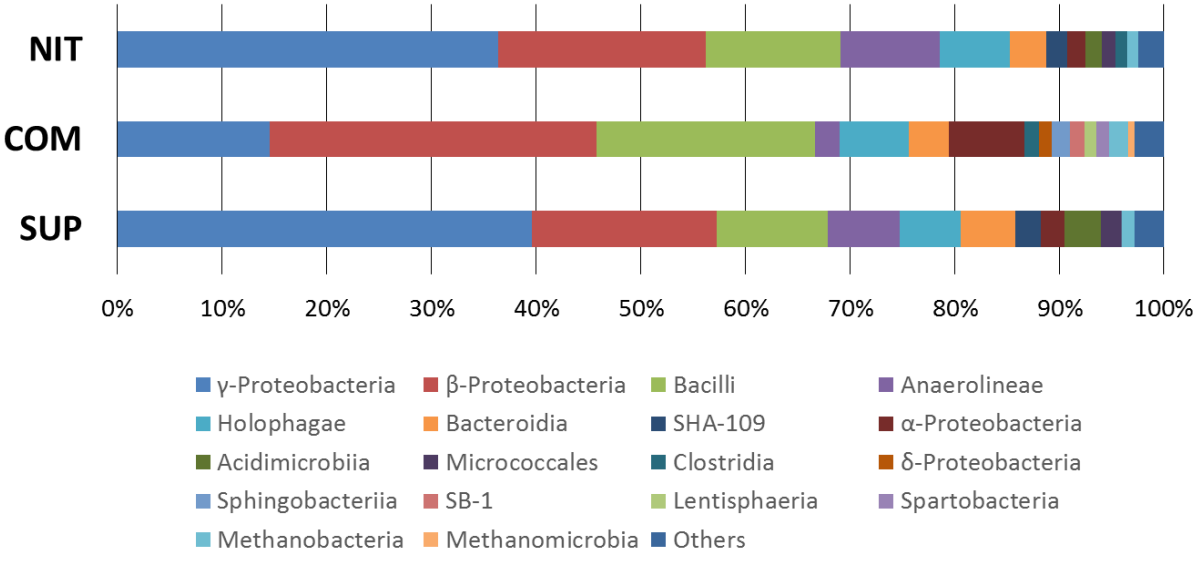

Fig. 15: Relative frequency [%] of Bacteria and Archaea on class-level identified in different microcosms

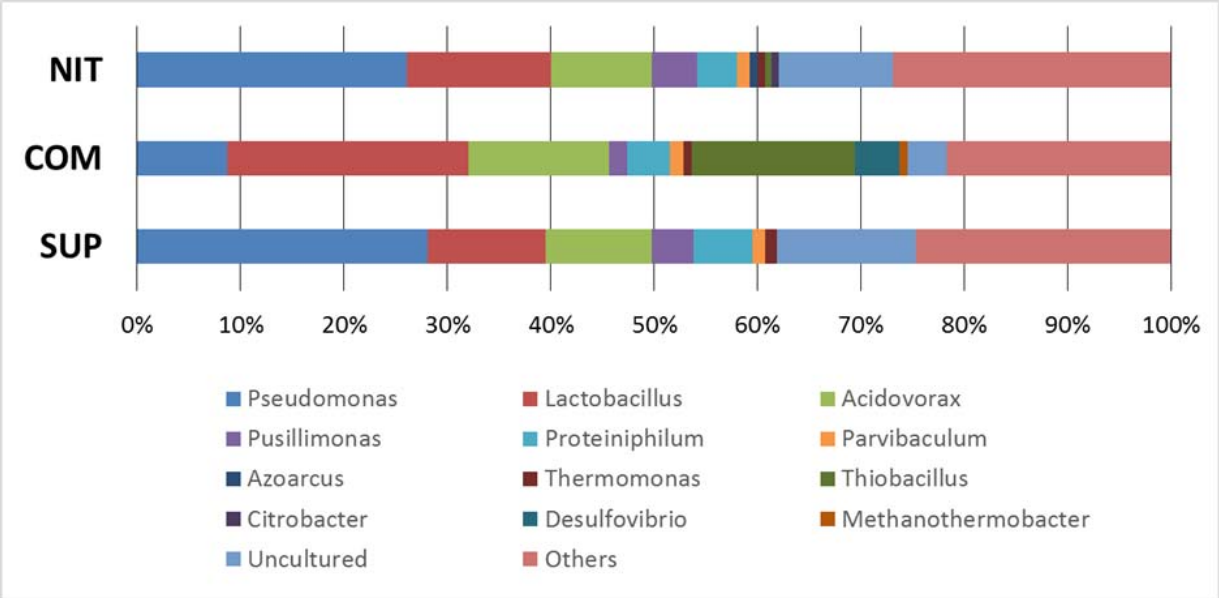

Fig. 16: Relative frequency [%] of Bacteria and Archaea on genus-level identified in different microcosms

4.5 Acceptor sided shifts in stable isotope ratios

Tab. 9 gives an overview about δ-values measured during the experiment. To individual reactors, nitrogen was added as KNO_3 and sulfur in form of Na_2SO_4. Isotopic analysis of these chemicals yielded in $\delta^{15}N$-value of 3.5 ‰ for KNO_3 and $\delta^{34}S$-value of 0.5 ‰ for Na_2SO_4, which agrees very well with the measured δ-values at the beginning of the experiment. In all imposed δ-values an analytical measuring error of ±0.4 ‰ for $\delta^{15}N$ and of ±0.6 ‰ for $\delta^{34}S$ must be considered in consequence of equipment performance.

In all microcosms significant acceptor sided shifts in $^{15}N/^{14}N$ isotope ratios were detected, whereas more prominent shifts occurred in NIT and SUP. Generally, the highest $\delta^{15}N$-shifts were observed in SUP where nitrate depletion was most prominent. In contrast, no significant shifts in $^{34}S/^{32}S$ isotope ratios were observed at COM.

Tab. 9: Acceptor sided stable isotope shifts ($\delta^{15}N$ for nitrate; $\delta^{34}S$ for sulfate) in different microcosms

NIT		**COM**			**SUP**	
Exp. Dur.	**$\delta^{15}N$**	**Exp. Dur.**	**$\delta^{15}N$**	**$\delta^{34}S$**	**Exp. Dur.**	**$\delta^{15}N$**
[d]	*[‰]*	*[d]*	*[‰]*	*[‰]*	*[d]*	*[‰]*
0	3.5	**0**	3.7	0.4	**0**	3.3
15	3.7	**22**	4.6	0.4	**8**	4.3
22	4.9	**139**	5.2	0.7	**57**	5.9
113	6.5	**242**	5.5	1.0	**113**	7.1
133	6.8				**233**	8.3
233	7.2					

Exp. Dur. = Experiment duration
Equipment performance: $\delta^{15}N$ = ±0.4 ‰ /// $\delta^{34}S$ = ±0.6 ‰

4.6 Statistical analysis of correlations between TEA- and TPH-decrease and acceptor sided shifts in stable isotope ratios

For statistical analysis of correlations between TEA- and TPH-decrease and measured shifts in acceptor sided stable isotope ratios linear regression analysis using the programming language R® were performed. Given that no significant shifts in $\delta^{34}S$-values were detected statistical analysis were only performed with nitrate- and TPH-decreases as independent variables (x) and shifts of $\delta^{15}N$-values as dependent variables (y). To check whether the existing data sets fulfill all necessary conditions for the application of a linear regression, Durbin-Watson-Tests and analysis via diagnostic plots were performed (*see Appendix*). All in R® programmed codes and results are given in the appendix of this work.

4.6.1 Correlations between nitrate depletion and acceptor sided $^{15}N/^{14}N$-shifts

In all experiments, the relation between the changes of acceptor sided $^{15}N/^{14}N$ stable isotope ratios over time in the residual nitrate fraction (R_t/R_0) and the corresponding decline in nitrate concentrations (C_t/C_0) could be described with a linear regression. For better demonstration of linear correlations, natural logarithms of (C_t/C_0) as independent variables (x) and of (R_t/R_0) as dependent variables (y) were formed. Results of performed linear regression analysis are shown in Tab. 10.

Tab. 10: Results of performed linear regression analysis with the changes of acceptor sided $^{15}N/^{14}N$ stable isotope ratios over time in the residual nitrate fraction (R_t/R_0) as dependent variables (y) and the respective decline in nitrate concentrations (C_t/C_0) as independent variables (x) for different microcosms

Symbols:	Shortcuts:
o = Measured values Solid line = Estimated linear regression line Dotted lines = 95%-confidence-band Dashed lines = 95%-prediction-band	E = Error Res. Std. Err. = Residual standard error Sig. Level = Significance level Coeff. Det. = Coefficient of determination N_{Tot} = Total number of values N_{Conf} = Number of values within 95%-confidence-band N_{Pred} = Number of values within 95%-prediction-band N_{Cook} = Number of values outside Cook's distance

NIT

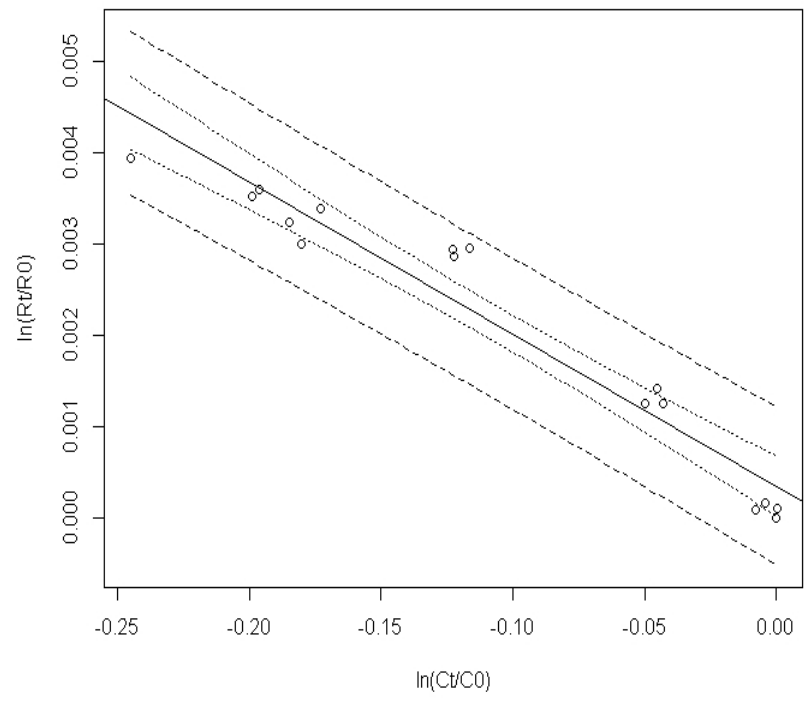

Regression parameters:

Intercept (a) = 0.00035
Slope (b) = -0.0167
Res. Std. Err. (σ) = 0.00037

Regression equation:

Y = 0.00035 + (-0.0167*x) + E

Significance parameters:

Sig. Level (α) = 0.05
p-value = $7.84*10^{-10}$
t-value = -14.52
Significance = Yes

Model quality:

Coeff. Det. (R^2) = 0.9377
N_{Tot} = 16
N_{Conf} = 8/16
N_{Pred} = 16/16
N_{Cook} = 0/16

COM

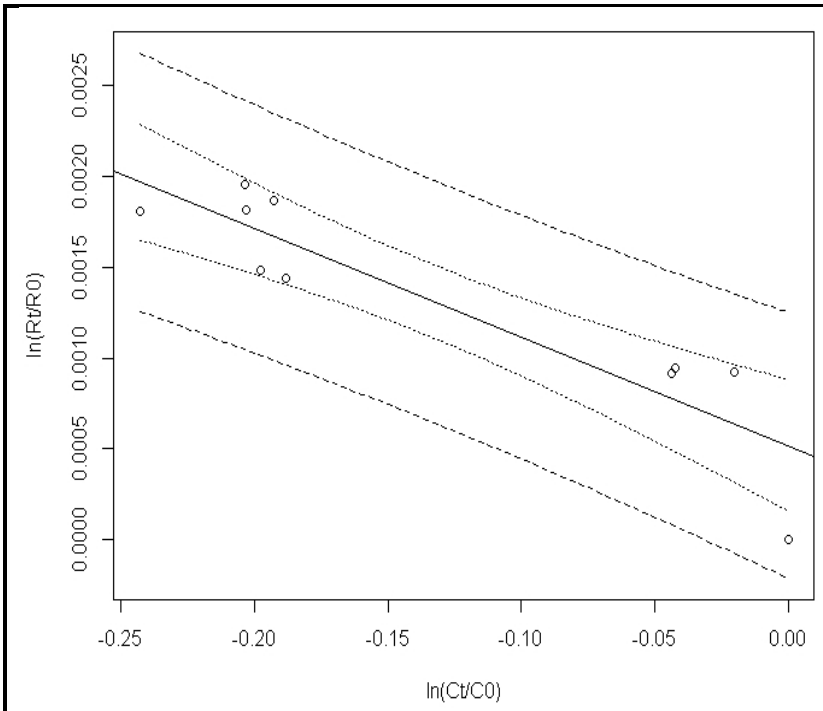

Regression parameters:

Intercept (a) = 0.00052
Slope (b) = -0.006
Res. Std. Err. (σ) = 0.00028

Regression equation:

Y = 0.00052 + (-0.006*x) + E

Significance parameters:

Sig. Level (α) = 0.05
p-value = 0.000293
t-value = -6.09
Significance = Yes

Model quality:

Coeff. Det. (R^2) = 0.8226
N_{Tot} = 10
N_{Conf} = 9/10
N_{Pred} = 10/10
N_{Cook} = 1/10

SUP

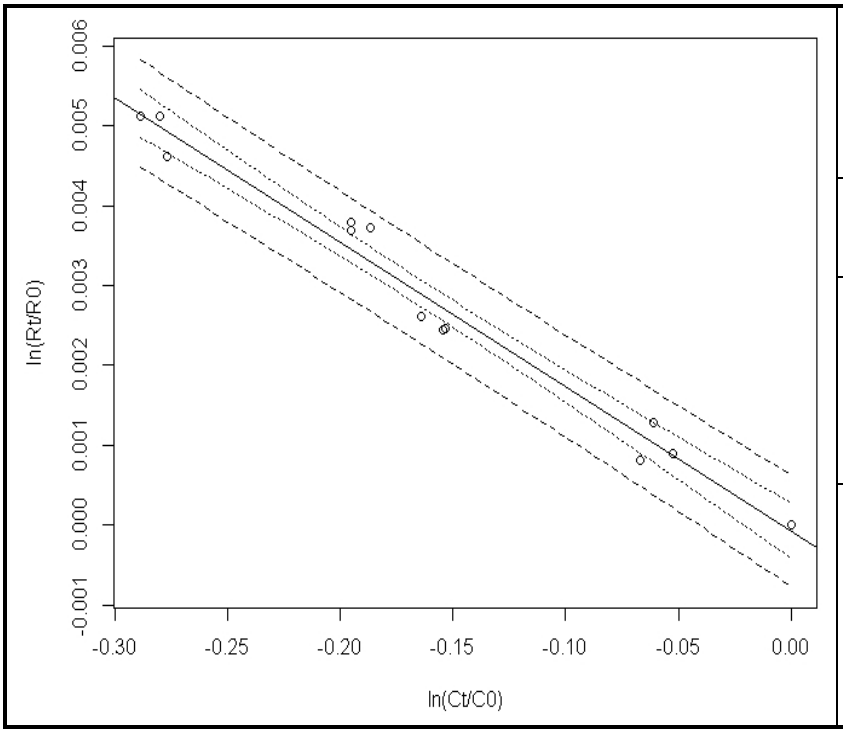

Regression parameters:

Intercept (a) = -0.00007
Slope (b) = -0.0181
Res. Std. Err. (σ) = 0.00028

Regression equation:

Y = -0.00007 + (-0.0181*x) + E

Significance parameters:

Sig. Level (α) = 0.05
p-value = $3.01*10^{-10}$
t-value = -21.098
Significance = Yes

Model quality:

Coeff. Det. (R^2) = 0.9759
N_{Tot} = 13
N_{Conf} = 5/13
N_{Pred} = 13/13
N_{Cook} = 0/13

For all microcosms linear regression models show good statistical correlations between nitrate depletion and shifts in acceptor sided $^{15}N/^{14}N$ stable isotope ratios. Tested against a significance level of α=0.05, for all microcosms a significant linear dependence of $\delta^{15}N$-values in the residual nitrate fraction on the respective decline in nitrate concentrations was found (p-values<0.05; t-values>|1.96|). Furthermore, good model qualities for all performed linear regressions were observed confirmed by R^2-values of at least 0.82. Besides, many values are located within the 95%-confidence-band and even all within the 95%-prediction-band. Moreover, only a few outliers outside of Cook's distance causing leverage effects were detected.

Tab. 11 shows for correlation between $\delta^{15}N$-shifts in the residual nitrate fraction and nitrate depletion detected slopes of the regression lines (b) and therefrom calculated kinetic isotope fractionation factors (α_N) and isotope enrichment factors (ε_N) in different microcosms. For NIT and SUP detected b-values and so α_N- and ε_N-values were relatively similar. However, for COM b-, α_N- and ε_N-values were lower, since in these reactors besides nitrate also sulfate was depleted. For better presentation of this dependence, Fig. 17 shows at different microcosms detected regression lines in one graph.

Tab. 11: For correlation between $\delta^{15}N$-shifts in the residual nitrate fraction and nitrate depletion detected slopes of the regression lines (b) and therefrom calculated kinetic isotope fractionation factors (α_N) and isotope enrichment factors (ε_N) at different microcosms

		NIT	COM	SUP
Slope of the regression line (b)		-0.0167	-0.006	-0.0181
Kinetic isotope fractionation factor (α_N)		0.9833	0.994	0.9819
Isotope enrichment factor (ε_N)	*[‰]*	-16.7	-6	-18.1

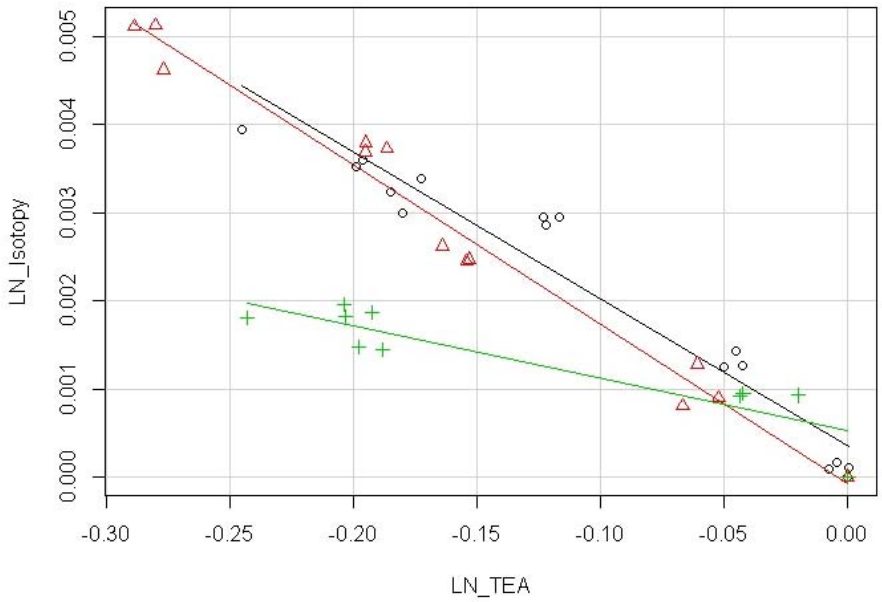

Fig. 17: Contrasting juxtaposition of linear regression lines obtained for correlation between δ[15]N-shifts in the residual nitrate fraction and nitrate depletion at NIT (o, black), at COM (+, green) as well as at SUP (Δ, red)

4.6.2 Correlations between TPH-degradation and acceptor sided $^{15}N/^{14}N$-shifts

In all experiments, significant linear correlations between the changes of acceptor sided $^{15}N/^{14}N$ stable isotope ratios over time in the residual nitrate fraction (R_t/R_0) as dependent variables (y) and the corresponding decline in TPH-concentrations (C_t/C_0) as independent variables (x) were found *(see Tab. 12)*. Again for better demonstration of linear correlations x- and y-values were logarithmized.

As in correlations with nitrate depletion, dependence of regression line slopes (b) and thus, of kinetic isotope fractionation factors ($\alpha_{N\text{-}TPH}$) and isotope enrichment factors ($\varepsilon_{N\text{-}TPH}$) on prevailing electron accepting conditions was also determined at correlations performed between TPH-decrease and shifts in acceptor sided $\delta^{15}N$-values *(see Tab. 13)*. Nevertheless, b-, $\alpha_{N\text{-}TPH}$- and $\varepsilon_{N\text{-}TPH}$-values were lower by approximately 50 % compared to correlations with nitrate depletion. For better representation in Fig. 18 at different microcosms detected regression lines are set against in one graph.

Tab. 12: Results of performed linear regression analysis with the changes of acceptor sided $^{15}N/^{14}N$ stable isotope ratios over time in the residual nitrate fraction (R_t/R_0) as dependent variables (y) and the respective decline in TPH-concentrations (C_t/C_0) as independent variables (x) for different microcosms

Symbols:	Shortcuts:
o = Measured values Solid line = Estimated linear regression line Dotted lines = 95%-confidence-band Dashed lines = 95%-prediction-band	E = Error Res. Std. Err. = Residual standard error Sig. Level = Significance level Coeff. Det. = Coefficient of determination N_{Tot} = Total number of values N_{Conf} = Number of values within 95%-confidence-band N_{Pred} = Number of values within 95%-prediction-band N_{Cook} = Number of values outside Cook's distance

NIT

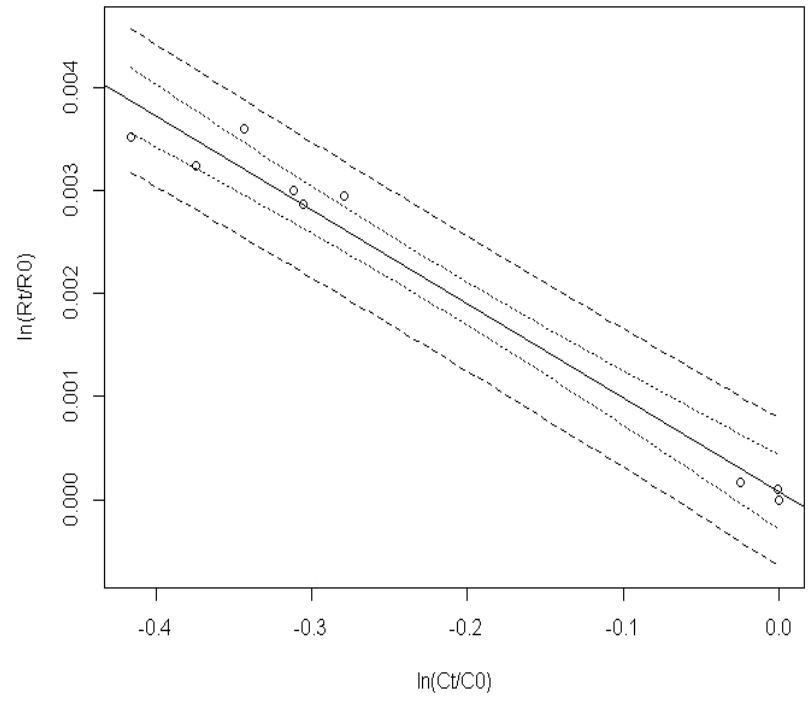

Regression parameters:

Intercept (a) = 0.00007
Slope (b) = -0.0091
Res. Std. Err. (σ) = 0.00026

Regression equation:

Y = 0.00007 + (-0.0091*x) + E

Significance parameters:

Sig. Level (α) = 0.05
p-value = $6.64*10^{-7}$
t-value = -16.742
Significance = Yes

Model quality:

Coeff. Det. (R^2) = 0.9756
N_{Tot} = 9
N_{Conf} = 6/9
N_{Pred} = 9/9
N_{Cook} = 0/9

COM

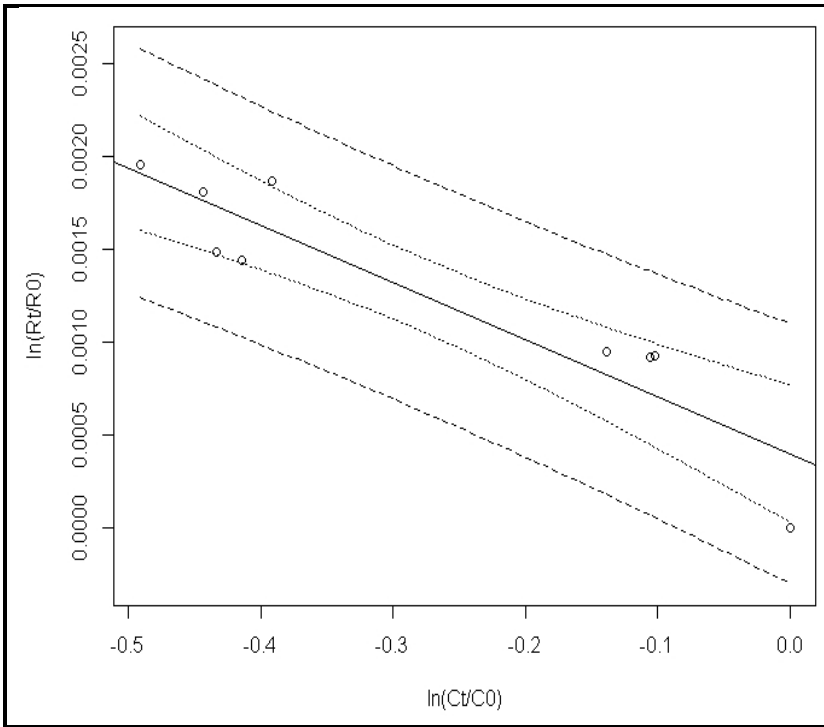

Regression parameters:

Intercept (a) = 0.0004
Slope (b) = -0.0031
Res. Std. Err. (σ) = 0.00025

Regression equation:

Y = 0.0004 + (-0.0031*x) + E

Significance parameters:

Sig. Level (α) = 0.05
p-value = 0.000327
t-value = -6.522
Significance = Yes

Model quality:

Coeff. Det. (R^2) = 0.8587
N_{Tot} = 9
N_{Conf} = 2/9
N_{Pred} = 9/9
N_{Cook} = 1/9

SUP

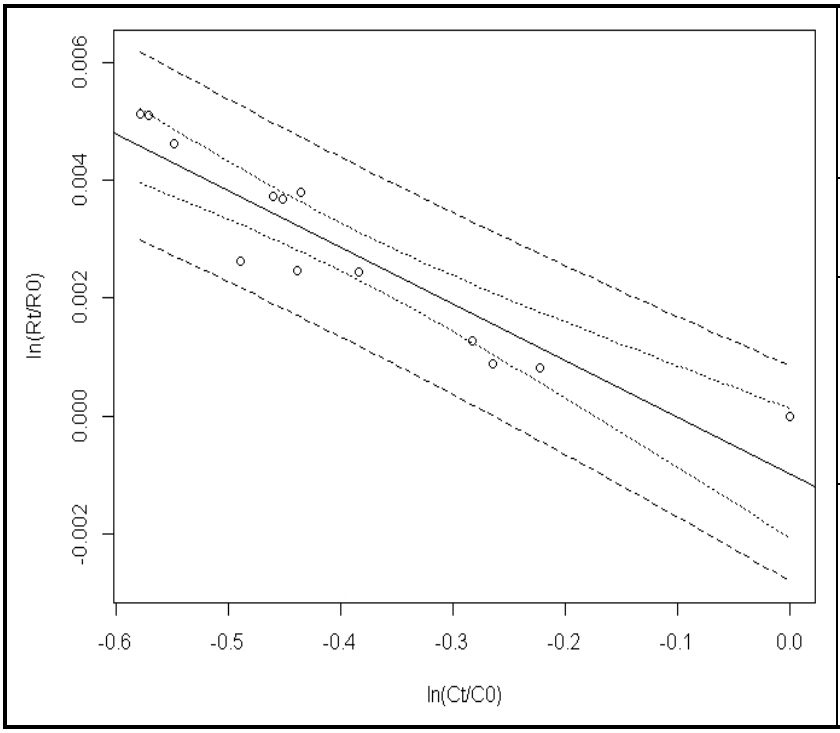

Regression parameters:

Intercept (a) = -0.00097
Slope (b) = -0.0096
Res. Std. Err. (σ) = 0.00067

Regression equation:

Y = -0.00097 + (-0.0096*x) + E

Significance parameters:

Sig. Level (α) = 0.05
p-value = $5.31*10^{-6}$
t-value = -8.175
Significance = Yes

Model quality:

Coeff. Det. (R^2) = 0.8587
N_{Tot} = 13
N_{Conf} = 4/13
N_{Pred} = 13/13
N_{Cook} = 1/13

Tab. 13: For correlation between $\delta^{15}N$-shifts in the residual nitrate fraction and TPH-degradation detected slopes of the regression lines (b) and therefrom calculated kinetic isotope fractionation factors ($\alpha_{N\text{-}TPH}$) and isotope enrichment factors ($\varepsilon_{N\text{-}TPH}$) at different microcosms

		NIT	COM	SUP
Slope of the regression line (b)		-0.0091	-0.0031	-0.0096
Kinetic isotope fractionation factor ($\alpha_{N\text{-}TPH}$)		0.9909	0.9969	0.9904
Isotope enrichment factor ($\varepsilon_{n\text{-}TPH}$)	*[‰]*	-9.1	-3.1	-9.6

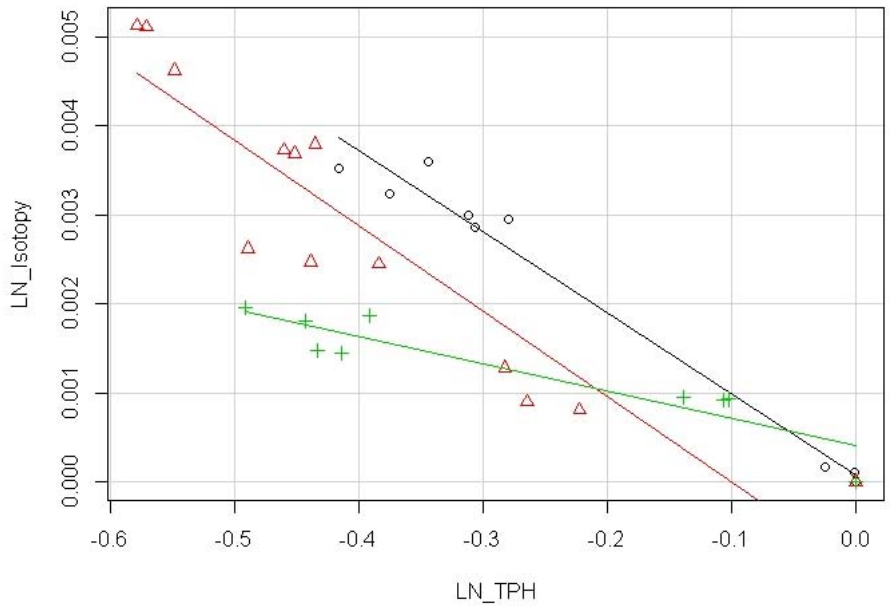

Fig. 18: Contrasting juxtaposition of linear regression lines obtained for correlation between $\delta^{15}N$-shifts in the residual nitrate fraction and TPH-degradation at NIT (o, black), at COM (+, green) as well as at SUP (Δ, red)

5 Discussion

5.1 Observed decline in concentrations of alternative TEA and TPH

Within the present study, anaerobic biodegradation of historically PH contaminated aquifer material supplemented with paraffin-rich crude oil was analyzed in lab-scale experiments using different alternative electron acceptors. Thereby, significant TPH-decrease was detected under all electron accepting conditions *(see Tab. 6 and Fig. 13)*. In NIT, average TEA-depletion was 0.024 $mmol*L^{-1}d^{-1}$, while corresponding TPH-degradation rate amounted to 24.8 $mg*kg^{-1}d^{-1}$ (0.07 $mmol*kg^{-1}d^{-1}$ according to n-C_{25}), corresponding in relation to the initial concentration to a decrease of 31.6 % over 233 days. In contrast, at SUP TEA-depletion was 0.032 $mmol*L^{-1}d^{-1}$ and TPH-degradation rate amounted to 28.3 $mg*kg^{-1}d^{-1}$ (0.08 $mmol*kg^{-1}d^{-1}$ according to n-C_{25}), equal to 43.2 % degradation over the same period. In COM nitrate depletion represented 0.026 $mmol*L^{-1}d^{-1}$, while the sulfate depletion rate was only 0.012 $mmol*L^{-1}d^{-1}$ over 233 days. During the same period TPH-degradation rate amounted to 27.6 $mg*kg^{-1}d^{-1}$ (0.08 $mmol*kg^{-1}d^{-1}$ according to n-C_{25}), corresponding to a decrease of 35.7 %. Similar degradation rates were also detected in other studies investigating anaerobic biodegradation of TPH. For example, Hasinger et al. (2012) obtained an average TPH-degradation rate of 28 $mg*kg^{-1}d^{-1}$ under nitrate-reducing conditions over an experiment period of 185 days in laboratory experiments conducted with aquifer material from the same site. However, it should be noted that degradation rates strongly depend on prevailing experiment conditions, including microbial community composition, and therefore can be very diverse (Blume et al., 2010). Besides reduction of nitrate and sulfate no relevant depletion of other TEA like ferric iron(III), manganese(IV) and CO_2 was observed.

In all microcosms, only little accumulation of nitrite as intermediate product of nitrate reduction *(see Fig. 11)* and no accumulation of sulfide as intermediate product of sulfate reduction was found. Besides, no precipitations like FeS_2 (pyrite) formed by these compounds were detected. For example at NIT only around 1.4 % of depleted nitrate were stoichiometrically recovered as nitrite. The occurrence of accumulation of nitrite or sulfide depends very much on the amount in which various enzymes are formed during anaerobic degradation process. So for example nitrite accumulation occurs if nitrate reductase, which induces reduction of nitrate to nitrite, is completely synthetized, while for further reduction of nitrite necessary nitrite reductase is not fully formed (Chyabutra et al., 2000; Fuchs et al., 2014). Since nitrite and sulfide have toxic effects on microorganisms and therefore can inhibit degradation process or even cause cell death (Chyabutra et al., 2000; O'Flaherty et al., 1998), no significant accumulations of these compounds should occur, as it was observed in the current experiment.

Comparing the results obtained at microcosms with different TEA amendment, differences and similarities can be found. While after 233 days NIT and COM showed similar average nitrate consumption rates, nitrate depletion in SUP was significantly higher. Thereby, in SUP the detected nitrate consumption was most notably higher in the first period of the experiment. In contrast to TEA, after 233 days no significant diverse TPH-degradation

rates between different microcosms were observed. Nevertheless, also here SUP showed higher TPH-degradation at the first period of the experiment. Given that the only difference between these and the other microcosms is in the addition of sodium molybdate for sulfate reduction suppression, a relation to this compound can be assumed *(see Chapter 5.5)*. In COM the observed sulfate depletion rate was much lower than simultaneously detected nitrate consumption. The preferential use of nitrate over sulfate if both alternative TEA are added together was already noted in other studies (e.g. Cunningham et al., 2000; Cunningham et al., 2001; Dou et al., 2008). This effect results from higher energy yield for microorganisms using nitrate as alternative TEA instead of sulfate (Roychoudhury and Merrett, 2006; Thauer et al., 1977; Wisotzky, 2011). So for degradation of n-C_6 Spormann and Widdel (2000) observed -492.8 kJ released Gibbs free energy per mol reduced nitrate, while released energy was only -44.2 kJ per mol sulfate reduced. Heider et al. (1999) and Widdel and Rabus (2001) established even by a factor of 15 higher Gibbs free energy available for microorganisms when using nitrate instead of sulfate. In addition, the observed effect can also be explained by the fact, that sulfate has a lower reactivity than nitrate (Thauer et al., 1977).

5.2 Stoichiometric considerations

For stoichiometric considerations, since the TPH-fraction has no uniform molar weight, concentrations were related to n-C_{25} as model compound. Using this compound appears justified because it elutes exactly in the middle of the observed retention time window between n-C_{10} and n-C_{40}. Furthermore, using the molar weight of an aliphatic rather than of an aromatic compound seems justified, since used aquifer material was contaminated with paraffin-rich crude oil which mainly contains n-alkanes. Following stoichiometric equations, for anaerobic biodegradation of 1 mol n-C_{25} either 30.4 mol of nitrate or 19 mol of sulfate are required, which results in stoichiometric ratios of 1:30.4 and 1:19.0, respectively (Haeseler et al., 2010). Considerably lower ratios were detected in the present study *(see Tab. 7)*. Thus, in NIT and in SUP ratios were 1:5.3 and 1:6.1, respectively (day 233). At COM ratios were 1:5.0 for nitrate and 1:2.0 for sulfate (day 242). Fundamentally lower ratios were also obtained in other studies. In a similar experiment Hasinger et al. (2012) detected a requirement of 4.3 mol nitrate for reducing 1 mol of n-C_{25}. Within the current experiment the observed lower ratios at COM can partly be explained by the fact that in these reactors for degradation of TPH besides nitrate also sulfate was used. Since all other reactors only contain nitrate and ferric iron(III) as well as manganese(IV) reduction was negligible, this explanation is insufficient. Moreover, in effect ratios would be even higher because those compounds containing less than 10 and more than 40 carbon atoms, which may also be degraded, are not considered in the calculation used for TPH-concentrations. For this reason, lower TEA-requirements observed in the experiment can only be explained by incomplete degradation of PH, which was confirmed by detection of several metabolites *(see Chapter 5.3)*.

5.3 Detected metabolites of PH-degradation

Microbial metabolism of PH to CO_2 and H_2O proceeds via several consecutive metabolic steps. So for the degradation of relatively inert PH, microorganisms primarily have to transform them into more polar and thus better water-soluble intermediate products (Blume et al., 2010; Fuchs et al., 2014). While under aerobic conditions this transformation process always starts with oxidation catalyzed by the enzyme monooxygenase or dioxygenase, activation of hydrocarbons follows fundamentally different and diverse pathways in absence of oxygen (Andrade et al., 2012; Grossi et al., 2008; Spormann and Widdel, 2000; Widdel and Rabus, 2001). Generally, in the course of all of these pathways intermediate products like succinates, alcohols and fatty acids are formed (Bian et al., 2015; Gieg and Suflita, 2002; Grossi et al., 2008; SLUG, 2000). Since these metabolites exhibit a higher polarity than their parent compounds (Beller et al., 1995; Cravo-Laureau et al., 2005; Gieg and Suflita, 2002), they pass into the aqueous phase and cannot be detected on unpolar GC-systems. Moreover, metabolites containing OH- or COOH-groups can form hydrogen bonds between the different compounds, which may cause weak volatility, insufficient thermal stability or even interactions of the compounds with the column surface and as a consequence, poor acquisition on detector (Schummer et al., 2009). One practical option in order to reduce polarity of these compounds and so to make them measurable is derivatisation (Cazes, 2004).

During the present experiment from aqueous supernatants extracted intermediate products were derivatized using BSTFA. Thereby, the active proton (H^+) in for example OH- or COOH-groups of metabolites is replaced by a trimethylsilyl-group ($Si[CH_3]_3$), which leads to formation of nonpolar trimethylsilylesters (Rontani et al., 2008; Schummer et al., 2009). Accordingly, qualitative and semi-quantitative analysis by GC-MS was performed. Thereby, several silylated succinates, alcohols and fatty acids could be identified respective to their mass spectra *(see Tab. 8)*. Nevertheless, it was not possible to relate all peaks of obtained GC-MS chromatograms to a special compound because many peaks were overlapping each other or were too small for reliable identification. At most mass spectra of identified trimethylsilylated metabolites the molecular ion peak $[M]^+$ specifying the molecular weight of the compound was only slightly pronounced. However, all mass spectra showed a predominant $[M - 15]^+$ ion peak, on which the molecular mass of the silylated compound can be calculated. This $[M - 15]^+$ ion peak is caused by the cleavage of one methyl-group (CH_3) from the molecule and is typical for silylated compounds (Cravo-Laureau et al., 2005; Rontani et al., 2008; Schummer et al., 2009). Hence, this ion peak was already detected in other studies dealing with trimethylsilylated intermediate products of PH-biodegradation (Callaghan et al., 2009; Cravo-Laureau et al., 2005; Gieg and Suflita, 2002; Rontani et al., 2008). In addition, all mass spectra analyzed in the present study show a peak at m/z 73 which derives from the trimethylsilyl-group in the derivatized metabolite (Gieg and Suflita, 2002; Pierce, 1968).

Looking at in different microcosms identified metabolites *(see. Tab. 8)* it becomes apparent that most of these compounds resulted from biodegradation of aliphatic hydrocarbons. Since the paraffin-rich crude oil used for the current experiment mainly contains n-alkanes this observation can be well explained. Anyway, also benzoic acid as typical metabolite of

benzene degradation was found (Schauer and Sietmann, 2010). If individual microcosms are compared, some metabolites were observed in all reactors, while others only prevailed in only nitrate (NIT and SUP) or also sulfate containing microcosms (COM). In contrast, between NIT and SUP no differences were observed according to qualitative metabolite recovery. This may be related to the fact that other microbial populations can proliferate under nitrate-reducing conditions compared to mixed electron accepting conditions.

When comparing GC-MS spectra obtained during this experiment in different microcosms semi-quantitatively *(see Fig. 14)*, amounts of metabolites found in NIT and SUP were similar, while significant lower amounts of intermediate products were detected at COM. This observation indicates more complete PH degradation under mixed electron accepting conditions. In a study performed by Boopathy (2004) faster and more complete biodegradation of hydrocarbons under mixed electron conditions was reported as well. First, this effect may be the result of a larger total amount of electron acceptors if both are added. Furthermore, one possible explanation for this observation relies on the fact that under mixed electron accepting conditions as well nitrate-reducing and sulfate-reducing microorganisms and thus, a more heterogeneous microbial population can establish. Since the anaerobic biodegradation of PH always requires collaboration of different microbial strains, where produced metabolites of one organism are substrate for the next one, this can lead to faster and more complete biodegradation of PH (Merretig-Bruns and Jelen, 2009). Exactly this effect could be observed within the current experiment, as microbial diversity was higher in COM (Chao-Index: 5942 // Shannon-Index: 8) than in NIT and SUP (Chao-Index: 3858 // Shannon-Index: 6). Finally, more complete degradation may also contribute to Gibbs free energy obtained by microorganisms from reduction of different compounds. Generally, released Gibbs free energy is higher by reducing nitrate than those gained by sulfate reduction (Roychoudhury and Merrett, 2006; Thauer et al., 1977; Wisotzky, 2011). Thus, if both nitrate and sulfate are available, most compounds are preferentially biodegraded using nitrate (Gödeke et al., 2003; Haeseler et al., 2010; Werner, 2009). But especially for more complex compounds the preferred metabolism was found using sulfate instead of nitrate as electron acceptor (Hasinger et al., 2012), which results from higher additional energy gain for microorganisms (Spormann and Widdel, 2000). In summary it can be stated that some compounds are degraded favorably under nitrate-reducing conditions, while others are more likely metabolized using sulfate as electron acceptor. From this it can be assumed that if both electron acceptors are available, more compounds can be degraded completely.

5.4 Identified microorganisms

Today many microorganisms capable of metabolising PH under anaerobic conditions using several alternative TEA like nitrate or sulfate are known (Grossi et al., 2008; Spormann and Widdel, 2000; Wentzel et al., 2007; Werner, 2009; Widdel and Rabus, 2001). Also within the present study numerous PH-degrading microorganisms were identified *(see Fig. 15 and Fig. 16).* Thereby, in all microcosms around 98-99 % of detected microorganisms belonged to the taxonomic group of Bacteria, while only 1-2 % were Archaea belonging to the class of Methanobacteria. This observation corresponds to the

fact that most PH degrading microorganisms are Bacteria (Leahy and Colwell, 1990; Widdel and Rabus, 2001). Among Bacteria especially those of the phylum Proteobacteria are well known for biodegradation of PH (Werner, 2009; Widdel and Rabus, 2001). Over 60 % of within the present study at different microcosms detected organisms were Proteobacteria belonging to the classes of β- and γ-Proteobacteria and Firmicutes belonging to the class of Bacilli. Thereby, in NIT and SUP γ-Proteobacteria dominated while in COM β-Proteobacteria and Bacilli were most prominent. Among β-Proteobacteria microorganisms of the genus *Acidovorax* and *Pusillimonas* were identified in all microcosms. For both of these two bacterial organisms capability for anaerobic PH-biodegradation was shown (Cao et al., 2011; Eriksson et al., 2003; Lu, 2014; Singleton et al., 2009). Additionally, organisms of the genus *Thiobacillus* were detected mainly in COM. This bacterial genus is known to perform anaerobic biodegradation of hydrocarbons in contaminated aquifers (Alfreider et al., 2002). Among γ-Proteobacteria especially organisms of the genus *Pseudomonas* were identified, for which the ability to mineralize n-alkanes and naphthalene using nitrate as electron acceptor is already proven (Grossi et al., 2008; Rockne et al., 2000). In the class of Bacilli microorganisms of the genus *Lactobacillus* were predominant. Although this microbial strain is rather known for its benevolent role in the production of dairy products like yoghurt (Omogbai et al., 2005) or cheese (Blaiotta et al., 2001), it has even potential for biodegradation of crude oil (Thavasi, 2006; Thavasi et al., 2011). By the way, also α-Proteobacteria like *Parvibaculum* were identified, which often occur at PH contaminated sites (Paixão et al., 2010) and thus presumably play an important role in the breakdown of these compounds (Schleheck et al., 2011). Moreover, it was possible to identify further microorganisms known for degradation of hydrocarbons under anaerobic conditions like genera belonging to the phylum of Chloroflexi (Savage et al., 2010). In COM also sulfate-reducing microorganisms belonging to the class of δ-Proteobacteria like *Desulfovibrio* were detected. Although biodegradation of n-alkanes by *Desulfovibrio* was even reported in the 1960s (Davis and Yarbrough, 1966), since then this process could not be observed again (Fukui et al., 1999). Also in the present experiment this bacterial strain did not play a major role in biodegradation of PH since no accumulation was observed.

5.5 The role of molybdenum

Molybdenum, a transition metal, has numerous biological functions (Dobbek, 2000). It forms the active center of many microbial enzymes. Furthermore, highly oxidized molybdates consisting of Mo(VI) and oxoanions (MoO_4^{2-}) show great solubility and therefore are readily bioavailable (Hagel, 2006). Since molybdate is stereochemically similar to sulfate and blocks the enzyme ATP-sulfurylase, even low concentrations can inhibit the process of sulfate reduction (Hasnain and Anderson, 2005; Ranade et al., 1999; Reuveny, 1976; Smith and Klug, 1980). In order to achieve exactly this effect, during the current experiment to one part of microcosms containing only nitrate as TEA sodium molybdate (Na_2MoO_4) was added (SUP). Thereby, in SUP notably higher nitrate- and TPH-degradation rates were observed within the first period of the experiment than in NIT. Given that the only difference between SUP and NIT is the addition of sodium molybdate,

a relation to this compound can be assumed. However, since even at the beginning of the experiment at microcosms detected sulfate concentrations were below the detection limit, this observation cannot be attributed to the inhibitory effect on sulfate-reduction caused by sodium molybdate. Hence, it is obvious to look for an explanation on the enzymatic level.

A possible explanation for the significantly higher nitrate reduction in SUP may rely on the molybdenum containing enzyme nitrate reductase. This enzyme catalyzes the reduction of nitrate to nitrite as the first step of nitrate reduction (Cypionka, 2010; Fuchs et al., 2014; Wisotzky, 2011). Since molybdenum constitutes an important part of nitrate reductase, it is obvious that the addition of molybdate enhances the activity of this enzyme and thus, reduction of nitrate to nitrite. Exactly this effect was shown in a study of Vega et al. (1971), where increasing activity of nitrate reductase was determined with gradually increasing amendment of molybdate. Looking at nitrite concentrations obtained within the present study *(see Fig. 11)*, this explanation can be confirmed. Especially during the first 28 days of the experiment a prominent increase in nitrite concentrations was observed in SUP, while significantly lower increases were detected at NIT. The fact that nitrite concentrations fell again in further progress of the experiment can be explained by higher expression of nitrite reductase induced by increasing nitrite quantities (Chyabutra et al., 2000).

A similar explanation can also be found for the higher TPH-degradation rates at SUP observed during the first period of the experiment *(see Tab. 6 and Fig. 13)*. For this, the so called molybdenum-hydroxylases may be responsible. These enzymes have the capability to hydroxylate a large number of aliphatic and aromatic hydrocarbons deriving necessary oxygen atom from cleavage of water rather than from O_2 (Dobbek, 2000; Hille, 1996; Hille, 2004). Thereby, alcohols and phenols are formed as intermediate products (Brückner, 2004; Fuchs et al., 2014). By the addition of molybdate, activity of these enzymes and therefore transformation of hydrocarbons to hydroxylated metabolites can be increased (Hille, 1996; Magalon et al., 2011). Since these intermediate products exhibit higher polarity and therefore cannot be measured with unpolar GC-FID-systems (Beller et al., 1995; Cravo-Laureau et al., 2005; Gieg and Suflita, 2002; Hasinger et al., 2012), this leads to decreasing detected TPH-concentrations. Within the present study exactly this process was observed. So especially during the first period of the experiment higher TPH-degradation rates and more rapid formation of metabolites were observed at SUP in contrast to the other reactors. At this point, however, it should be noted that amendment of molybdate can only accelerate hydroxylation of hydrocarbons to intermediate products but not the whole process of PH-degradation. Moreover, higher concentrations of molybdate have toxic effects on organisms and environment (Biswas et al., 2009; Blume et al., 2010; Ranade et al., 1999), wherefore this compound is not suitable for improvement of biodegradation process.

5.6 Observed shifts in acceptor sided stable isotope ratios

Since microorganisms use lighter isotopes in preference to heavier ones, during biodegradation isotope ratios of compounds involved into the reaction are shifted. Thereby, an enrichment of heavier isotopes in residual substrates and of lighter isotopes in

degradation products appears, which as well at side of PH as of TEA leads to a shift from lighter to heavier isotopes and so to increasing δ-values (Cichocka et al., 2008; Fischer et al., 2004; Meckenstock et al., 2004; Nagel et al., 2011). In contrast to most existing studies, in which during the process of anaerobic PH-biodegradation occurring pollutant sided shifts in $^{13}C/^{12}C$ isotope ratios are reviewed (e.g. Jaeckel et al., 2014; Meckenstock et al., 1999; Morasch et al., 2001; Richnow et al., 2003; Stelzer et al., 2006), within the present study shifts of stable isotope ratios were analyzed on side of TEA. Thus, δ-values of acceptor sided shifts in $^{15}N/^{14}N$ and $^{34}S/^{32}S$ isotope ratios were determined for nitrate and sulfate, respectively *(see Tab. 9)*. Thereby, in all microcosms significant shifts in $\delta^{15}N$-values were seen. While in NIT $\delta^{15}N$-value increased by 3.7 over 242 days, SUP showed significantly higher increase of 5. This observation can be explained by the fact that in SUP depletion rate of nitrate was even higher. In contrast, COM showed the lowest increase of $\delta^{15}N$-value with 1.8 over 242 days, which was conditioned by simultaneous depletion of sulfate. Looking at $\delta^{34}S$-values no significant shifts were observed at COM, which can be explained by the fact that also in these microcosms nitrate was used preferentially over sulfate. To date there are existing only a few studies dealing with acceptor sided shifts in $\delta^{15}N$- and $\delta^{34}S$-values during anaerobic biodegradation of PH (e.g. Fischer et al., 2004; Gödeke et al., 2003; Knöller et al., 2011; Su et al., 2013). But since these studies were performed under completely different experimental conditions, a comparison to the presently obtained δ-values is not possible.

5.7 Observed correlations between TEA- and TPH-decrease and acceptor sided shifts in stable isotope ratios

During the present study the observed TEA- and TPH-decreases (C_t/C_0) in different microcosms were contrasted with simultaneously occurring changes of acceptor sided stable isotope ratios in the residual nitrate fraction (R_t/R_0). Since no significant changes in $^{34}S/^{32}S$ isotope ratios were detected over the experiment period, comparisons were only performed with shifts in $\delta^{15}N$-values. Thereby, in all microcosms significant linear correlations with R^2-values higher than 0.82 were found *(see Tab. 10 and Tab. 12)*. Additionally, kinetic isotope fractionation factors (α) as well as isotope enrichment factors (ε) were calculated from obtained slopes of the regression lines (b) *(see Tab. 11 and Tab. 13)*. Thereby, at all microcosms the observed b-, $\alpha_{N\text{-}TPH}$- and $\varepsilon_{N\text{-}TPH}$-values for correlations with TPH-degradation were lower by approximately 50 % in comparison to correlations with nitrate depletion. Comparing between detected b-, α- and ε-values in different microcosms, as well for correlations with nitrate depletion as for correlation with TPH-decrease NIT and SUP showed similar values. In contrast, significantly lower values were observed in COM. This fact confirms dependence of b-, α- and ε-values on prevailing electron accepting conditions and on the existing microbial consortium which also was pointed out in other studies (Knöller et al., 2011; Nijenhuis et al., 2005; Nikolausz et al., 2006).

Basically, from correlations between $\delta^{15}N$-shifts and respective nitrate depletion calculated ε_N-values are between -40 and -5 ‰ for degradation of pollutants with nitrate as sole TEA (Lehmann et al., 2003). So in batch experiments performed by Knöller et al. (2011)

ε_N-values between -16.2 and -8.6 ‰ were found for nitrate-reducing degradation of toluene and succinate. Also in the present experiment similar ε_N-values were observed. Thus, in NIT and SUP ε_N-values were -16.7 ‰ and -18.1 ‰, respectively. In contrast, at COM for $^{15}N/^{14}N$ fractionation detected ε_N-value constitutes only -6 ‰, for which no comparable isotope enrichment factor was found in literature.

In contrast, within this study detected $\varepsilon_{N\text{-}TPH}$-values for NIT, SUP and COM calculated from correlations between $\delta^{15}N$-shifts and TPH-decrease were -9.1 ‰, -9.6 ‰ and -3.1 ‰, respectively. These $\varepsilon_{N\text{-}TPH}$-values observed in the present study represent a novelty, since in commonly available literature dealing with anaerobic biodegradation of PH no isotope enrichment factors calculated from correlation of acceptor sided isotope ratios with respective TPH-decrease were found.

5.8 *In situ* monitoring of PH-biodegradation based on acceptor sided stable isotope ratios as a new monitoring approach

In recent years there have been great efforts to use shifts in stable isotope ratios for qualitative and quantitative *in situ* monitoring of PH-biodegradation (Förstner, 2012; Meckenstock et al., 2004; Stelzer, 2008). The big advantage of this method relies on the fact that abiotic concentration-reducing processes, like volatilization, sorption or dilution, which only lead to relocation but not to degradation of pollutants have no significant influence on isotope fractionation (Aelion et al., 2009; Harrington et al., 1999; Hunkeler et al., 2004; Slater et al., 2000; Wisotzky, 2011). Thus, analysis of stable isotope ratios allows in contrast to other monitoring methods direct detection of PH-biodegradation (Hunkeler et al., 2008; Meckenstock et al., 2004). In most cases for prediction of TPH-depletion necessary isotope enrichment factors (ε) are calculated from correlations between shifts in pollutant sided $^{13}C/^{12}C$ isotope ratios and respective TPH-decline (e.g. Fischer et al., 2008; Kniemeyer et al., 2007; Meckenstock et al., 1999; Richnow et al., 2003; Vieth and Wilkes, 2006; Wilkes et al., 2008). Nevertheless, this method is problematic because due to different chain lengths of PH dilution of the measured isotopic shifts occurs, which can lead to incorrect predictions (Aelion et al., 2009; Hunkeler et al., 2008; Meckenstock et al., 2004; Morasch et al., 2004; Stelzer, 2008). Hence, in the present study shifts in acceptor sided isotope ratios were used. Thus, the observed TPH-decreases (C_t/C_0) in different microcosms were contrasted with simultaneously occurring changes of acceptor sided stable isotope ratios in the residual nitrate fraction (R_t/R_0). Thereby, good statistical correlations between $^{15}N/^{14}N$ shifts and TPH-depletion were found for all microcosms which allowed for the calculation of corresponding $\varepsilon_{N\text{-}TPH}$-values. This renders the prediction of anaerobic biodegradation based on isotope fractionation on side of TEA possible, whereby at complex compounds like PH occurring pollutant sided dilution effect of isotope shifts can be avoided. For this reason, this method for *in situ* monitoring of anaerobic PH-biodegradation can be regarded as very promising.

Anyway, for application in practice also in this case it has to be noted that prevailing electron accepting conditions and existing microbial consortia influence the slope of the regression line (b) and therefore the obtained $\varepsilon_{N\text{-}TPH}$-value, as it was shown in the current

as well as in other studies (Knöller et al., 2011; Nijenhuis et al., 2005; Nikolausz et al., 2006). Since at contaminated sites predominating environmental conditions and therefore existing microbial consortia can be very diverse, this can lead to over- or underestimation of actually occurring degradation process, which is the most prominent reason calling for caution in a possible application of this method in the field. Therefore, it is essential to calculate the obtained $\varepsilon_{N\text{-}TPH}$-values from correlations between acceptor sided isotope fractionation and respective TPH-decrease also under other electron accepting conditions using different microbial strains and PH-matrices, wherefore numerous lab-scale experiments simulating different circumstances as well as field tests still need to be carried out. Only after $\varepsilon_{N\text{-}TPH}$-values occurring under various conditions have been determined, this method can be applied in practice for reliable *in situ* monitoring of anaerobic PH-biodegradation.

6 Conclusion and Outlook

Within the present study, long-term microbial degradation experiments for anaerobic biodegradation of PH were carried out in the laboratory scale. Thereby, biodegradation of a PH-contaminated sandy aquifer material was simulated in batch reactors (i) with nitrate as sole TEA, (ii) with both nitrate and sulfate amendment as well as (iii) with nitrate under sulfate reduction suppression.

The analysis of microbial community composition showed diverse consortia prevailing in different microcosms. Generally, biodegradation of TPH was most complete at microcosms containing both nitrate and sulfate, since at these microcosms significantly lower amounts of metabolites were detected. These observations indicate the usefulness of a mixed electron accepting system to remove PH under anaerobic conditions. Since to date only a few studies dealing with biodegradation under mixed electron accepting conditions are available, further research is necessary in this area. In contrast, no significantly different degradation rates were detected between microcosms with nitrate as sole TEA and those under sulfate reduction suppression. Only during the first period of the experiment higher TPH-degradation rates were observed in microcosms containing sodium molybdate for sulfate reduction suppression. In the present study this effect was found to be caused by higher activity of molybdenum-hydroxylases in consequence of sodium molybdate amendment which leads to accelerate hydroxylation of hydrocarbons to intermediate products. So it could be shown that sodium molybdate can expedite the initial activation of PH, i.e. the rate limiting step, but not the whole degradation process. Nevertheless, higher concentrations of molybdate have toxic effects on organisms and environment, wherefore this compound is not suitable for improvement of biodegradation process.

Furthermore, the main objective of this study was reached, since good correlations between acceptor sided shifts in isotope ratios and respective TPH-decreases were found for all microcosms. So it was shown that qualitative and quantitative *in situ* monitoring of PH-biodegradation can also be conducted based on acceptor sided isotope fractionation, whereby at complex compounds like PH occurring pollutant sided dilution effect of isotope shifts can be avoided. For that reason, this method for *in situ* monitoring of anaerobic PH-biodegradation can be regarded as very promising. Nonetheless, results obtained in the present study only show the first steps towards a possible application, i.e. the conceptual applicability of this method. Since correlations can be very diverse in different environmental conditions, for a possible future practical application further studies on this topic are required on lab-scale as well as in the field.

7 References

7.1 Bibliography

Aeckersberg, F., Bak, F. and Widdel, F. (1991): Anaerobic oxidation of saturated hydrocarbons to CO_2 by a new type of sulfate-reducing bacterium. Archives of Microbiology 156, p. 5-14

Aeckersberg, F., Rainey, F.A. and Widdel, F. (1998): Growth, natural relationships, cellular fatty acids and metabolic adaptation of sulfate-reducing bacteria that utilize long-chain alkanes under anoxic conditions. Achieves of Microbiology 170, p. 361-369

Aelion, C.M., Höhener, P., Hunkeler, D. and Aravena, R. (2009): Environmental Isotopes in Biodegradation and Bioremediation. 1st edition. CRC Press, Boca Raton

Alfreider, A., Vogt, C. and Babel, W. (2002): Microbial Diversity in an *in situ* Reactor System Treating Monochlorobenzene Contaminated Groundwater as Revealed by 16S Ribosomal DNA Analysis. Systematic and Applied Microbiology 25, p. 232-240

Andrade L.L., Leite, D.CA., Ferreira, E.M., Ferreira, L.Q., Paula, G.R., Maguire, M.J., Hubert, C.RJ., Peixoto, R.S., Domingues, R.MCP. and Rosado, A.S. (2012): Microbial diversity and anaerobic hydrocarbon degradation potential in an oil-contaminated mangrove sediment. BMC Microbiology 12, p. 186-195

Atlas, R.M. (1981): Microbial Degradation of Petroleum Hydrocarbons: an Environmental Perspective. Microbiological Reviews 45, p. 180-209

Ball, H.A., Johnson, H.A., Reinhard, M. and Spormann, A.M. (1996): Initial reactions in anaerobic ethylbenzene oxidation by a denitrifying bacterium, strain EB1. Journal of Bacteriology 178, p. 5755-5761

Beller, H. R. and Edwards, E.A (2000): Anaerobic toluene activation by benzylsuccinate synthase in a highly enriched methanogenic culture. Applied Environmental Microbiology 66, p. 5503-5505

Beller, H.R. and Spormann, A.M. (1997): Anaerobic activation of toluene and o-xylene by addition to fumarate in denitrifying strain T. Journal of Bacteriology 179, p. 670-676

Beller, H.R., Ding, W.H. and Reinhard, M. (1995). Byproducts of anaerobic alkylbenzene metabolism useful as indicators of *in situ* bioremediation. Environmental Science and Technology 29, p. 2864-2870

Bian, X.Y., Mbadinga, S.M., Liu, Y.F., Yang, S.Z., Liu, Y.F., Ye, R.Q., Gu, Y.D. and Mu, B.Z. (2015): Insight into the Anaerobic Biodegradation Pathway of n-Alkanes in Oil Reservoirs by Detection of Signature Metabolites. Scientific Reports 5, p. 9801-9813

Biegert, T., Fuchs, G. and Heider, J. (1996): Evidence that oxidation of toluene in the denitrifying bacterium Thauera aromatica is initiated by formation of benzylsuccinate from toluene and fumarate. European Journal of Biochemistry 238, p. 661-668

Biswas, K.C., Woodards, N.A., Xu, H. and Barton L.L. (2009): Reduction of molybdate by sulfate-reducing bacteria. Biometals 22, p. 131-139

Blaiotta, G., Moschetti, G., Simeoli, E., Andolfi, R., Villani, F. and Coppola, S. (2001): Monitoring lactic acid bacteria strains during 'Cacioricotta' cheese production by restriction endonuclease analysis and pulsed-field gel electrophoresis. Journal of Dairy Research 68, p. 139-144

Blume, H.P., Brümmer, G.W., Horn, R., Kandeler, E., Kögel-Knabner, I., Kretzschmar, R., Stahr, K. and Wilke, B.M. (2010): Lehrbuch der Bodenkunde. 16th edition. Spektrum Akademischer Verlag, Heidelberg

Boetius, A., Ravenschlag, K., Schubert, C.J., Rickert, D., Widdel, F., Gieseke, A., Amann, R., Jørgensen, B.B., Witte, U. and Pfannkuche, O. (2000): A marine microbial consortium apparently mediating anaerobic oxidation of methane. Nature 407, p. 623-626

Boley, C. (Ed.), Adam, D., Bente, S., Börger, R., Dausch, G., Englert, K. et al. (2012): Handbuch Geotechnik. 1st edition. Vieweg+Teubner Verlag, Wiesbaden

Boll, M., Fuchs, G and Heider, J. (2002): Anaerobic oxidation of aromatic compounds and hydrocarbons. Current Opinion in Chemical Biology 6, p. 604-611

Boopathy, R. (2003): Use of anaerobic soil slurry reactors for the removal of petroleum hydrocarbons in soil. International Biodeterioration & Biodegradation 52, p. 161-166

Boopathy, R. (2004): Anaerobic biodegradation of no. 2 diesel fuel in soil - A soil column study. Bioresource Technology 94, p. 143-151

Brückner, R. (2004): Reaktionsmechanismen: Organische Reaktionen, Stereochemie, Moderne Synthesemethoden. 3rd edition. Spektrum Akademischer Verlag, Heidelberg

Caldwell, M.E., Garrett, R.M., Prince, R.C. and Suflita, J.M. (1998): Anaerobic Biodegradation of Long-Chain n-Alkanes under Sulfate-Reducing Conditions. Environmental Science and Technology 32, p. 2191-2195

Callaghan, A.V., Davidova, I.A., Savage-Ashlock, K., Parisi, V.A., Gieg, L.M., Suflita, J.M., Kukor, J.J. and Wawrik, B. (2010): Diversity of benyzl- and alkylsuccinate synthase genes in hydrocarbon-impacted environments and enrichment cultures. Environmental Science & Technology 44, p. 7287-7294

Callaghan, A.V., Gieg, L.M., Kropp, K.G., Suflita, J.M. and Young, L.Y. (2006): Comparison of Mechanisms of Alkane Metabolism under Sulfate-Reducing Conditions among Two Bacterial Isolates and a Bacterial Consortium. Applied and Environmental Microbiology 72, p. 4274-4282

Callaghan, A.V., Tierney, M., Phelps, C.D. and Young L.Y. (2009): Anaerobic Biodegradation of n-Hexadecane by a Nitrate-Reducing Consortium. Applied and Environmental Microbiology 75, p. 1339-1344

Callaghan, A.V., Warwik, B., Chadain, S.M.N., Young, L.Y. and Zylstra, G.J. (2008): Anaerobic alkane-degrading strain AK-01 contains two alkylsuccinate synthase genes. Biochemical and Biophysical Research Communications 366, p. 142-148

Cao, B., Ma, T., Ren, Y., Ren, Y., Li, G., Li, P., Guo, X., Ding, P. and Feng, L. (2011): Complete Genome Sequence of Pusillimonas sp. T7-7, a Cold-Tolerant Diesel Oil-Degrading Bacterium Isolated from the Bohai Sea in China. Journal of Bacteriology 193, p. 4021-4022

Cazes, J. (Ed.) (2004): Analytical Instrumentation Handbook. 3rd edition. CRC Press, Boca Raton

Chyabutra, C. and Ju, L.K. (2000): Degradation of n-Hexadecane and Its Metabolites by Pseudomonas aeruginosa under Microaerobic and Anaerobic Denitrifying Conditions. Applied and Environmental Microbiology 66, p. 493-498

Cichocka, D., Imfeld, G., Richnow, H.H. and Nijenhuis, I. (2008): Variability in microbial carbon isotope fractionation of tetra- and trichloroethene upon reductive dechlorination. Chemosphere 71, p. 639-648

Clark, I. and Fritz, P. (1997): Environmental isotopes in hydrogeology. 1st edition. CRC Press, Boca Raton

Cooney, J.J., Silver, S.A. and Beck, E.A. (1985): Factors influencing hydrocarbon degradation in three freshwater lakes. Microbial Ecology 11, p. 127-137

Cravo-Laureau, C., Grossi, V., Raphel, D., Matheron, R. and Hirschler-Réa, A. (2005): Anaerobic n-Alkane Metabolism by a Sulfate-Reducing Bacterium, Desulfatibacillum aliphaticivorans Strain CV2803. Applied and Environmental Microbiology 71, p. 3458-3467

Cravo-Laureau, C., Matheron, R., Joulian, C., Cayol, J.L. and Hirschler-Réa, A. (2004): Desulfatibacillum alkenivorans sp. nov., a novel n-alkene-degrading, sulfate-reducing bacterium, and emended description of the genus Desulfatibacillum. International Journal of Systematic and Evolutionary Microbiology 54, p. 1639-1642

Cunningham, J.A., Hopkins, G.D., Lebron, C.A. and Reinhard, M. (2000): Enhanced anaerobic bioremediation of groundwater contaminated by fuel hydrocarbons at Seal Beach, California. Biodegradation 11, p. 159-170

Cunningham, J.A., Rahme, H., Hopkins, G.D., Lebron, C. and Reinhard, M. (2001): Enhanced *In Situ* Bioremediation of BTEX-Contaminated Groundwater by Combined Injection of Nitrate and Sulfate. Environmental & Science Technology 35, p. 1663-1670

Cypionka, H. (2010): Grundlagen der Mikrobiologie. 4th edition. Springer Verlag, Berlin-Heidelberg

Das, S. (2014): Microbial Biodegradation and Bioremediation. 1st edition. Elsevier, London

Davidova, I.A., Gieg, L.M., Nanny, M., Kropp, K.G. and Suflita, J.M. (2005): Stable isotopic studies of n-alkane metabolism by a sulfate-reducing bacterial enrichment culture. Applied and Environmental Microbiology 71, p. 8174-8182

Davis, J.B and Yarbrough, H.F (1966): Anaerobic oxidation of hydrocarbons by Desulfovibrio desulfuricans. Chemical Geology 1, p. 137-144

Dendrou, S., Dendrou, B. and Tumay, M. (2000): Advanced Risk-Based Biodegradation Study Using Environmental Information System and the Holistic Macroengineering Approach. In: Wise, D.L., Trantolo, D.J., Cichon, E.J., Inyang, H.I. and Stottmeister, U. (Eds.): Remediation Engineering of Contaminated Soils. 1st edition. Marcel Dekker Inc., New York

Dobbek, H. (2000): Röntgenstrukturanalyse von Molybdän-haltigen Kohlenmonoxid-Dehydrogenasen. Dissertation. Technical University, Munich

Dou, J., Liu, X., Hu, Z. and Deng, D. (2008): Anaerobic BTEX biodegradation linked to nitrate and sulfate reduction. Journal of Hazardous Materials 151, p. 720-729

Eggeling, L. and Bott, M. (2005): Handbook of Cornebacterium glutamicum. 1st edition. CRC Press, Boca Raton

Ehrenreich, P., Behrends, A. Harder, J. and Widdel, F. (2000): Anaerobic oxidation of alkanes by newly isolated denitrifying bacteria. Archives of Microbiology 173, p. 58-64

Eriksson, M., Sodersten, E., Yu, Z., Dalhammar, G. and Mohn, W.W. (2003): Degradation of Polycyclic Aromatic Hydrocarbons at Low Temperature under Aerobic and Nitrate-Reducing Conditions in Enrichment Cultures from Northern Soils. Applied and Environmental Microbiology 69, p. 275-284

Evans, P.J., Mang, D.T., Kim, K.S. and Young, L.Y. (1991): Anaerobic degradation of toluene by a denitrifying bacterium. Applied and Environmental Microbiology 57, p. 1139-1145

Fischer, A., Herklotz, I., Hermann, S., Thullner, M., Weeling, S.A.B., Stams, A.J.M., Schlomann, M., Richnow, H.H. and Vogt, C. (2008): Combined carbon and hydrogen isotope fractionation investigations for elucidating benzene biodegradation pathways. Environmental Science & Technology 42, p. 4356-4363

Fischer, A., Vieth, A., Knöller, K., Wachter, T., Dahmke, A. and Richnow, H.H. (2004): Charakterisierung des mikrobiellen Schadstoffabbaus mithilfe von isotopenchemischen Methoden. Grundwasser - Zeitschrift der Fachsektion Hydrogeologie 3, p. 159-172

Förstner, U. (2012): Umweltschutztechnik. 8th edition. Springer Verlag, Berlin-Heidelberg

Fuchs, G. (Ed.), Eitinger, T., Heider, J., Kemper, B., Kothe, E., Overmann, J., Schink, B., Schneider, E. and Unden, G. (2014): Allgemeine Mikrobiologie. 9th edition. Georg Thieme Verlag, Stuttgart

Fukui, M., Harms, G., Rabus, R., Schramm, A., Widdel, F., Zengler, K., Boreham, C. and Wilkes, H. (1999): Anaerobic degradation of oil hydrocarbons by sulfate-reducing and nitrate-reducing bacteria. Microbial Ecology of Oil Fields, s.p.

Gieg, L.M. and Suflita, J.M. (2002): Detection of Anaerobic Metabolites of Saturated and Aromatic Hydrocarbons in Petroleum-Contaminated Aquifers. Environmental and Science and Technology 36, p. 3755-3762

Gilewicz, M., Monpert, G., Acquaviva, M., Mille, G. and Bertrand, J.C. (1991): Anaerobic oxidation of 1-n-heptadecene by a marine denitrifying bacterium. Applied Microbiology and Biotechnology 36, p. 252-256

Gödeke, S., Weiß, H., Trabitzsch, R., Vogt, C., Wachter, T. and Schirmer, M. (2003): Benzenabbau im Grundwasser unter verschiedenen Redox-Bedingungen. Zeitschrift der Fachsektion Hydrogeologie 4, p. 232-237

Granzin, S. and Valtl, M. (2015): Verdachtsflächenkataster und Altlastenatlas. Report of the Austrian Federal Environment Agency. Austrian Federal Environment Agency, Vienna

Grossi, V., Cravo-Laureau, C., Guyoneaud, R., Ranchou-Peyruse, A. and Hirschler-Réa, M.A. (2008): Metabolism of n-alkanes and n-alkenes by anaerobic bacteria: A summary. Organic Geochemistry 39, p. 1197-1203

Grossi, V., Cravo-Laureau, C., Méou, A., Raphel, D., Garzino, F. and Hirschler-Réa, A. (2007): Anaerobic 1-Alkene Metabolism by the Alkane- and Alkene-Degrading Sulfate Reducer Desulfatibacillum aliphaticivorans Strain CV2803. Applied and Environmental Microbiology 73, p. 7882-7890

Grossi, V., Cravo-Laureau, C., Rontani, J.F., Cros, M. and Hirschler-Réa, A. (2011): Anaerobic oxidation of n-alkenes by sulphate-reducing bacteria from the genus Desulfatiferula: n-Ketones as potential metabolites. Research in Microbiology 162, p. 915-922

Haeseler, F., Behar, F., Garnier, D. and Chenet, P.Y. (2010): First stoichiometric model of oil biodegradation in natural petroleum systems Part I - The BioClass 0D approach. Organic Geochemistry 41, p. 1156-1170

Hagel, C. (2006): Struktur und Funktion der Ethylbenzol Dehydrogenase, einer anaeroben Kohlenwasserstoff-Hydroxylase. Dissertation. University Darmstadt, Darmstadt

Hamby, D.M. (1996): Site remediation techniques supporting environmental restoration activities: A review, http://web.engr.oregonstate.edu/~hambydm/papers/remedrev.pdf (Access on 11/08/15)

Harrington, R.R., Poulson, S.R., Drever, J.I., Colberg, P.J.S. and Kelly, E.F. (1999): Carbon isotope systematics of monoaromatic hydrocarbons: vaporization and adsorption experiments. Organic Geochemistry 30, p. 765-775

Harwood, C.S., Burchardt, G., Herrmann H. and Fuchs, G. (1999): Anaerobic metabolism of aromatic compounds via the benzoyl-CoA pathway. FEMS Microbiology Reviews 22, p. 439-458

Hasinger, M., Scherr, K.E., Bogolte, B.T., Soja, G., Todorovic, D. and Loibner, A.P. (2011): Biologische Sanierung von MKW und PAK in der gesättigten Bodenzone - Selektive Unterstützung von mikrobiologischen Abbauprozessen, http://www.umweltfoerderung.at/uploads/2011_technarbeitshilfe_abbauprozesse2.pdf (Access on 09/12/14)

Hasinger, M., Scherr, K.E., Lundaa, T., Bräuer, L., Zach, C. and Loibner, A.P. (2012): Changes in iso- and n-alkane distribution during biodegradation of crude oil under nitrate and sulphate reducing conditions. Journal of Biotechnology 157, p. 490-498

Hasnain I.M. and Anderson, G.K. (2005): Molybdate inhibition of sulphate reduction in two-phase anaerobic digestion. Process Biochemistry 40, p. 2079-2089

Heider, J. (2007): Adding handles to unhandy substrates: anaerobic hydrocarbon activation mechanism. Current Opinion in Chemical Biology 11, p. 188-194

Heider, J. (2008): Anaerober Kohlenwasserstoff-Abbau - Es geht auch ohne Sauerstoff. BIOspektrum 14, p. 28-31

Heider, J., Spormann, A.M., Beller, H.R. and Widdel, F. (1999): Anaerobic bacterial metabolism of hydrocarbons. FEMS Microbiology Reviews 22, p. 459-473

Hessische Landesamt für Umwelt und Geologie - HLUG (2005): Auswertung von Mineralöl-Gaschromatogrammen, http://www.hlug.de/fileadmin/dokumente/altlasten/handbuch/hba35_web.pdf (Access on 09/12/14)

Hille, R. (1996): The Mononuclear Molybdenum Enzymes. Chemical Reviews 96, p. 2757-2816

Hille, R. (2002): Molybdenum and tungsten in biology. Trends in Biochemical Science 27, p. 360-367

Hille, R. (2004): Molybdenum-containing hydroxylases. Archives of Biochemistry and Biophysics 433, p. 107-116

Hinrichs, K.U., Hayes, J., Sylva, S., Brewer, P. and DeLong, E. (1999): Methane consuming archaebacteria in marine sediments. Nature 398, p. 802-805

Hoefs, J. (2015). Stable Isotope Geochemistry. 7th edition. Springer Verlag, Berlin-Heidelberg

Hofstetter, T.B., Schwarzenbach, R.P. and Bernasconi, S.M. (2008): Assessing Transformation Processes of Organic Compounds Using Stable Isotope Fractionation. Environmental Science & Technology 42, p. 7737-7743

Holliger, C. and Zehnder, A.J.B. (1996): Anaerobic biodegradation of hydrocarbons. Current Opinion in Biotechnology 7, p. 326-330

Hunkeler, D., Anderson, N., Aravena, R., Bernasconi, S.M. and Butler, B.J. (2001): Hydrogen and Carbon Isotope Fractionation during Aerobic Biodegradation of Benzene. Environmental & Science Technology 35, p. 3462-3467

Hunkeler, D., Chollet, N., Pittet, X., Aravena, R., Cherry, J.A. and Parker, B.L. (2004): Effect of source variability and transport processes on carbon isotope ratios of TCE and PCE in two sandy aquifers. Journal of Contaminant Hydrology 74, p. 265-282

Hunkeler, D., Meckenstock, R.U., Lollar, B.S., Schmidt, T. and Wilson, K.T. (2008): A Guide for Assessing Biodegradation and Source Identification of Organic Ground Water Contaminants using Compound Specific Isotope Analysis (CSIA). Report on behalf of the United States Environmental Protection Agency. Office of Research and Development, Ada

International Energy Agency - IEA (2014): Key World Energy Statistics 2014, http://www.iea.org/publications/freepublications/publication/keyworld2014.pdf (Access on 09/08/15)

Jaeckel, U., Vogt, C., Fischer, A., Richnow, H.H. and Musat, F. (2014): Carbon and hydrogen stable isotope fractionation associated with the anaerobic degradation of propane and butane by marine sulfate-reducing bacteria. Environmental Microbiology 16, p. 130-140

Johnson, H.A., Pelletier, D.A. and Spormann, A.M. (2001): Isolation and characterization of anaerobic ethylbenzene dehydrogenase, a novel Mo-Fe-S enzyme. Journal of Bacteriology 183, p. 4536-4542

Johnston, D.T., Farquhar, J., Summons, R.E., Shen, Y., Kaufman, A.J., Masterson, A.L. and Canfield, D.E. (2008): Sulfur isotope biogeochemistry of the Proterozoic McArthur Basin. Geochimica et Cosmochimica Acta 72, p. 4278-4290

Jones, D.M., Head, I.M., Gray, M.D., Adams, J.J., Rowan, A.K., Aitken, C.M., Bennett, B., Huang, H., Brown, A., Bowler, B.F.J., Oldenburg, T., Erdmann, M. and Larter S.R. (2008): Crude-oil biodegradation via methanogenesis in subsurface petroleum reservoirs. Nature 451, p. 176-180

Kane, S.R., Beller, H.R., Legler, T.C. and Anderson, R.T. (2002): Biochemical and genetic evidence of benzylsuccinate synthase in toluene-degrading, ferric iron-reducing Geobacter metallireducens. Biodegradation 13, p. 149-154

Kato, T., Haruki, M., Imanaka, T., Morikawa, M. and Kanaya, S. (2001): Isolation and characterization of long-chain-alkane degrading Bacillus thermoleovorans from deep subterranean petroleum reservoirs. Journal of Bioscience and Bioengineering 91, p. 64-70

Kendall, C. and Caldwell, E.A. (1998): Fundamentals of Isotope Geochemistry. In: Kendall, C. and McDonnell, J.J. (Eds.): Isotope Tracers in Catchment Hydrology. 1st edition. Elsevier Science B.V., Amsterdam

Kiss, S., Pasca, D. and Dragan-Bularda, M. (Eds.) (1998): Enzymology of Disturbed Soils. 1st Edition. Elsevier Science B.V., Amsterdam

Kniemeyer, O. and Heider, J. (2001a): (S)-1-Phenylethanol dehydrogenase of Azoarcus sp. strain EbN1, an enzyme of anaerobic ethylbenzene catabolism. Achieves of Microbiology 176, p. 129-135

Kniemeyer, O. and Heider, J. (2001b): Ethylbenzene dehydrogenase, a novel hydrocarbon-oxidizing molybdenum/iron-sulfur/heme enzyme. Journal of Biological Chemistry 276, p. 21381-21386

Kniemeyer, O., Fischer, T., Wilkes, H., Glöckner, F.O. and Widdel, F. (2003): Anaerobic Degradation of Ethylbenzene by a New Type of Marine Sulfate-Reducing Bacterium. Applied and Environmental Microbiology 69, p. 760-768

Kniemeyer, O., Musat, F., Sievert, S.M., Knittel, K., Wilkes, H., Blumenberg, M., Michaelis, W., Classen, A., Bolm, C., Joye, S.B. and Widdel, F. (2007): Anaerobic oxidation of short-chain hydrocarbons by marine sulfate-reducing bacteria. Nature 449, p. 898-902

Knöller, K., Vogt, C., Haupt, M., Feisthauer, S. and Richnow, H.H. (2011): Experimental investigation of nitrogen and oxygen isotope fractionation in nitrate and nitrite during denitrification. Biogeochemistry 103, p. 371-384

Kopinke, F.D., Georgi, A., Voskamp, M. and Richnow H.H. (2005): Carbon Isotope Fractionation of Organic Contaminants Due to Retardation on Humic Substances: Implications for Natural Attenuation Studies in Aquifers. Environmental Science & Technology 39, p. 6052-6062

Kropp, K.G., Davidova, I.A. and Suflita, J.M. (2000): Anaerobic oxidation of n-dodecane by an addition reaction in a sulfate-reducing bacterial enrichment culture. Applied and Environmental Microbiology 66, p. 5393-5398

Kube, M., Heider, J., Amann, J., Hufnagel, P., Kuhner, S., Beck, A., Reinhardt, R. and Rabus, R. (2004): Genes involved in the anaerobic degradation of toluene in a denitrifying bacterium, strain EbN1. Archives of Microbiology 181, p. 182-194

Lal, B. and Khanna, S. (1996): Degradation of crude oil by Acinetobacter calcoaceticus and Alcaligenes odorans. Journal of Applied Bacteriology 81, p. 355-362

Langenhoff, A.A.M., Nijenhuis, I., Tan, N.C.G., Briglia, M., Zehnder, A.J.B. and Schraa, G. (1997a): Characterisation of a mangenese-reducing, toluene-degrading enrichment culture. FEMS Microbiology Ecology 24, p. 113-125

Langenhoff, A.A.M., Brouwers-Ceiler, D.L., Engelberting, J.H.L., Quist, J.J., Wolkenfelt, J.G.P.M., Zehnder, A.J.B. and Schraa, G. (1997b): Microbial reduction of manganese coupled to toluene oxidation. FEMS Microbiology Ecology 22, p. 119-127

Le Corfec, Y. (2011): Sites et sols pollués - Gestion des passifs environnementaux. 1st edition. Dunod, Paris

Leahy, J.G. and Colwell, R.R. (1990): Microbial Degradation of Hydrocarbons in the Environment. Microbiological Reviews 54, p. 305-315

Lehmann, M.F., Reichert, P., Bernasconi, S.M., Barbieri, A. and McKenzie, J.A. (2003): Modelling nitrogen and oxygen isotope fractionation during denitrification in a lacustrine redox-transition zone. Geochimica et Cosmochimica Acta 67, p. 2529-2542

Leuthner, B. and Heider, J. (2000): Anaerobic toluene catabolism of Thauera aromatica: the bbs operon codes for enzymes of β oxidation of the intermediate benzylsuccinate. Journal of Bacteriology 182, p. 272-277

Leutwein, C. and Heider, J. (2002): (R)-Benzylsuccinyl-CoA dehydrogenase of Thauera aromatica, an enzyme of the anaerobic toluene catabolic pathway. Archives of Microbiology 178, p. 517-524

Lovley, D.R., Baedecker, M.J., Lonergan, D.J., Cozzarelli, I.M., Phillips, E.J.P. and Siegel, O.I. (1989): Oxidation of aromatic contaminants coupled to microbial iron reduction. Nature 339, p. 297-300

Lu, L., Yazdi, H., Jin, S., Zuo, Y., Fallgren, P.H. and Ren Z.J. (2014): Enhanced bioremediation of hydrocarbon-contaminated soil using pilot-scale bioelectrochemical systems. Journal of Hazardous Materials 274, p. 8-15

Lu, Z. (2014): Identifying Dominant Anaerobic Microorganisms for Degradation of Benzene. Dissertation. University of Saskatchewan, Saskatoon

Magalon, A., Fedor, J.G., Walburga, A. and Weiner, J.H. (2011): Molybdenum enzymes in bacteria and their maturation. Coordination Chemistry Reviews 255, p. 1159-1178

Marquardt, H., Schäfer, S.G. and Barth, H. (Eds.) (2013): Toxikologie. 3rd edition. Wissenschaftliche Verlagsgesellschaft, Stuttgart

Meckenstock, R.U., Morasch, B., Griebler, C. and Richnow, H.H. (2004): Stable isotope fractionation analysis as a tool to monitor biodegradation in contaminated aquifers. Journal of Contaminant Hydrology 75, p. 215-255

Meckenstock, R.U., Morasch, B., Warthmann, R., Schink, B., Annweiler, E., Michaelis, W. and Richnow, H.H. (1999): $^{13}C/^{12}C$ isotope fractionation of aromatic hydrocarbons during microbial degradation. Environmental Microbiology 1, p. 409-414

Merretig-Bruns, U. and Jelen, E. (2009): Anaerobic Biodegradation of Detergent Surfactants. Materials 2, p. 181-206

Michels, J., Track, T., Gehrke, U. and Sell, D. (2001): Leitfaden - Biologische Verfahren zur Bodensanierung. Report on behalf of the German Federal Ministry of Education and Research. German Federal Environment Agency, Dessau-Roßlau

Mizuno, O., Li, Y.Y. and Noike, T. (1998): The behavior of sulfate-reducing bacteria in acidogenic phase of anaerobic digestion. Water Research 32, p. 1626-1634

Morasch, B. and Meckenstock, R.U. (2005): Anaerobic degradation of p-xylene by a sulfatereducing enrichment culture. Current Microbiology 51, p. 127-130

Morasch, E., Richnow, H.H., Schink, B. and Meckenstock R.U. (2001): Stable Hydrogen and Carbon Isotope Fractionation during Microbial Toluene Degradation: Mechanistic and Environmental Aspects. Applied and Environmental Microbiology 67, p. 4842-4849

Morasch, E., Richnow, H.H., Schink, B., Vieth, A. and Meckenstock R.U. (2002): Carbon and Hydrogen Stable Isotope Fractionation during Aerobic Bacterial Degradation of Aromatic Hydrocarbons. Applied and Environmental Microbiology 68, p. 5191-5194

Morasch, E., Richnow, H.H., Vieth, A., Schink, B. and Meckenstock R.U. (2004): Stable Isotope Fractionation Caused by Glycyl Radical Enzymes during Bacterial Degradation of Aromatic Compounds. Applied and Environmental Microbiology 70, p. 2935-2940

Mortimer, C.E., Müller, U. and Beck, J. (2014): Chemie - Das Basiswissen der Chemie. 11th edition. Georg Thieme Verlag, Stuttgart

Mosey, F.E (1983): Mathematical modelling of the anaerobic digestion process: regulatory mechanisms for the formation of short-chain volatile acids from glucose. Water Science and Technology 15, p. 209-232

Myers, C.R. and Nealson, K.H. (1988): Bacterial manganese reduction and growth with manganese oxide as the sole electron acceptor. Science 240, p. 1319-1321

Nagel, A., Strauss, H., Stephan, M. and Achten, C. (2011): Nachweis von Natural Attenuation mittels Isotopenuntersuchungen an einem ehemaligen Kokereistandort. Grundwasser - Zeitschrift der Fachsektion Hydrogeologie 16, p. 235-245

National Institute of Standards and Technology - NIST (2015): The NIST WebBook, http://webbook.nist.gov/chemistry/ (Access on 16/08/15)

Nijenhuis, I., Andert, J., Beck, K., Kästner, M., Diekert, G. and Richnow, H.H. (2005): Stable Isotope Fractionation of Tetrachloroethene during Reductive Dechlorination by Sulfurospirillum multivorans and Desulfitobacterium sp. Strain PCE-S and Abiotic Reactions with Cyanocobalamin. Applied and Environmental Microbiology 71, p. 3413-3419

Nikolausz, M., Nijenhuis, I., Ziller, K., Richnow, H.H. and Kästner, M. (2006): Stable carbon isotope fractionation during degradation of dichloremethane by methylotrophic bacteria. Environmental Microbiology 8, p. 156-164

O'Flaherty, V., Mahony, T., O'Kennedy, R. and Colleran, E. (1998): Effect of pH on growth kinetics and sulphide toxicity thresholds of a range of methanogenic, syntrophic and sulphate-reducing bacteria. Process Biochemistry 33, p. 555-569

Omogbai, B.A., Ikenebomeh, M.J. and Ojeaburu, S.I. (2005): Microbial utilization of stachyose in soymilk yogurt production. African Journal of Biotechnology 4, p. 905-908

Paixão, D.A., Dimitrov, M.R., Pereira, R.M., Accorsini, F.R., Vidotti, M.B. and Lemos, E.G. (2010): Molecular analysis of the bacterial diversity in a specialized consortium for diesel oil degradation. Revista Brasiliera de Ciência do Solo 34, p. 773-781

Parey, K., Demmer, U., Warketin, E., Wynen, A., Ermler, U. and Dahl, C. (2013): Structural, Biochemical and Genetic Characterization of Dissimilatory ATP Sulfurylase from Allochromatium vinosum. PLOS ONE 8, s.p.

Peters, K.E., Walters, C.C. and Moldowan, J.N. (2005): Biodegradation parameters. In: Peters, K.E., Walters, C.C. and Moldowan, J.N. (Eds.): The Biomarker Guide. 2nd edition. Cambridge University Press, Cambridge

Pierce, A. E. (1968): Silylation of organic compounds - A Technique for Gasphase Analysis. 1st edition. Pierce Chemical Company, Rockford

Prince, R.C., Garrett, R.M., Bare, R.E., Grossman, M.J., Townsend, T., Suflita, J.M., Lee, K., Owens, E.H., Sergy, G.A., Braddock, J.F., Lindstrom, J.E. and Lessard, R.R. (2003): The roles of photooxidation and biodegradation in long-term weathering of crude and heavy fuel oils. Spill Science and Technology Bulletin 8, p. 145-156

Rabus, R. and Widdel, F. (1995): Anaerobic degradation of ethylbenzene and other aromatic hydrocarbons by new denitrifying bacteria. Achieves of Microbiology 163, p. 96-103

Rabus, R., Kube, M., Heider, J., Beck, A., Heitmann, K., Widdel, F. and Reinhardt, R. (2005): The complete genome of an aromatic-degrading denitrifying bacterium, strain EbN1. Archieves of Microbiology 183, p. 27-36

Rabus, R., Nordhaus, R., Ludwig, W. and Widdel, F. (1993): Complete oxidation of toluene under strictly anaerobic conditions by a new sulfate-reducing bacterium. Applied Environmental Microbiology 59, p. 1444-1451

Rabus, R., Wilkes, H., Behrends, A., Armstroff, A., Fischer, T., Pierik, A.J. and Widdel, F. (2001): Anaerobic initial reaction of n-alkanes in a denitrifying bacterium: evidence for (1-methylpentyl)succinate as initial product and for involvement of an organic radical in n-hexane metabolism. Journal of Bacteriology 183, p. 1707-1715

Radwan, S.S., Sorkhoh, N.A., Felzmann, H. and El-Desouky, A.F. (1996): Uptake and utilization of n-octacosane and n-nonacosane by Arthrobacter nicotianae KCC B35. Journal of Applied Bacteriology 80, p. 370-374

Ranade, D.R., Dighe, A.S., Bhirangi, S.S., Panhalkar, V.S. and Yeole, T.Y. (1999): Evaluation of the use of sodium molybdate to inhibit sulphate reduction during anaerobic digestion of distillery waste. Bioresource Technology 68, p. 287-291

Rayleigh, J.W.S. (1896): Theoretical considerations respecting the separation of gases by diffusion and similar processes. Philosophical Magazine 42, p. 493-498

Rehm, H. J., and Reiff, I. (1981): Mechanisms and occurrence of microbial oxidation of long-chain alkanes. In: Fiechter, A. (Ed.): Advances in biochemical engineering. 19th edition. Springer Verlag, Berlin-Heidelberg

Reichenauer, T.G., Fries-Hanl, W., Edelmann, E., Hofer, H., Weisgram, M., Müller, D. and Dörrie, T. (2011): Expositionsabschätzung und Risikoanalyse - Arbeitshilfe zur Expositionsabschätzung und Risikoanalyse an kontaminierten Standorten. Report on behalf of the Austrian Federal Ministry of Agriculture, Forestry, Environment and Water Management. Austrian Federal Environment Agency, Vienna

Reuveny, Z. (1976): Derepression of ATP sulfurylase by the sulfate analogs molybdate and selenate in cultured tobacco cells. Proceedings of the National Academy of Science 74, p. 619-622

Richnow, H.H., Annweiler, E., Michaelis, W. and Meckenstock R.U. (2003): Microbial *in situ* degradation of aromatic hydrocarbons in a contaminated aquifer monitored by carbon isotope fractionation. Journal of Contaminant Hydrology 65, p. 101-120

Rockne, K.J., Chee-Sanford, J.C., Sanford, R.A., Hedlund, B.P., Staley, J.T. and Strand, S.E. (2000): Anaerobic naphthalene degradation by microbial pure cultures under nitrate-reducing conditions. Applied and Environmental Microbiology 66, p.1595-1601

Rontani, J.F. and Aubert, C. (2008): Hydrogen and Trimethylsilyl Transfers During EI Mass Spectral Fragmentation of Hydroxycarboxylic and Oxocarboxylic Acid Trimethylsilyl Derivates. Journal of the American Society for Mass Spectrometry 19, p. 66-75

Rosenberg, E. and Ron, E.Z. (1999): High- and low-molecular-mass microbial surfactants. Applied Microbiology and Biotechnology 52, p. 154–162

Roychoudhury, A.M. and Merrett, G.L. (2006): Redox pathways in a petroleum contaminated shallow sandy aquifer: Iron and sulfate reductions. Science of the Total Environment 366, p. 262-274

Rueter, P., Rabus, R., Wilkes, H., Aeckersberg, F., Rainey, F.A., Jannasch, H.W. and Widdel, F. (1994): Anaerobic oxidation of hydrocarbons in crude oil by new types of sulphate-reducing bacteria. Nature 372, p. 455-458

Sächsisches Landesamt für Umwelt und Geologie - SLUG (2000): Materialien zur Altlastenbehandlung Nr.1/2000 - Mikrobiologische Sanierungsverfahren, http://www.umwelt.sachsen.de/umwelt/download/boden/mza1_00.pdf (Access on 09/12/14)

Safinowski M and Meckenstock, R.U. (2006): Methylation is the initial reaction in anaerobic naphthalene degradation by a sulfatereducing enrichment culture. Environmental Microbiology 8, p. 347-352

Savage, K.N., Krumholz, L.R., Gieg, L.M., Parisi, V.A., Suflita, J.M., Allen, J., Philp, R.P. and Elshahed, M.S. (2010): Biodegradation of low-molecular-weight alkanes under mesophilic, sulfate-reducing conditions: metabolic intermediates and community patterns. FEMS Microbiology Ecology 72, p. 485-495

Schauer, F. and Sietmann, R. (2010): Angewandte Mikrobiologie - Erdöl abbauende Mikroorganismen. BioSpectrum 16, p. 502-507

Scherr, K.E., Aichberger, H., Braun, R. and Loibner, A.P. (2007): Influence of soil fractions on microbial degradation behavior of mineral hydrocarbons. European Journal of Soil Biology 43, p. 341-350

Scherr, K.E., Hasinger, M., Mayer, P. and Loibner A.P. (2009): Effect of vegetable oil addition on bioaccessibility and biodegradation of polycyclic aromatic hydrocarbons in historically contaminated soils. Journal of Chemical Technology and Biotechnology 84, p. 827-835

Scherr, K.E., Lundaa, T., Close, V., Bochmann, G. and Loibner, A.P. (2012): Changes in bacterial communities from anaerobic digesters during petroleum hydrocarbon degradation. Journal of Biotechnology 157, p. 564-572

Scherr, K.E., Nahold, M.M., Lantschbauer, W. and Loibner, A.P. (2011): Sequential application of electron donors and humic acids for the anaerobic bioremediation of chlorinated aliphatic hydrocarbons. New Biotechnology 29, p. 116-125

Schink, B. (1985): Degradation of unsaturated hydrocarbons by methanogenic enrichments cultures. FEMS Microbiology Ecology 3, p. 69-77

Schinner, F. and Sonnleitner, R. (1997): Bodenökologie: Mikrobiologie und Bodenenzymatik Band III - Pflanzenschutzmittel, Agrarhilfsstoffe und organische Umweltchemikalien. 1st edition. Springer Verlag, Berlin-Heidelberg

Schleheck, D., Weiss, M., Pitluck, S., Bruce, D., Land, M.L., Han, S., Saunders, E., Tapia, R., Detter, C., Brettin, T., Han, J., Woyke, T., Goodwin, L., Pennacchio, L., Nolan, M., Cook, A.M., Kjelleberg, S. and Thomas, T. (2011): Complete genome sequence of Parvibaculum lavamentivorans type strain (DS-1). Standards in Genomic Science 5, p. 298-310

Schneiker, S., Martins dos Santos, V.A., Bartels, D., Bekel, T., Brecht, M., Buhrmester, J., Chernikova, T.N., Denaro, R., Ferrer, M. et al. (2006): Genome sequence of the ubiquitous hydrocarbondegrading marine bacter Alcanivorax borkumensis. Natural Biotechnology 24, p. 997-1004

Schummer, C., Delhomme, O., Appenzeller, B.M.R., Wennig, R. and Millet, M. (2009): Comparison of MTBSTFA and BSTFA in derivatization reactions of polar compounds prior to GC/MS analysis. Talanta 77, p. 1473-1482

Setti, L., Lanzarini, G., Pifferi, P.G. and Spagna, G. (1993): Further research into the aerobic degradation of n-alkanes in a heavy oil by a pure culture of a Pseudomonas sp.. Chemosphere 26, p. 1151-1157

Sikkema, J., De Bont, J.A.N. and Poolman, B. (1995): Mechanisms of membrane toxicity of hydrocarbons. Microbiology Reviews 59, p. 201-222

Singer, M.E. and Finnerty, W.R. (1984): Microbial metabolism of straight-chain and branched alkanes. In: Atlas, R.M. (Ed.): Petroleum microbiology. 1st edition. Macmillan Publishing Co., New York

Singleton, D.R., Ramirez, L.G. and Aitken, M.D. (2009): Characterization of a Polycyclic Aromatic Hydrocarbon Degradation Gene Cluster in a Phenanthrene-Degrading Acidovorax Strain. Applied and Environmental Microbiology 75, p. 2613-2620

Slater, G.F., Ahad, J.M.E., Sherwood Lollar, B., Allen-King, R. and Sleep, B. (2000): Carbon isotope effects resulting from equilibrium sorption of dissolved VOCs. Analytical Chemistry 72, p. 5669-5672

Smith, R.L. and Klug, M.J. (1980): Electron Donors Utilized by Sulfate-Reducing Bacteria in Eutrophic Lake Sediments. Applied and Environmental Microbiology 42, p. 116-121

So, C.M. and Young, L.Y. (1999): Initial reactions in anaerobic alkane degradation by a sulfate reducer, strain AK-01. Applied and Environmental Microbiology 65, p. 5532-5540

So, C.M. and Young, L.L. (2001): Anaerobic Biodegradation of Alkanes by Enriched Consortia under Four Different Reducing Conditions. Environmental Toxicology and Chemistry 20, p. 473-478

So, C.M., Phelps, C.E. and Young, L.Y. (2003): Anaerobic Transformation of Alkanes to Fatty Acids by a Sulfate-Reducing Bacterium, Strain Hxd3. Applied and Environmental Microbiology 69, p. 3892-3900

Song, H.G., Pedersen, T.A., and Bartha, R. (1986): Hydrocarbon mineralization in soil: relative bacterial and fungal contribution. Soil Biology & Biochemistry 18, p. 109-111

Spormann, A.M. and Widdel, F. (2000): Metabolism of alkylbenzenes, alkanes, and other hydrocarbons in anaerobic bacteria. Biodegradation 11, p. 85-105

Steinbach, A., Seifert, R., Annweiler, E. and Michaelis, W. (2004): Hydrogen and Carbon Isotope Fractionation during Anaerobic Biodegradation of Aromatic Hydrocarbonss - A Field Study. Environmental & Science Technology 38, p. 609-616

Stelzer, N. (2008): Entwicklung eines Testsystems zur Erfassung der *in situ* Biodegradation im Grundwasser. Dissertation. Christian-Albrecht University, Kiel

Stelzer, N., Fischer, A., Kästner, M. and Richnow, H.H. (2006): Analyse des anaeroben Benzolabbaus - Vergleich von In-situ-Mikrokosmen, Elektronenakzeptorbilanzen und Isotopenfraktionierungsprozessen. Grundwasser - Zeitschrift der Fachsektion Hydrogeologie 11, p. 247-258

Stögbauer, A. (2004): Schwefelisotopenfraktionierung in abwasserbelasteten Sedimenten - Biogeochemische Umsetzungen und deren Auswirkungen auf den Schwermetallhaushalt. Dissertation. University Karlsruhe, Karlsruhe

Stroo, H.F., Ward, C.H. and Herbs, C. (Eds.) (2010): *In Situ* Remediation of Chlorinated Solvent Plumes. 1st edition. Springer Verlag, New York

Su, X., Lv, H., Zhang, W., Zhang, Y. and Jiao, X. (2013): Evaluation of petroleum hydrocarbon biodegradation in shallow groundwater by hydrogeochemical indicators and C, S-isotopes. Environmental Earth Science 69, p. 2091-2101

Ternes, W. (2013): Biochemie der Elemente - Anorganische Chemie biologischer Prozesse. 1st edition. Springer Verlag, Berlin-Heidelberg

Thauer, R.K., Jungermann, K. and Decker, K. (1977): Energy conservation in chemotrophic anaerobic bacteria. Bacteriological Reviews 41, p. 100-180

Thavasi, R. (2006): Biosurfactants from marine hydrocarbonoclastic bacteria and their application in marine oil pollution abatement. Dissertation. Annamalai University, Tamil Nadu

Thavasi, R., Jayalakshmi, S. and Banat, I.M. (2011): Application of biosurfactant produced from peanut oil cake by Lactobacillus delbrueckii in biodegradation of crude oil. Bioresource Technology 102, p. 3366-3372

The International Tanker Owners Pollution Federation - ITOPF (2015): Oil Tanker Spill Statistics 2014, http://www.itopf.com/fileadmin/data/Documents/Company_Lit/Oil_Spill_Stats_2014FINALlowres.pdf (Access on 04/06/15)

Tucker, M.D., Barton, L.L. and Thomson, B.M. (1997): Reduction and immobilization of molybdate by Desulfovibrio desulfuricans. Journal of Environmental Quality 26, p. 1146-1152

Ulrich, A.C. and Edwards, E.A. (2003): Physiological and molecular characterization of anaerobic benzene-degrading mixed cultures. Environmental Microbiology 5, p. 92-102

Van Beilen, J.B., Li, Z., Duetz, W.A., Smits, T.H. and Witholt, B. (2003): Diversity of alkane hydroxylase systems in the environment. Oil & Gas Science and Technology 58, p. 427-440

Van Beilen, J.B., Smits, T.H., Whyte, L.G., Schorcht, S., Röthlisberger, M., Plaggemeier, T., Engesser, K.H. and Witholt, B. (2002): Alkane hydroxylase homologues in gram-positive strains. Environmental Microbiology 4, p. 676-682

Vega, J.M., Herrera, J., Aparicio, P.J., Paneque, A. and Losada, M. (1971): Role of Molybdenum in Nitrate Reduction by Chlorella. Plant Physiology 48, p. 294-299

Vieth, A. and Wilkes, H. (2006): Deciphering biodegradation effects on light hydrocarbons in crude oils using their stable carbon isotopic composition: A case study from the Fullfaks oil field, offshore Norway. Geochimica Cosmochimica Acta 70, p. 651-665

Wang, L., Tang, Y., Wang, S., Liu, R.L., Liu, M.Z., Zhang, Y., Liang, F.L. and Feng, L. (2006): Isolation and characterization of a novel thermophilic Bacillus strain degrading long-chain n-alkanes. Extremophiles 10, p. 347-356

Wang, Z. and Fingas, M.F. (2003): Development of oil hydrocarbon fingerprinting and identification techniques. Marine Pollution Bulletin 47, p. 423-452

Watson, J.S., Jones, D.M., Swannell, R.P.J. and Van Duin, A.C.T. (2002): Formation of carboxylic acids during aerobic biodegradation of crude oil and evidence of microbial oxidation of hopanes. Organic Geochemistry 33, p. 1153-1169

Wawra, E., Dolznig, H. and Müllner, E. (2003): Chemie erleben - Anorganische, organische und analytische Chemie für Mediziner und Naturwissenschaftler. 1st edition. Facultas Verlag, Vienna

Weiner, E.R. (2012): Applications of Environmental Aquatic Chemistry: A Practical Guide for Environmental Professionals. 3rd edition. CRC Press, Boca Raton

Wentzel, A., Ellingsen, T.E., Kotlar, H.K., Zotchev, S.B. and Throne-Holst, M. (2007): Bacterial metabolism of long-chain n-alkanes. Applied Microbiology and Biotechnology 76, p. 1209-1221

Werner, I. (2009): Untersuchungen zum Stoffwechsel des anaeroben Alkanabbaus. Dissertation. University Bremen, Bremen

Widdel, F. and Rabus, R. (2001): Anaerobic biodegradation of saturated and aromatic hydrocarbons. Current Opinion in Biotechnology 12, p. 259-276

Widdel, F., Knittel, K. and Galushko, A. (2010): Anaerobic hydrocarbon-degrading microorganisms: an overview. In: Timmis, K.N. (Ed.): Handbook of hydrocarbon and lipid microbiology. 1st edition. Springer-Verlag, Berlin-Heidelberg

Wiedemeier, T.H., Rifai, H.S., Newell, C.J. and Wilson, J.T. (1999): Natural Attenuation of Fuels and Chlorinated Solvents in the Subsurface. 1st edition. John Wiley & Sons, Inc., Hoboken

Wilkes, H., Kuehner, S., Bolm, C., Fischer, T., Classen, A., Widdel, F. and Rabus, R. (2003): Formation of n-alkane- and cycloalkane-derived organic acid during anaerobic growth of a denitrifying bacterium with crude oil. Organic Geochemistry 34, p. 1313-1323

Wilkes, H., Rabus, R., Fischer, T., Armstroff, A., Behrends, A. and Widdel, F. (2002): Anaerobic degradation of n-hexane in a denitrifying bacterium: Further degradation of the initial intermediate (1-methylpentyl)succinate via C-skeleton rearrangement. Archives of Microbiology 177, p. 235-243

Wilkes, H., Vieth, A. and Elias, R. (2008): Constraints on the quantitative assessment of in-reservoir biodegradation using compound-specific stable carbon isotopes. Organic Geochemistry 39, p. 1215-1221

Wisotzky, F. (2011): Angewandte Grundwasserchemie, Hydrogeologie und hydrogeochemische Modellierung - Grundlagen, Anwendungen und Problemlösungen. 1st edition. Springer Verlag, Berlin-Heidelberg

Xiong, S., Li, X., Chen, J., Zhao, N., Zhang, H. and Zhang, X. (2015): Cruide oil degradation by bacterial consortia under four different redox and temperature conditions. Applied Microbiology and Biotechnology 99, p. 1451-1461

Yuste, L., Corbella, M.E., Turiegano, M.J., Karlson, U., Puyet, A. and Rojo, F. (2000): Characterization of bacterial strains able to grow on high molecular mass residues from crude oil processing. FEMS Microbiology Ecology 32, p. 69-75

Zhang, X. and Young, Y. (1997): Carboxylation as an Initial Reaction in the Anaerobic Metabolism of Naphthalene and Phenanthrene by Sulfidogenic Consortia. Applied and Environmental Microbiology 63, p. 4759-4764

Zobell, C.E. (1946): Action of Microörganisms on Hydrocarbons. Bacteriological Reviews 10, p. 1-49

7.2 Table of figures

7.3 Table of tables

8 Appendix (Statistical analysis with R®)

This appendix contains all for statistical analysis in R® programmed codes (red). Furthermore, results of calculations (blue) and resulting graphs are given. Moreover, results are commented (cursive script) in Chapter 8.1.1.

8.1 Correlations between nitrate depletion and acceptor sided $^{15}N/^{14}N$-shifts

8.1.1 Microcosms with nitrate amendment

Data import:

```
> no3 <- read.csv("NO3_x.csv")
> no3

   LN_Isotopy       LN_TEA
1  0.0000000000  0.000000000
2  0.0001081030  0.000091200
3  0.0001663880 -0.004346160
4  0.0000886736 -0.007780624
5  0.0012507780 -0.050086309
6  0.0012612280 -0.042955901
7  0.0014249260 -0.045259951
8  0.0029462040 -0.123026764
9  0.0028667180 -0.122211650
10 0.0029561400 -0.116660395
11 0.0033931980 -0.172856011
12 0.0032342900 -0.184842738
13 0.0029958800 -0.180080016
14 0.0035196450 -0.198866163
15 0.0036000720 -0.196323250
16 0.0039452080 -0.245113415
```

The data were imported in csv-format.

Linear regression model:

```
> reg_no3 <- lm(LN_Isotopy~LN_TEA, data=no3)
> summary(reg_no3)

Call:
lm(formula = LN_Isotopy ~ LN_TEA, data = no3)

Residuals:
       Min         1Q     Median         3Q        Max
-4.906e-04 -2.776e-04 -8.344e-05  2.282e-04  6.626e-04

Coefficients:
             Estimate Std. Error t value Pr(>|t|)
(Intercept)  0.0003480  0.0001533    2.27   0.0395 *
LN_TEA      -0.0166771  0.0011488  -14.52 7.84e-10 ***
---
Signif. codes:  0 '***' 0.001 '**' 0.01 '*' 0.05 '.' 0.1 ' ' 1

Residual standard error: 0.0003744 on 14 degrees of freedom
Multiple R-squared: 0.9377,     Adjusted R-squared: 0.9333
F-statistic: 210.7 on 1 and 14 DF,  p-value: 7.843e-10
```

Call:

- *Specification of the model formula.*

Residuals:

- *Specification of the distribution of deviations of the real values from the estimated regression line.*

Coefficients:

- *Specification of intercept (a) and slope (b) of the estimated regression line in the first column called "Estimate".*
- *Specification of t-values (third column) and p-values (fourth column). A significant correlation exists when t-value>|1.96| and p-value<0.05 (=significance level α).*

Last block:

- *Specification of standard deviation of estimator expressed as residual standard error.*
- *Specification of multiple R squared (=R²-value). This value specifies what percentage of statistical spread of y-values is explained by the model. Models with R²-values higher than 0.7 (70%) exhibit good model quality.*

Graphical presentation of linear regression:

```
> plot(no3$LN_TEA, no3$LN_Isotopy,
xlab="ln(Ct/C0)", ylab="ln(Rt/R0)")
> abline(reg_no3)
> aux_values <-
data.frame(LN_TEA=seq(min(no3$LN_TEA),
max(no3$LN_TEA), length=100))
> conf_band <- predict(reg_no3,
aux_values, interval="conf")
> pred_band <- predict(reg_no3,
aux_values, interval="pred")
> plot(no3$LN_TEA, no3$LN_Isotopy,
xlab="ln(Ct/C0)", ylab="ln(Rt/R0)",
ylim=c(min(pred_band[,2]),
max(pred_band[,3])))
> abline(reg_no3)
> matlines(aux_values$LN_TEA,
conf_band, lty=c("blank", "dotted",
"dotted"), col=c("black", "black",
"black"))
> matlines(aux_values$LN_TEA,
pred_band, lty=c("blank", "dashed",
"dashed"), col=c("black", "black",
"black"))
```

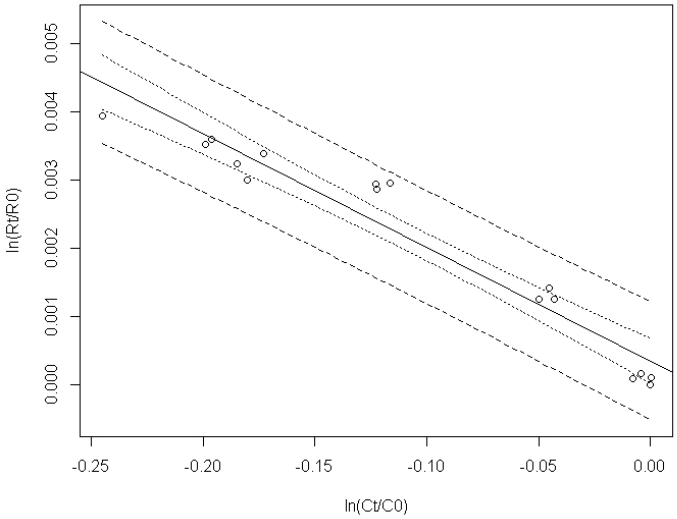

- *o = Measured values*
- *Solid line = Estimated linear regression line*
- *Dotted lines = 95%-confidence-band:*
  In this area the y-values for given x-values are situated with 95% probability.
- *Dashed lines = 95%-prediction-band:*
  In this area the y-values for henceforth measured x-values are situated with 95% probability. This band is always wider than the 95%-confidence-band.

Diagnostic plots:

```
> oldpar <- par(oma=c(0,0,3,0), mfrow=c(2,2))
> plot(reg_no3)
> par(oldpar)
```

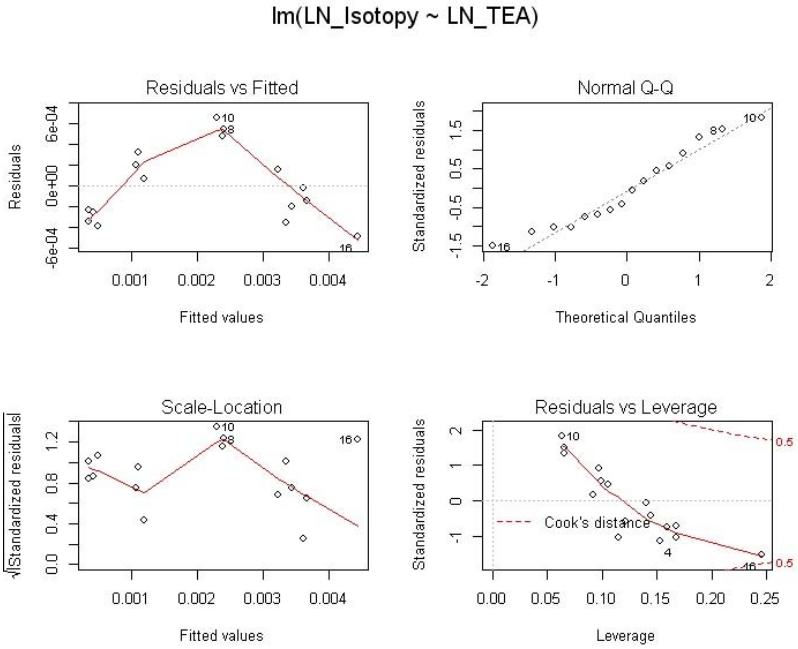

- *Plot 1 – Residuals vs Fitted:*
  - *This is a scatter plot where the residuals are plotted over the fitted values.*
  - *By means of this plot can be checked whether the residuals spread around 0, which is required for carrying out a linear regression.*
  - *Ideally, the residuals should spread around 0. In this case the average error represented by the red line would be 0.*
  - *In the present model the red line is located very close to 0, wherefore this requirement for linear regression is fulfilled.*
- *Plot 2 – Normal Q-Q:*
  - *This is a scatter plot where the standardized residuals are plotted over the theoretical quantiles.*
  - *By means of this plot can be checked whether the standardized residuals and so the x- and y-values are normally distributed, which is required for carrying out a linear regression.*
  - *Ideally, all points should be located on the red dashed line. In this case standardized residuals and so x- and y-values would be normally distributed.*
  - *In the present model all points are located around the red dashed line, wherefore this requirement for linear regression is fulfilled.*
- *Plot 3 – Scale-Location:*
  - *This is a scatter plot where the roots of absolute values of standardized residuals are plotted over the fitted values.*
  - *By means of this plot can be checked whether the standardized residuals and so the y-values are equally spreading with increasing x-values (=homoscedasticity), which is required for carrying out a linear regression.*
  - *Ideally, the red line shows no continuous trend. In this case homoscedasticity prevails.*
  - *In the present model the red line shows no continuous trend, wherefore this requirement for linear regression is fulfilled.*
- *Plot 4 – Residuals vs. Leverage:*
  - *This is a scatter plot where the standardized residuals are plotted over the leverage.*
  - *By means of this plot can be checked whether the model contains outliers which have a high leverage effect and so can distort the model.*

- *Ideally, the model includes no or even less values with a high leverage effect outside the so called Cook's distance, which is represented by the red dashed line.*
- *In the present model no value is located outside of Cook's distance, wherefore no distortion of the model exists.*

Durbin-Watson-Test:

```
> library(car)
Loading required package: MASS
Loading required package: nnet
> dwt(reg_no3, max.lag=1, simulate=TRUE, reps=1000, method=c("normal"))

 lag   Autocorrelation    D-W Statistic     p-value
   1       -0.49622215      2.220287738       0.012
 Alternative hypothesis: rho != 0
```

An important requirement for performing linear regression is the absence of autocorrelation between x-values and errors. By means of the so called Durbin-Watson-Test x-values and errors can be tested for autocorrelation.

Thereby, the presence of autocorrelation can be determined over given Durbin-Watson Statistic (third column):

- *Durbin-Watson Statistic around 0 = positive autocorrelation*
- *Durbin-Watson Statistic between 1 and 3 = no autocorrelation*
- *Durbin-Watson Statistic around 0 = negative autocorrelation*

In the present model Durbin-Watson Statistic is 2.22, wherefore no autocorrelation between x-values and errors exists and so this requirement for linear regression is fulfilled.

8.1.2 Microcosms with both nitrate and sulfate

Data import:

```
> so4no3n <- read.csv("SO4-NO3-N_x.csv")
> so4no3n

LN_Isotopy      LN_TEA
1  0.000000000  0.00000000
2  0.000925560 -0.02023704
3  0.000916845 -0.04375519
4  0.000945220 -0.04244362
5  0.001440680 -0.18833615
6  0.001480476 -0.19779832
7  0.001818678 -0.20317581
8  0.001954921 -0.20364560
9  0.001810059 -0.24298321
10 0.001864758 -0.19260218
```

Linear regression model:

```
> reg_so4no3n <- lm(LN_Isotopy~LN_TEA, data=so4no3n)
> summary(reg_so4no3n)

Call:
lm(formula = LN_Isotopy ~ LN_TEA, data = so4no3n)

Residuals:
       Min         1Q     Median         3Q        Max
-0.0005199 -0.0001910  0.0001118  0.0001906  0.0002850

Coefficients:
             Estimate Std. Error t value Pr(>|t|)
(Intercept)  0.0005199  0.0001571   3.309 0.010710 *
LN_TEA      -0.0059612  0.0009789  -6.090 0.000293 ***
---
Signif. codes:  0 '***' 0.001 '**' 0.01 '*' 0.05 '.' 0.1 ' ' 1

Residual standard error: 0.0002758 on 8 degrees of freedom
Multiple R-squared: 0.8226,     Adjusted R-squared: 0.8004
F-statistic: 37.09 on 1 and 8 DF,  p-value: 0.0002927
```

Graphical presentation of linear regression:

```
> plot(so4no3n$LN_TEA, so4no3n$LN_Isotopy,
xlab="ln(Ct/C0)", ylab="ln(Rt/R0)")
> abline(reg_so4no3n)
> aux_values <-
data.frame(LN_TEA=seq(min(so4no3n$LN_TEA),
max(so4no3n$LN_TEA), length=100))
> conf_band <- predict(reg_so4no3n,
aux_values, interval="conf")
> pred_band <- predict(reg_so4no3n,
aux_values, interval="pred")
> plot(so4no3n$LN_TEA, so4no3n$LN_Isotopy,
xlab="ln(Ct/C0)", ylab="ln(Rt/R0)",
ylim=c(min(pred_band[,2]),
max(pred_band[,3])))
> abline(reg_so4no3n)
> matlines(aux_values$LN_TEA, conf_band,
lty=c("blank", "dotted", "dotted"),
col=c("black", "black", "black"))
> matlines(aux_values$LN_TEA, pred_band,
lty=c("blank", "dashed", "dashed"),
col=c("black", "black", "black"))
```

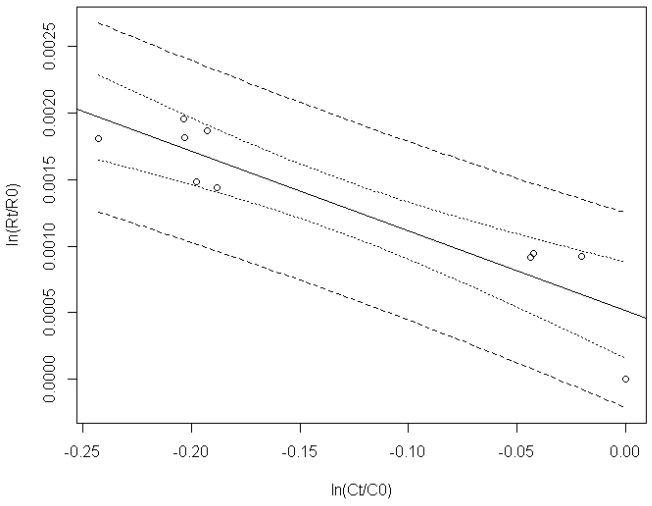

Diagnostic plots:

```
> oldpar <- par(oma=c(0,0,3,0), mfrow=c(2,2))
> plot(reg_so4no3n)
> par(oldpar)
```

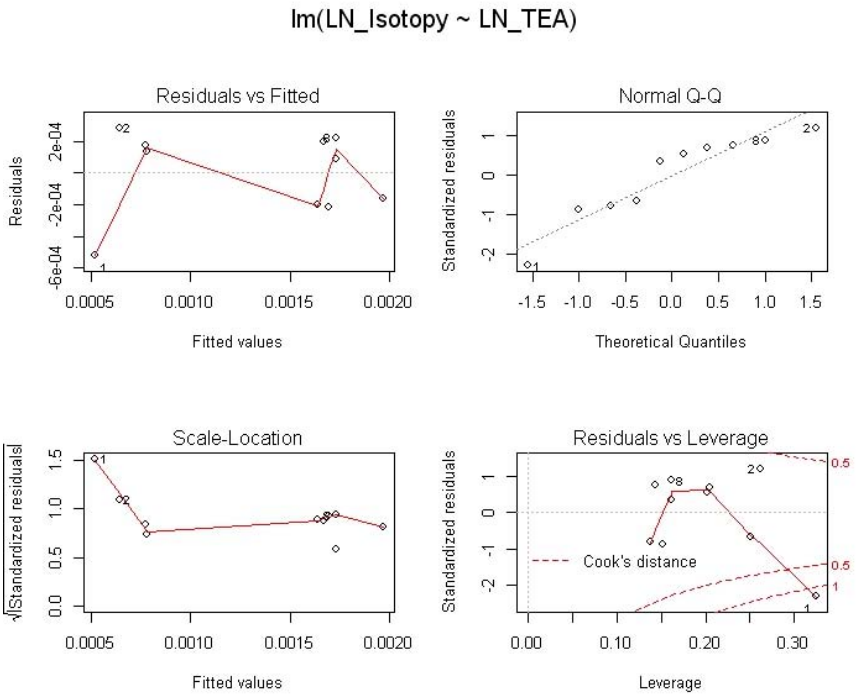

Durbin-Watson-Test:

```
> library(car)
> dwt(reg_so4no3n, max.lag=1, simulate=TRUE, reps=1000, method=c("normal"))

lag Autocorrelation D-W Statistic p-value
   1      -0.2341868      1.960626   0.686
 Alternative hypothesis: rho != 0
```

8.1.3 Microcosms with nitrate under sulfate reduction suppression

Data import:

```
> no3mol <- read.csv("NO3-Mol_x.csv")
> no3mol

   LN_Isotopy      LN_TEA
1  0.000000000  0.00000000
2  0.001278904 -0.06091283
3  0.000897098 -0.05231574
4  0.000808968 -0.06677116
5  0.002466700 -0.15311008
6  0.002447810 -0.15419393
7  0.002619797 -0.16389093
8  0.003792598 -0.19501278
9  0.003688339 -0.19518668
10 0.003723093 -0.18640390
11 0.005113931 -0.28882191
12 0.004623307 -0.27685235
13 0.005124508 -0.27994745
```

Linear regression model:

```
> reg_no3mol <- lm(LN_Isotopy~LN_TEA, data=no3mol)
> summary(reg_no3mol)

Call:
lm(formula = LN_Isotopy ~ LN_TEA, data = no3mol)

Residuals:
       Min         1Q     Median         3Q        Max
-3.286e-04 -2.706e-04  2.096e-05  2.287e-04  4.222e-04

Coefficients:
             Estimate Std. Error t value Pr(>|t|)
(Intercept) -6.988e-05  1.567e-04  -0.446    0.664
LN_TEA      -1.808e-02  8.571e-04 -21.098 3.01e-10 ***
---
Signif. codes:  0 ‘***’ 0.001 ‘**’ 0.01 ‘*’ 0.05 ‘.’ 0.1 ‘ ’ 1

Residual standard error: 0.0002759 on 11 degrees of freedom
Multiple R-squared: 0.9759,     Adjusted R-squared: 0.9737
F-statistic: 445.1 on 1 and 11 DF,  p-value: 3.01e-10
```

Graphical presentation of linear regression:

```
> plot(no3mol$LN_TEA, no3mol$LN_Isotopy,
xlab="ln(Ct/C0)", ylab="ln(Rt/R0)")
> abline(reg_no3mol)
> aux_values <-
data.frame(LN_TEA=seq(min(no3mol$LN_TEA),
max(no3mol$LN_TEA), length=100))
> conf_band <- predict(reg_no3mol,
aux_values, interval="conf")
> pred_band <- predict(reg_no3mol,
aux_values, interval="pred")
> plot(no3mol$LN_TEA, no3mol$LN_Isotopy,
xlab="ln(Ct/C0)", ylab="ln(Rt/R0)",
ylim=c(min(pred_band[,2]),
max(pred_band[,3])))
> abline(reg_no3mol)
> matlines(aux_values$LN_TEA, conf_band,
lty=c("blank", "dotted", "dotted"),
col=c("black", "black", "black"))
> matlines(aux_values$LN_TEA, pred_band,
lty=c("blank", "dashed", "dashed"),
col=c("black", "black", "black"))
```

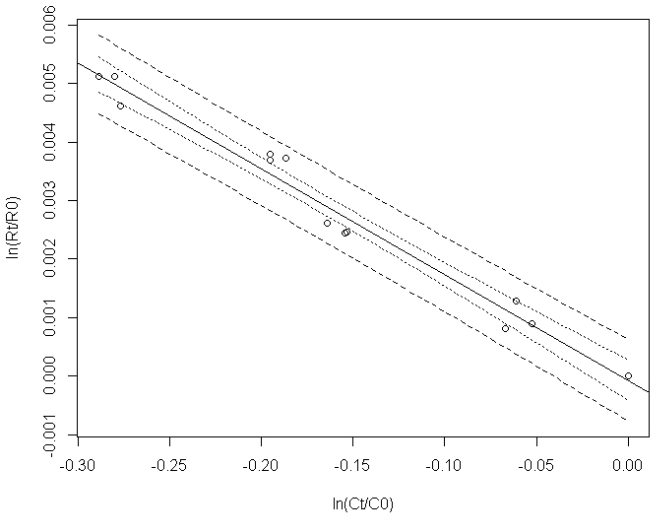

Diagnostic plots:

```
> oldpar <- par(oma=c(0,0,3,0), mfrow=c(2,2))
> plot(reg_no3mol)
> par(oldpar)
```

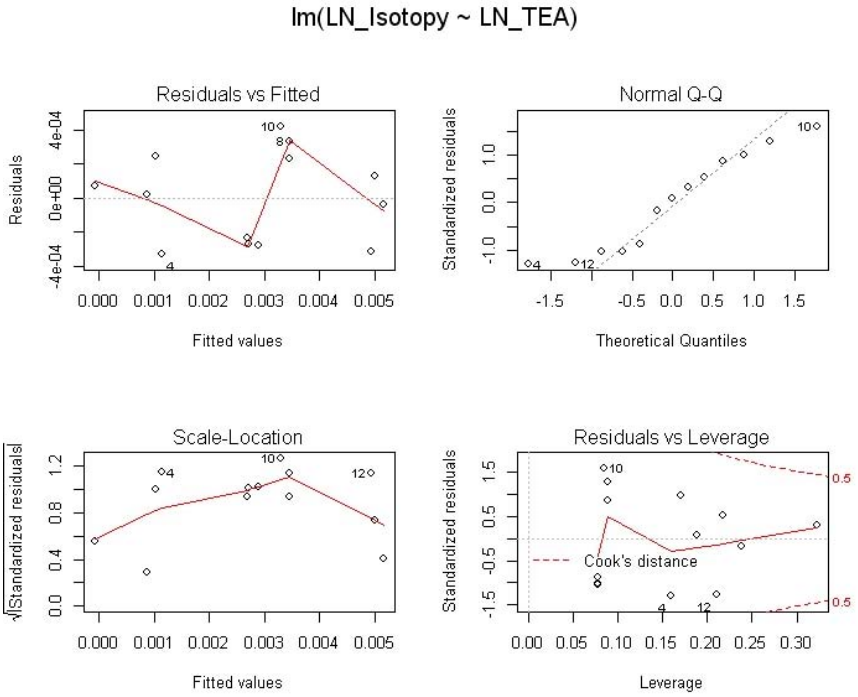

Durbin-Watson-Test:

```
> library(car)
Loading required package: MASS
Loading required package: nnet
> dwt(reg_no3mol, max.lag=1, simulate=TRUE, reps=1000, method=c("normal"))

 lag Autocorrelation D-W Statistic p-value
   1       0.143895      1.574337   0.256
 Alternative hypothesis: rho != 0
```

8.1.4 Contrasting scatterplot

Data import:

```
> n_total <- read.csv("N-total_x.csv")
> n_total
```

	LN_Isotopy	LN_TEA	Type
1	0.0000000000	0.000000000	NO3-Mol
2	0.0012789040	-0.060912832	NO3-Mol
3	0.0008970980	-0.052315744	NO3-Mol
4	0.0008089680	-0.066771160	NO3-Mol
5	0.0024667000	-0.153110075	NO3-Mol
6	0.0024478100	-0.154193930	NO3-Mol
7	0.0026197970	-0.163890928	NO3-Mol
8	0.0037925980	-0.195012778	NO3-Mol
9	0.0036883390	-0.195186675	NO3-Mol
10	0.0037230930	-0.186403896	NO3-Mol
11	0.0051139310	-0.288821910	NO3-Mol
12	0.0046233070	-0.276852346	NO3-Mol
13	0.0051245080	-0.279947454	NO3-Mol
14	0.0000000000	0.000000000	NO3
15	0.0001081030	0.000091200	NO3
16	0.0001663880	-0.004346160	NO3
17	0.0000886736	-0.007780624	NO3
18	0.0012507780	-0.050086309	NO3
19	0.0012612280	-0.042955901	NO3
20	0.0014249260	-0.045259951	NO3
21	0.0029462040	-0.123026764	NO3
22	0.0028667180	-0.122211650	NO3
23	0.0029561400	-0.116660395	NO3
24	0.0033931980	-0.172856011	NO3
25	0.0032342900	-0.184842738	NO3
26	0.0029958800	-0.180080016	NO3
27	0.0035196450	-0.198866163	NO3
28	0.0036000720	-0.196323250	NO3
29	0.0039452080	-0.245113415	NO3
30	0.0000000000	0.000000000	SO4NO3
31	0.0009255600	-0.020237042	SO4NO3
32	0.0009168450	-0.043755189	SO4NO3
33	0.0009452200	-0.042443622	SO4NO3
34	0.0014406800	-0.188336152	SO4NO3
35	0.0014804760	-0.197798320	SO4NO3
36	0.0018186780	-0.203175807	SO4NO3
37	0.0019549210	-0.203645598	SO4NO3
38	0.0018100590	-0.242983208	SO4NO3
39	0.0018647580	-0.192602184	SO4NO3

Scatterplot:

```
> scatterplot(LN_Isotopy~LN_TEA | Type, data=n_total, reg.line=lm, smooth=FALSE, spread=FALSE,
boxplots=FALSE, span=0.5, by.groups=TRUE)
```

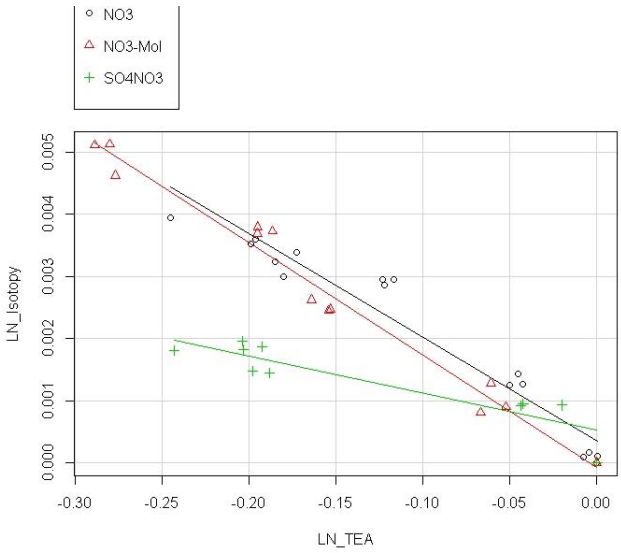

8.2 Correlations between TPH-degradation and acceptor sided $^{15}N/^{14}N$-shifts

8.2.1 Microcosms with nitrate amendment

Data import:

```
> no3 <- read.csv("NO3.csv")
> no3

LN_Isotopy       LN_TPH
1 0.000000000  0.000000000
2 0.000108103 -0.000360535
3 0.000166388 -0.024516952
4 0.002946204 -0.279389415
5 0.002866718 -0.305894831
6 0.003234290 -0.374938354
7 0.002995880 -0.311900613
8 0.003519645 -0.416677803
9 0.003600072 -0.343661987
```

Linear regression model:

```
> reg_no3 <- lm(LN_Isotopy~LN_TPH, data=no3)
> summary(reg_no3)

Call:
lm(formula = LN_Isotopy ~ LN_TPH, data = no3)

Residuals:
       Min         1Q     Median         3Q        Max
-3.556e-04 -1.319e-04  1.930e-06  7.631e-05  3.908e-04

Coefficients:
             Estimate Std. Error t value Pr(>|t|)
(Intercept)  7.463e-05  1.521e-04   0.491    0.639
LN_TPH      -9.121e-03  5.448e-04 -16.742 6.64e-07 ***
---
Signif. codes:  0 ‘***’ 0.001 ‘**’ 0.01 ‘*’ 0.05 ‘.’ 0.1 ‘ ’ 1

Residual standard error: 0.0002622 on 7 degrees of freedom
Multiple R-squared: 0.9756,     Adjusted R-squared: 0.9722
F-statistic: 280.3 on 1 and 7 DF,  p-value: 6.636e-07
```

Graphical presentation of linear regression:

```
> plot(no3$LN_TPH, no3$LN_Isotopy,
xlab="ln(Ct/C0)", ylab="ln(Rt/R0)")
> abline(reg_no3)
> aux_values <-
data.frame(LN_TPH=seq(min(no3$LN_TPH),
max(no3$LN_TPH), length=100))
> conf_band <- predict(reg_no3, aux_values,
interval="conf")
> pred_band <- predict(reg_no3, aux_values,
interval="pred")
> plot(no3$LN_TPH, no3$LN_Isotopy,
xlab="ln(Ct/C0)", ylab="ln(Rt/R0)",
ylim=c(min(pred_band[,2]), max(pred_band[,3])))
> abline(reg_no3)
> matlines(aux_values$LN_TPH, conf_band,
lty=c("blank", "dotted", "dotted"),
col=c("black", "black", "black"))
> matlines(aux_values$LN_TPH, pred_band,
lty=c("blank", "dashed", "dashed"),
col=c("black", "black", "black"))
```

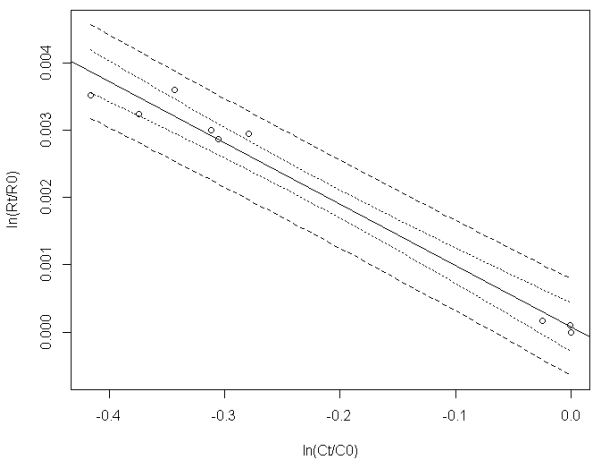

Diagnostic plots:

```
> oldpar <- par(oma=c(0,0,3,0), mfrow=c(2,2))
> plot(reg_no3)
> par(oldpar)
```

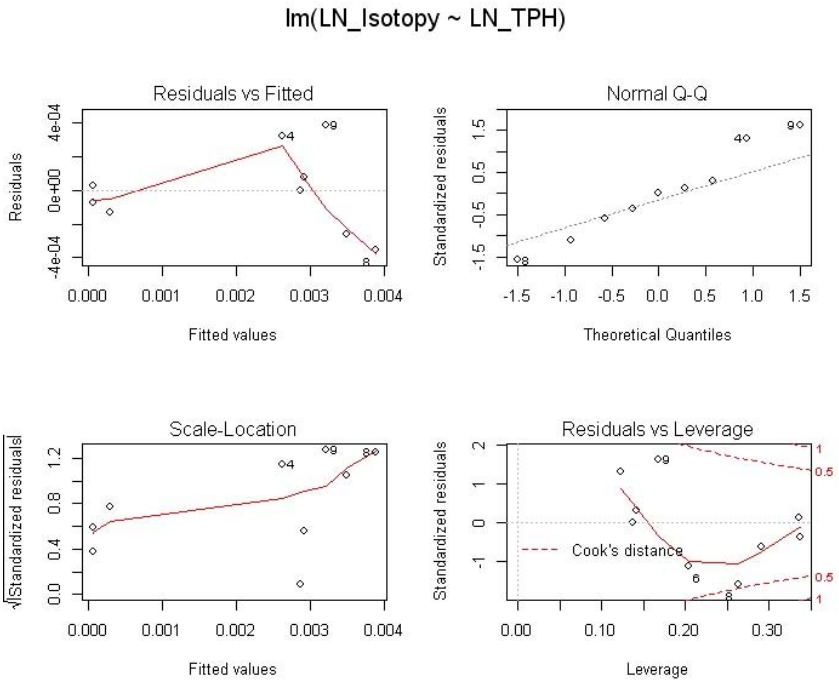

Durbin-Watson-Test:

```
> library(car)
Loading required package: MASS
Loading required package: nnet
> dwt(reg_no3, max.lag=1, simulate=TRUE, reps=1000, method=c("normal"))

 lag Autocorrelation D-W Statistic p-value
   1       -0.471781      2.758264   0.354
 Alternative hypothesis: rho != 0
```

8.2.2 Microcosms with both nitrate and sulfate

Data import:

```
> so4no3n <- read.csv("SO4-NO3-N.csv")
> so4no3n

LN_Isotopy     LN_TPH
1 0.000000000  0.0000000
2 0.000925560 -0.1018041
3 0.000916845 -0.1060583
4 0.000945220 -0.1382087
5 0.001440680 -0.4140068
6 0.001480476 -0.4330036
7 0.001954921 -0.4912127
8 0.001810059 -0.4432078
9 0.001864758 -0.3916973
```

Linear regression model:

```
> reg_so4no3n <- lm(LN_Isotopy~LN_TPH, data=so4no3n)
> summary(reg_so4no3n)

Call:
lm(formula = LN_Isotopy ~ LN_TPH, data = so4no3n)

Residuals:
       Min         1Q     Median         3Q        Max
-3.986e-04 -2.317e-04  4.779e-05  1.919e-04  2.610e-04

Coefficients:
             Estimate Std. Error t value Pr(>|t|)
(Intercept)  0.0003986  0.0001565   2.547 0.038297 *
LN_TPH      -0.0030768  0.0004718  -6.522 0.000327 ***
---
Signif. codes:  0 ‘***’ 0.001 ‘**’ 0.01 ‘*’ 0.05 ‘.’ 0.1 ‘ ’ 1

Residual standard error: 0.0002521 on 7 degrees of freedom
Multiple R-squared: 0.8587,     Adjusted R-squared: 0.8385
F-statistic: 42.54 on 1 and 7 DF,  p-value: 0.0003273
```

Graphical presentation of linear regression:

```
> plot(so4no3n$LN_TPH, so4no3n$LN_Isotopy,
xlab="ln(Ct/C0)", ylab="ln(Rt/R0)")
> abline(reg_so4no3n)
> aux_values <-
data.frame(LN_TPH=seq(min(so4no3n$LN_TPH),
max(so4no3n$LN_TPH), length=100))
> conf_band <- predict(reg_so4no3n,
aux_values, interval="conf")
> pred_band <- predict(reg_so4no3n,
aux_values, interval="pred")
> plot(so4no3n$LN_TPH, so4no3n$LN_Isotopy,
xlab="ln(Ct/C0)", ylab="ln(Rt/R0)",
ylim=c(min(pred_band[,2]),
max(pred_band[,3])))
> abline(reg_so4no3n)
> matlines(aux_values$LN_TPH, conf_band,
lty=c("blank", "dotted", "dotted"),
col=c("black", "black", "black"))
> matlines(aux_values$LN_TPH, pred_band,
lty=c("blank", "dashed", "dashed"),
col=c("black", "black", "black"))
```

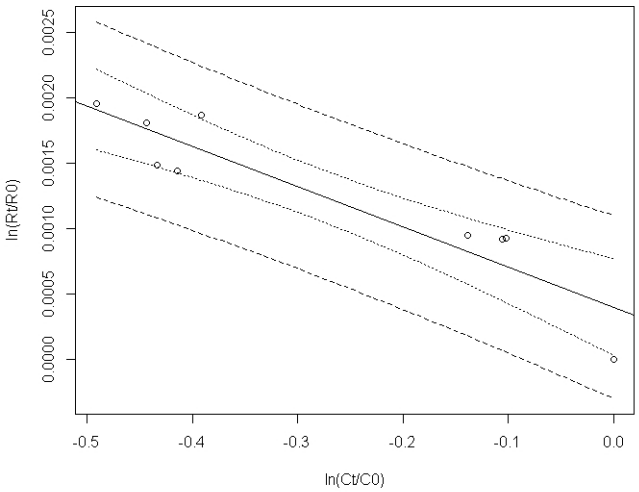

Diagnostic plots:

```
> oldpar <- par(oma=c(0,0,3,0), mfrow=c(2,2))
> plot(reg_so4no3n)
> par(oldpar)
```

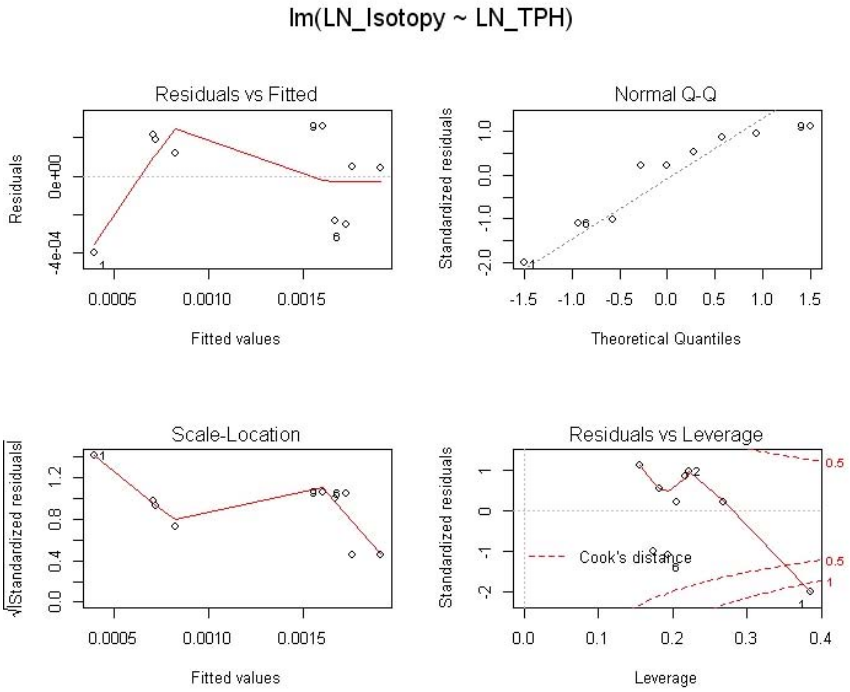

Durbin-Watson-Test:

```
> library(car)
Loading required package: MASS
Loading required package: nnet
> dwt(reg_so4no3n, max.lag=1, simulate=TRUE, reps=1000, method=c("normal"))

 lag Autocorrelation D-W Statistic p-value
   1      0.02784455      1.434169   0.158
 Alternative hypothesis: rho != 0
```

8.2.3 Microcosms with nitrate under sulfate reduction suppression

Data import:

```
> no3mol <- read.csv("NO3-Mol.csv")
> no3mol

LN_Isotopy     LN_TPH
1  0.000000000  0.0000000
2  0.001278904 -0.2822812
3  0.000897098 -0.2644707
4  0.000808968 -0.2220482
5  0.002466700 -0.4384862
6  0.002447810 -0.3835180
7  0.002619797 -0.4894903
8  0.003792598 -0.4350065
9  0.003688339 -0.4517191
10 0.003723093 -0.4604547
11 0.005113931 -0.5709789
12 0.004623307 -0.5485870
13 0.005124508 -0.5789696
```

Linear regression model:

```
> reg_no3mol <- lm(LN_Isotopy~LN_TPH, data=no3mol)
> summary(reg_no3mol)

Call:
lm(formula = LN_Isotopy ~ LN_TPH, data = no3mol)

Residuals:
       Min         1Q     Median         3Q        Max
-0.0011072 -0.0004611  0.0002745  0.0005395  0.0009670

Coefficients:
             Estimate Std. Error t value Pr(>|t|)
(Intercept) -0.0009670  0.0004982  -1.941   0.0783 .
LN_TPH      -0.0095895  0.0011730  -8.175 5.31e-06 ***
---
Signif. codes:  0 ‘***’ 0.001 ‘**’ 0.01 ‘*’ 0.05 ‘.’ 0.1 ‘ ’ 1

Residual standard error: 0.0006678 on 11 degrees of freedom
Multiple R-squared: 0.8587,     Adjusted R-squared: 0.8458
F-statistic: 66.83 on 1 and 11 DF,  p-value: 5.315e-06
```

Graphical presentation of linear regression:

```
> plot(no3mol$LN_TPH, no3mol$LN_Isotopy,
xlab="ln(Ct/C0)", ylab="ln(Rt/R0)")
> abline(reg_no3mol)
> aux_values <-
data.frame(LN_TPH=seq(min(no3mol$LN_TPH),
max(no3mol$LN_TPH), length=100))
> conf_band <- predict(reg_no3mol,
aux_values, interval="conf")
> pred_band <- predict(reg_no3mol,
aux_values, interval="pred")
> plot(no3mol$LN_TPH, no3mol$LN_Isotopy,
xlab="ln(Ct/C0)", ylab="ln(Rt/R0)",
ylim=c(min(pred_band[,2]),
max(pred_band[,3])))
> abline(reg_no3mol)
> matlines(aux_values$LN_TPH, conf_band,
lty=c("blank", "dotted", "dotted"),
col=c("black", "black", "black"))
> matlines(aux_values$LN_TPH, pred_band,
lty=c("blank", "dashed", "dashed"),
col=c("black", "black", "black"))
```

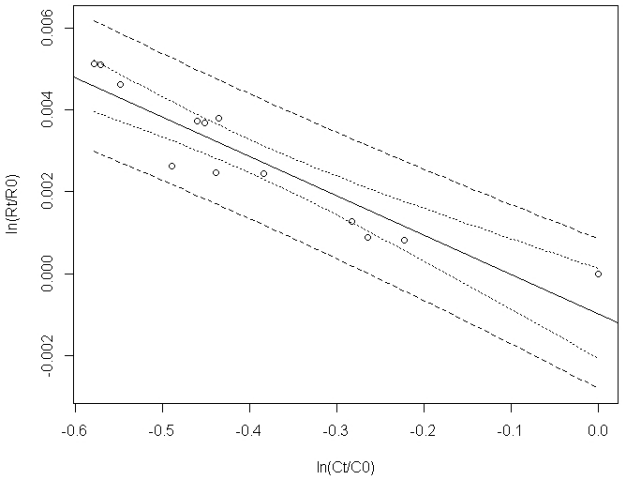

Diagnostic plots:

```
> oldpar <- par(oma=c(0,0,3,0), mfrow=c(2,2))
> plot(reg_no3mol)
> par(oldpar)
```

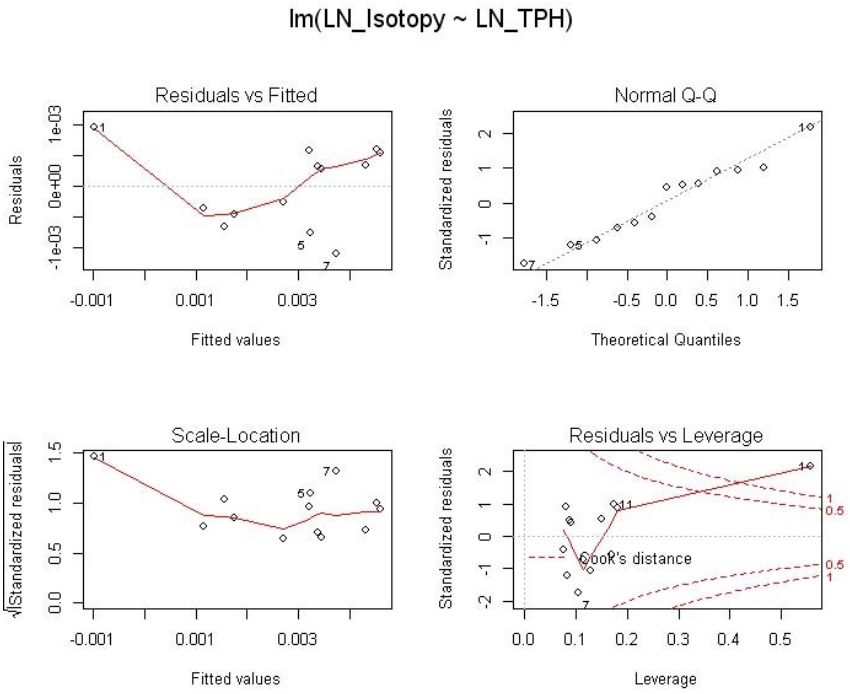

Durbin-Watson-Test:

```
> library(car)
Loading required package: MASS
Loading required package: nnet
> dwt(reg_no3mol, max.lag=1, simulate=TRUE, reps=1000, method=c("normal"))

 lag Autocorrelation D-W Statistic p-value
   1       0.1374605      1.574601   0.294
 Alternative hypothesis: rho != 0
```

8.2.4 Contrasting scatterplot

Data import:

```
> n_total <- read.csv("N-total.csv")
> n_total
```

```
> n_total <- read.csv("N-total.csv")
> n_total
    LN_Isotopy       LN_TPH    Type
1  0.000000000  0.000000000 NO3-Mol
2  0.001278904 -0.282281198 NO3-Mol
3  0.000897098 -0.264470652 NO3-Mol
4  0.000808968 -0.222048197 NO3-Mol
5  0.002466700 -0.438486235 NO3-Mol
6  0.002447810 -0.383517991 NO3-Mol
7  0.002619797 -0.489490271 NO3-Mol
8  0.003792598 -0.435006454 NO3-Mol
9  0.003688339 -0.451719070 NO3-Mol
10 0.003723093 -0.460454702 NO3-Mol
11 0.005113931 -0.570978942 NO3-Mol
12 0.004623307 -0.548587038 NO3-Mol
13 0.005124508 -0.578969616 NO3-Mol
14 0.000000000  0.000000000     NO3
15 0.000108103 -0.000360535     NO3
16 0.000166388 -0.024516952     NO3
17 0.002946204 -0.279389415     NO3
18 0.002866718 -0.305894831     NO3
19 0.003234290 -0.374938354     NO3
20 0.002995880 -0.311900613     NO3
21 0.003519645 -0.416677803     NO3
22 0.003600072 -0.343661987     NO3
23 0.000000000  0.000000000  SO4NO3
24 0.000925560 -0.101804135  SO4NO3
25 0.000916845 -0.106058317  SO4NO3
26 0.000945220 -0.138208737  SO4NO3
27 0.001440680 -0.414006794  SO4NO3
28 0.001480476 -0.433003626  SO4NO3
29 0.001954921 -0.491212733  SO4NO3
30 0.001810059 -0.443207793  SO4NO3
31 0.001864758 -0.391697309  SO4NO3
```

Scatterplot:

```
> scatterplot(LN_Isotopy~LN_TPH | Type, data=n_total, reg.line=lm, smooth=FALSE, spread=FALSE,
boxplots=FALSE, span=0.5, by.groups=TRUE)
```